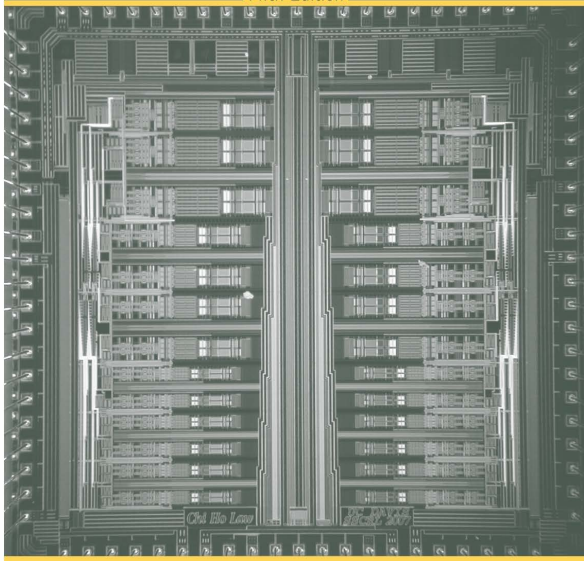


# ANALYSIS AND DESIGN OF ANALOG INTEGRATED CIRCUITS

Paul R. Gray ■ Paul J. Hurst ■ Stephen H. Lewis ■ Robert G. Meyer

Fifth Edition



EX-1013 0001

Kangxi Communication Technologies (Shanghai) Co., Ltd. v. Skyworks Solutions, Inc.



# ANALYSIS AND DESIGN OF ANALOG INTEGRATED CIRCUITS

Fifth Edition

**PAUL R. GRAY**

*University of California, Berkeley*

**PAUL J. HURST**

*University of California, Davis*

**STEPHEN H. LEWIS**

*University of California, Davis*

**ROBERT G. MEYER**

*University of California, Berkeley*



WILEY

*New York / Chichester / Weinheim / Brisbane / Singapore / Toronto*

PUBLISHER	Don Fowley
ACQUISITIONS EDITOR	Daniel Sayre
SENIOR PRODUCTION EDITOR	Valerie A. Vargas
EXECUTIVE MARKETING MANAGER	Christopher Ruel
DESIGNER	Arthur Medina
PRODUCTION MANAGEMENT SERVICES	Elm Street Publishing Services
EDITORIAL ASSISTANT	Carolyn Weisman
MEDIA EDITOR	Lauren Sapira

Cover courtesy of Chi Ho Law.

This book was set in 10/12 Times Roman by Thomson Digital and printed and bound by Hamilton Printing Company. The cover was printed by Phoenix Color, Inc.

This book was printed on acid-free paper. ☺

Copyright 2009 © John Wiley & Sons, Inc. All rights reserved.

No part of this publication may be reproduced, stored in a retrieval system or transmitted in any form or by any means, electronic, mechanical, photocopying, recording, scanning or otherwise, except as permitted under Sections 107 or 108 of the 1976 United States Copyright Act, without either the prior written permission of the Publisher, or authorization through payment of the appropriate per-copy fee to the Copyright Clearance Center Inc., 222 Rosewood Drive, Danvers, MA 01923, website [www.copyright.com](http://www.copyright.com). Requests to the Publisher for permission should be addressed to the Permissions Department, John Wiley & Sons, Inc., 111 River Street, Hoboken, NJ 07030-5774, (201) 748-6011, fax (201) 748-6008, website <http://www.wiley.com/go/permissions>. To order books or for customer service please call 1-800-CALL-WILEY (255-5945).

<http://www.wiley.com/college/gray>

***Library of Congress Cataloging-in-Publication Data***

Analysis and design of analog integrated circuits / Paul R. Gray . . . [et al.]. — 5th ed.  
p. cm.

Includes bibliographical references and index.

ISBN 978-0-470-24599-6 (cloth: alk. paper)

1. Linear integrated circuits-Computer-aided design. 2. Metal oxide semiconductors-Computer-aided design. 3. Bipolar transistors-Computer-aided design.

I. Gray, Paul R., 1942-

TK7874.A588 2009

621.3815-dc21

08-043583

Printed in the United States of America

10 9 8 7 6 5 3 2 1

*To Liz, Barbara, Robin, and Judy*

# Preface

Since the publication of the first edition of this book, the field of analog integrated circuits has developed and matured. The initial groundwork was laid in bipolar technology, followed by a rapid evolution of MOS analog integrated circuits. Thirty years ago, CMOS technologies were fast enough to support applications only at audio frequencies. However, the continuing reduction of the minimum feature size in integrated-circuit (IC) technologies has greatly increased the maximum operating frequencies, and CMOS technologies have become fast enough for many new applications as a result. For example, the bandwidth in some video applications is about 4 MHz, requiring bipolar technologies as recently as about twenty-three years ago. Now, however, CMOS easily can accommodate the required bandwidth for video and is being used for radio-frequency applications. Today, bipolar integrated circuits are used in some applications that require very low noise, very wide bandwidth, or driving low-impedance loads.

In this fifth edition, coverage of the bipolar 741 op amp has been replaced with a low-voltage bipolar op amp, the NE5234, with rail-to-rail common-mode input range and almost rail-to-rail output swing. Analysis of a fully differential CMOS folded-cascode operational amplifier (op amp) is now included in Chapter 12. The 560B phase-locked loop, which is no longer commercially available, has been deleted from Chapter 10.

The SPICE computer analysis program is now readily available to virtually all electrical engineering students and professionals, and we have included extensive use of SPICE in this edition, particularly as an integral part of many problems. We have used computer analysis as it is most commonly employed in the engineering design process—both as a more accurate check on hand calculations, and also as a tool to examine complex circuit behavior beyond the scope of hand analysis.

An in-depth look at SPICE as an indispensable tool for IC robust design can be found in *The SPICE Book*, 2nd ed., published by J. Wiley and Sons. This text contains many worked out circuit designs and verification examples linked to the multitude of analyses available in the most popular versions of SPICE. The *SPICE Book* conveys the role of simulation as an integral part of the design process, but not as a replacement for solid circuit-design knowledge.

This book is intended to be useful both as a text for students and as a reference book for practicing engineers. For class use, each chapter includes many worked problems; the problem sets at the end of each chapter illustrate the practical applications of the material in the text. All of the authors have extensive industrial experience in IC design and in the teaching of courses on this subject; this experience is reflected in the choice of text material and in the problem sets.

Although this book is concerned largely with the analysis and design of ICs, a considerable amount of material also is included on applications. In practice, these two subjects are closely linked, and a knowledge of both is essential for designers and users of ICs. The latter compose the larger group by far, and we believe that a working knowledge of IC design is a great advantage to an IC user. This is particularly apparent when the user must choose from among a number of competing designs to satisfy a particular need. An understanding of the IC structure is then useful in evaluating the relative desirability of the different designs under extremes of environment or in the presence of variations in supply voltage. In addition, the IC user is in a

much better position to interpret a manufacturer's data if he or she has a working knowledge of the internal operation of the integrated circuit.

The contents of this book stem largely from courses on analog integrated circuits given at the University of California at the Berkeley and Davis campuses. The courses are senior-level electives and first-year graduate courses. The book is structured so that it can be used as the basic text for a sequence of such courses. The more advanced material is found at the end of each chapter or in an appendix so that a first course in analog integrated circuits can omit this material without loss of continuity. An outline of each chapter is given below with suggestions for material to be covered in such a first course. It is assumed that the course consists of three hours of lecture per week over a fifteen-week semester and that the students have a working knowledge of Laplace transforms and frequency-domain circuit analysis. It is also assumed that the students have had an introductory course in electronics so that they are familiar with the principles of transistor operation and with the functioning of simple analog circuits. Unless otherwise stated, each chapter requires three to four lecture hours to cover.

Chapter 1 contains a summary of bipolar transistor and MOS transistor device physics. We suggest spending one week on selected topics from this chapter, with the choice of topics depending on the background of the students. The material of Chapters 1 and 2 is quite important in IC design because there is significant interaction between circuit and device design, as will be seen in later chapters. A thorough understanding of the influence of device fabrication on device characteristics is essential.

Chapter 2 is concerned with the technology of IC fabrication and is largely descriptive. One lecture on this material should suffice if the students are assigned the chapter to read.

Chapter 3 deals with the characteristics of elementary transistor connections. The material on one-transistor amplifiers should be a review for students at the senior and graduate levels and can be assigned as reading. The section on two-transistor amplifiers can be covered in about three hours, with greatest emphasis on differential pairs. The material on device mismatch effects in differential amplifiers can be covered to the extent that time allows.

In Chapter 4, the important topics of current mirrors and active loads are considered. These configurations are basic building blocks in modern analog IC design, and this material should be covered in full, with the exception of the material on band-gap references and the material in the appendices.

Chapter 5 is concerned with output stages and methods of delivering output power to a load. Integrated-circuit realizations of Class A, Class B, and Class AB output stages are described, as well as methods of output-stage protection. A selection of topics from this chapter should be covered.

Chapter 6 deals with the design of operational amplifiers (op amps). Illustrative examples of dc and ac analysis in both MOS and bipolar op amps are performed in detail, and the limitations of the basic op amps are described. The design of op amps with improved characteristics in both MOS and bipolar technologies are considered. This key chapter on amplifier design requires at least six hours.

In Chapter 7, the frequency response of amplifiers is considered. The zero-value time-constant technique is introduced for the calculations of the  $-3$ -dB frequency of complex circuits. The material of this chapter should be considered in full.

Chapter 8 describes the analysis of feedback circuits. Two different types of analysis are presented: two-port and return-ratio analyses. Either approach should be covered in full with the section on voltage regulators assigned as reading.

Chapter 9 deals with the frequency response and stability of feedback circuits and should be covered up to the section on root locus. Time may not permit a detailed discussion of root locus, but some introduction to this topic can be given.

In a fifteen-week semester, coverage of the above material leaves about two weeks for Chapters 10, 11, and 12. A selection of topics from these chapters can be chosen as follows. Chapter 10 deals with nonlinear analog circuits and portions of this chapter up to Section 10.2 could be covered in a first course. Chapter 11 is a comprehensive treatment of noise in integrated circuits and material up to and including Section 11.4 is suitable. Chapter 12 describes fully differential operational amplifiers and common-mode feedback and may be best suited for a second course.

We are grateful to the following colleagues for their suggestions for and/or evaluation of this book: R. Jacob Baker, Bernhard E. Boser, A. Paul Brokaw, Iwen Chao, John N. Churchill, David W. Cline, Kenneth C. Dyer, Ozan E. Erdoğan, John W. Fattaruso, Weinan Gao, Edwin W. Greeneich, Alex Gros-Balthazard, Tünde Gyurics, Ward J. Helms, Kaveh Hosseini, Timothy H. Hu, Shafiq M. Jamal, John P. Keane, Haideh Khorramabadi, Pak Kim Lau, Thomas W. Matthews, Krishnaswamy Nagaraj, Khalil Najafi, Borivoje Nikolić, Keith O'Donoghue, Robert A. Pease, Lawrence T. Pileggi, Edgar Sánchez-Sinencio, Bang-Sup Song, Richard R. Spencer, Eric J. Swanson, Andrew Y. J. Szeto, Yannis P. Tsvividis, Srikanth Vaidianathan, T. R. Viswanathan, Chong-Kuang Wang, Dong Wang, and Mo Maggie Zhang. We are also grateful to Darrel Akers, Mu Jane Lee, Lakshmi Rao, Nattapol Sitthimahachaikul, Haoyue Wang, and Mo Maggie Zhang for help with proofreading, and to Chi Ho Law for allowing us to use on the cover of this book a die photograph of an integrated circuit he designed. Finally, we would like to thank the staffs at Wiley and Elm Street Publishing Services for their efforts in producing this edition.

The material in this book has been greatly influenced by our association with the late Donald O. Pederson, and we acknowledge his contributions.

*Berkeley and Davis, CA, 2008*

***Paul R. Gray***  
***Paul J. Hurst***  
***Stephen H. Lewis***  
***Robert G. Meyer***

# Contents

## CHAPTER 1

### Models for Integrated-Circuit Active Devices 1

- 1.1 Introduction 1
- 1.2 Depletion Region of a *pn* Junction 1
  - 1.2.1 Depletion-Region Capacitance 5
  - 1.2.2 Junction Breakdown 6
- 1.3 Large-Signal Behavior of Bipolar Transistors 8
  - 1.3.1 Large-Signal Models in the Forward-Active Region 8
  - 1.3.2 Effects of Collector Voltage on Large-Signal Characteristics in the Forward-Active Region 14
  - 1.3.3 Saturation and Inverse-Active Regions 16
  - 1.3.4 Transistor Breakdown Voltages 20
  - 1.3.5 Dependence of Transistor Current Gain  $\beta_F$  on Operating Conditions 23
- 1.4 Small-Signal Models of Bipolar Transistors 25
  - 1.4.1 Transconductance 26
  - 1.4.2 Base-Charging Capacitance 27
  - 1.4.3 Input Resistance 28
  - 1.4.4 Output Resistance 29
  - 1.4.5 Basic Small-Signal Model of the Bipolar Transistor 30
  - 1.4.6 Collector-Base Resistance 30
  - 1.4.7 Parasitic Elements in the Small-Signal Model 31
  - 1.4.8 Specification of Transistor Frequency Response 34
- 1.5 Large-Signal Behavior of Metal-Oxide-Semiconductor Field-Effect Transistors 38
  - 1.5.1 Transfer Characteristics of MOS Devices 38
  - 1.5.2 Comparison of Operating Regions of Bipolar and MOS Transistors 45
  - 1.5.3 Decomposition of Gate-Source Voltage 47
  - 1.5.4 Threshold Temperature Dependence 47
  - 1.5.5 MOS Device Voltage Limitations 48
- 1.6 Small-Signal Models of MOS Transistors 49
  - 1.6.1 Transconductance 50
  - 1.6.2 Intrinsic Gate-Source and Gate-Drain Capacitance 51
  - 1.6.3 Input Resistance 52
  - 1.6.4 Output Resistance 52
  - 1.6.5 Basic Small-Signal Model of the MOS Transistor 52
  - 1.6.6 Body Transconductance 53
  - 1.6.7 Parasitic Elements in the Small-Signal Model 54
  - 1.6.8 MOS Transistor Frequency Response 55
- 1.7 Short-Channel Effects in MOS Transistors 59
  - 1.7.1 Velocity Saturation from the Horizontal Field 59
  - 1.7.2 Transconductance and Transition Frequency 63
  - 1.7.3 Mobility Degradation from the Vertical Field 65
- 1.8 Weak Inversion in MOS Transistors 65
  - 1.8.1 Drain Current in Weak Inversion 66
  - 1.8.2 Transconductance and Transition Frequency in Weak Inversion 69
- 1.9 Substrate Current Flow in MOS Transistors 71
  - A.1.1 Summary of Active-Device Parameters 73

## CHAPTER 2 Bipolar, MOS, and BiCMOS Integrated-Circuit Technology 78

- 2.1 Introduction 78
- 2.2 Basic Processes in Integrated-Circuit Fabrication 79
  - 2.2.1 Electrical Resistivity of Silicon 79
  - 2.2.2 Solid-State Diffusion 80
  - 2.2.3 Electrical Properties of Diffused Layers 82
  - 2.2.4 Photolithography 84
  - 2.2.5 Epitaxial Growth 86
  - 2.2.6 Ion Implantation 87
  - 2.2.7 Local Oxidation 87
  - 2.2.8 Polysilicon Deposition 87
- 2.3 High-Voltage Bipolar Integrated-Circuit Fabrication 88
- 2.4 Advanced Bipolar Integrated-Circuit Fabrication 92
- 2.5 Active Devices in Bipolar Analog Integrated Circuits 95
  - 2.5.1 Integrated-Circuit *npn* Transistors 96
  - 2.5.2 Integrated-Circuit *pnp* Transistors 107
- 2.6 Passive Components in Bipolar Integrated Circuits 115
  - 2.6.1 Diffused Resistors 115
  - 2.6.2 Epitaxial and Epitaxial Pinch Resistors 119
  - 2.6.3 Integrated-Circuit Capacitors 120
  - 2.6.4 Zener Diodes 121
  - 2.6.5 Junction Diodes 122
- 2.7 Modifications to the Basic Bipolar Process 123
  - 2.7.1 Dielectric Isolation 123
  - 2.7.2 Compatible Processing for High-Performance Active Devices 124
  - 2.7.3 High-Performance Passive Components 127
- 2.8 MOS Integrated-Circuit Fabrication 127

- 2.9 Active Devices in MOS Integrated Circuits 131
  - 2.9.1 *n*-Channel Transistors 131
  - 2.9.2 *p*-Channel Transistors 144
  - 2.9.3 Depletion Devices 144
  - 2.9.4 Bipolar Transistors 145
- 2.10 Passive Components in MOS Technology 146
  - 2.10.1 Resistors 146
  - 2.10.2 Capacitors in MOS Technology 148
  - 2.10.3 Latchup in CMOS Technology 151
- 2.11 BiCMOS Technology 152
- 2.12 Heterojunction Bipolar Transistors 153
- 2.13 Interconnect Delay 156
- 2.14 Economics of Integrated-Circuit Fabrication 156
  - 2.14.1 Yield Considerations in Integrated-Circuit Fabrication 157
  - 2.14.2 Cost Considerations in Integrated-Circuit Fabrication 159
- A.2.1 SPICE Model-Parameter Files 162

## CHAPTER 3 Single-Transistor and Multiple-Transistor Amplifiers 169

- 3.1 Device Model Selection for Approximate Analysis of Analog Circuits 170
- 3.2 Two-Port Modeling of Amplifiers 171
- 3.3 Basic Single-Transistor Amplifier Stages 173
  - 3.3.1 Common-Emitter Configuration 174
  - 3.3.2 Common-Source Configuration 178
  - 3.3.3 Common-Base Configuration 182
  - 3.3.4 Common-Gate Configuration 185
  - 3.3.5 Common-Base and Common-Gate Configurations with Finite  $r_o$  187
    - 3.3.5.1 Common-Base and Common-Gate Input Resistance 187
    - 3.3.5.2 Common-Base and Common-Gate Output Resistance 189

3.3.6	Common-Collector Configuration (Emitter Follower)	191	3.5.6.8	Offset Voltage Drift in the Source-Coupled Pair	236
3.3.7	Common-Drain Configuration (Source Follower)	194	3.5.6.9	Small-Signal Characteristics of Unbalanced Differential Amplifiers	237
3.3.8	Common-Emitter Amplifier with Emitter Degeneration	196			
3.3.9	Common-Source Amplifier with Source Degeneration	199	A.3.1	Elementary Statistics and the Gaussian Distribution	244
3.4	Multiple-Transistor Amplifier Stages	201			
3.4.1	The CC-CE, CC-CC, and Darlington Configurations	201	<b>CHAPTER 4</b>		
3.4.2	The Cascode Configuration	205	<b>Current Mirrors, Active Loads, and References</b>	251	
3.4.2.1	The Bipolar Cascode	205	4.1	Introduction	251
3.4.2.2	The MOS Cascode	207	4.2	Current Mirrors	251
3.4.3	The Active Cascode	210	4.2.1	General Properties	251
3.4.4	The Super Source Follower	212	4.2.2	Simple Current Mirror	253
3.5	Differential Pairs	214	4.2.2.1	Bipolar	253
3.5.1	The dc Transfer Characteristic of an Emitter-Coupled Pair	214	4.2.2.2	MOS	255
3.5.2	The dc Transfer Characteristic with Emitter Degeneration	216	4.2.3	Simple Current Mirror with Beta Helper	258
3.5.3	The dc Transfer Characteristic of a Source-Coupled Pair	217	4.2.3.1	Bipolar	258
3.5.4	Introduction to the Small-Signal Analysis of Differential Amplifiers	220	4.2.3.2	MOS	260
3.5.5	Small-Signal Characteristics of Balanced Differential Amplifiers	223	4.2.4	Simple Current Mirror with Degeneration	260
3.5.6	Device Mismatch Effects in Differential Amplifiers	229	4.2.4.1	Bipolar	260
3.5.6.1	Input Offset Voltage and Current	230	4.2.4.2	MOS	261
3.5.6.2	Input Offset Voltage of the Emitter-Coupled Pair	230	4.2.5	Cascode Current Mirror	261
3.5.6.3	Offset Voltage of the Emitter-Coupled Pair: Approximate Analysis	231	4.2.5.1	Bipolar	261
3.5.6.4	Offset Voltage Drift in the Emitter-Coupled Pair	233	4.2.5.2	MOS	264
3.5.6.5	Input Offset Current of the Emitter-Coupled Pair	233	4.2.6	Wilson Current Mirror	272
3.5.6.6	Input Offset Voltage of the Source-Coupled Pair	234	4.2.6.1	Bipolar	272
3.5.6.7	Offset Voltage of the Source-Coupled Pair: Approximate Analysis	235	4.2.6.2	MOS	275
			4.3	Active Loads	276
			4.3.1	Motivation	276
			4.3.2	Common-Emitter–Common-Source Amplifier with Complementary Load	277
			4.3.3	Common-Emitter–Common-Source Amplifier with Depletion Load	280
			4.3.4	Common-Emitter–Common-Source Amplifier with Diode-Connected Load	282
			4.3.5	Differential Pair with Current-Mirror Load	285
			4.3.5.1	Large-Signal Analysis	285
			4.3.5.2	Small-Signal Analysis	286
			4.3.5.3	Common-Mode Rejection Ratio	291

4.4 Voltage and Current References 297

4.4.1 Low-Current Biasing 297

4.4.1.1 Bipolar Widlar Current Source 297

4.4.1.2 MOS Widlar Current Source 300

4.4.1.3 Bipolar Peaking Current Source 301

4.4.1.4 MOS Peaking Current Source 302

4.4.2 Supply-Insensitive Biasing 303

4.4.2.1 Widlar Current Sources 304

4.4.2.2 Current Sources Using Other Voltage Standards 305

4.4.2.3 Self-Biasing 307

4.4.3 Temperature-Insensitive Biasing 315

4.4.3.1 Band-Gap-Referenced Bias Circuits in Bipolar Technology 315

4.4.3.2 Band-Gap-Referenced Bias Circuits in CMOS Technology 321

A.4.1 Matching Considerations in Current Mirrors 325

A.4.1.1 Bipolar 325

A.4.1.2 MOS 328

A.4.2 Input Offset Voltage of Differential Pair with Active Load 330

A.4.2.1 Bipolar 330

A.4.2.2 MOS 332

**CHAPTER 5**  
**Output Stages 341**

5.1 Introduction 341

5.2 The Emitter Follower as an Output Stage 341

5.2.1 Transfer Characteristics of the Emitter-Follower 341

5.2.2 Power Output and Efficiency 344

5.2.3 Emitter-Follower Drive Requirements 351

5.2.4 Small-Signal Properties of the Emitter Follower 352

5.3 The Source Follower as an Output Stage 353

5.3.1 Transfer Characteristics of the Source Follower 353

5.3.2 Distortion in the Source Follower 355

5.4 Class B Push-Pull Output Stage 359

5.4.1 Transfer Characteristic of the Class B Stage 360

5.4.2 Power Output and Efficiency of the Class B Stage 362

5.4.3 Practical Realizations of Class B Complementary Output Stages 366

5.4.4 All-*npn* Class B Output Stage 373

5.4.5 Quasi-Complementary Output Stages 376

5.4.6 Overload Protection 377

5.5 CMOS Class AB Output Stages 379

5.5.1 Common-Drain Configuration 380

5.5.2 Common-Source Configuration with Error Amplifiers 381

5.5.3 Alternative Configurations 388

5.5.3.1 Combined Common-Drain Common-Source Configuration 388

5.5.3.2 Combined Common-Drain Common-Source Configuration with High Swing 390

5.5.3.3 Parallel Common-Source Configuration 390

**CHAPTER 6**  
**Operational Amplifiers with Single-Ended Outputs 400**

6.1 Applications of Operational Amplifiers 401

6.1.1 Basic Feedback Concepts 401

6.1.2 Inverting Amplifier 402

6.1.3 Noninverting Amplifier 404

6.1.4 Differential Amplifier 404

6.1.5 Nonlinear Analog Operations 405

6.1.6 Integrator, Differentiator 406

6.1.7 Internal Amplifiers 407

6.1.7.1 Switched-Capacitor Amplifier 407

6.1.7.2 Switched-Capacitor Integrator 412

- 6.2 Deviations from Ideality in Real Operational Amplifiers 415
    - 6.2.1 Input Bias Current 415
    - 6.2.2 Input Offset Current 416
    - 6.2.3 Input Offset Voltage 416
    - 6.2.4 Common-Mode Input Range 416
    - 6.2.5 Common-Mode Rejection Ratio (CMRR) 417
    - 6.2.6 Power-Supply Rejection Ratio (PSRR) 418
    - 6.2.7 Input Resistance 420
    - 6.2.8 Output Resistance 420
    - 6.2.9 Frequency Response 420
    - 6.2.10 Operational-Amplifier Equivalent Circuit 420
  - 6.3 Basic Two-Stage MOS Operational Amplifiers 421
    - 6.3.1 Input Resistance, Output Resistance, and Open-Circuit Voltage Gain 422
    - 6.3.2 Output Swing 423
    - 6.3.3 Input Offset Voltage 424
    - 6.3.4 Common-Mode Rejection Ratio 427
    - 6.3.5 Common-Mode Input Range 427
    - 6.3.6 Power-Supply Rejection Ratio (PSRR) 430
    - 6.3.7 Effect of Overdrive Voltages 434
    - 6.3.8 Layout Considerations 435
  - 6.4 Two-Stage MOS Operational Amplifiers with Cascodes 438
  - 6.5 MOS Telescopic-Cascode Operational Amplifiers 439
  - 6.6 MOS Folded-Cascode Operational Amplifiers 442
  - 6.7 MOS Active-Cascode Operational Amplifiers 446
  - 6.8 Bipolar Operational Amplifiers 448
    - 6.8.1 The dc Analysis of the NE5234 Operational Amplifier 452
    - 6.8.2 Transistors that Are Normally Off 467
    - 6.8.3 Small-Signal Analysis of the NE5234 Operational Amplifier 469
    - 6.8.4 Calculation of the Input Offset Voltage and Current of the NE5234 477
- CHAPTER 7**
  - Frequency Response of Integrated Circuits 490**
    - 7.1 Introduction 490
    - 7.2 Single-Stage Amplifiers 490
      - 7.2.1 Single-Stage Voltage Amplifiers and the Miller Effect 490
        - 7.2.1.1 The Bipolar Differential Amplifier: Differential-Mode Gain 495
        - 7.2.1.2 The MOS Differential Amplifier: Differential-Mode Gain 499
      - 7.2.2 Frequency Response of the Common-Mode Gain for a Differential Amplifier 501
      - 7.2.3 Frequency Response of Voltage Buffers 503
        - 7.2.3.1 Frequency Response of the Emitter Follower 505
        - 7.2.3.2 Frequency Response of the Source Follower 511
      - 7.2.4 Frequency Response of Current Buffers 514
        - 7.2.4.1 Common-Base Amplifier Frequency Response 516
        - 7.2.4.2 Common-Gate Amplifier Frequency Response 517
    - 7.3 Multistage Amplifier Frequency Response 518
      - 7.3.1 Dominant-Pole Approximation 518
      - 7.3.2 Zero-Value Time Constant Analysis 519
      - 7.3.3 Cascode Voltage-Amplifier Frequency Response 524
      - 7.3.4 Cascode Frequency Response 527
      - 7.3.5 Frequency Response of a Current Mirror Loading a Differential Pair 534
      - 7.3.6 Short-Circuit Time Constants 536
    - 7.4 Analysis of the Frequency Response of the NE5234 Op Amp 539
      - 7.4.1 High-Frequency Equivalent Circuit of the NE5234 539
      - 7.4.2 Calculation of the  $-3$ -dB Frequency of the NE5234 540
      - 7.4.3 Nondominant Poles of the NE5234 542

7.5 Relation Between Frequency Response and Time Response 542

**CHAPTER 8  
Feedback 553**

8.1 Ideal Feedback Equation 553

8.2 Gain Sensitivity 555

8.3 Effect of Negative Feedback on Distortion 555

8.4 Feedback Configurations 557

8.4.1 Series-Shunt Feedback 557

8.4.2 Shunt-Shunt Feedback 560

8.4.3 Shunt-Series Feedback 561

8.4.4 Series-Series Feedback 562

8.5 Practical Configurations and the Effect of Loading 563

8.5.1 Shunt-Shunt Feedback 563

8.5.2 Series-Series Feedback 569

8.5.3 Series-Shunt Feedback 579

8.5.4 Shunt-Series Feedback 583

8.5.5 Summary 587

8.6 Single-Stage Feedback 587

8.6.1 Local Series-Series Feedback 587

8.6.2 Local Series-Shunt Feedback 591

8.7 The Voltage Regulator as a Feedback Circuit 593

8.8 Feedback Circuit Analysis Using Return Ratio 599

8.8.1 Closed-Loop Gain Using Return Ratio 601

8.8.2 Closed-Loop Impedance Formula Using Return Ratio 607

8.8.3 Summary—Return-Ratio Analysis 612

8.9 Modeling Input and Output Ports in Feedback Circuits 613

**CHAPTER 9  
Frequency Response and Stability of Feedback Amplifiers 624**

9.1 Introduction 624

9.2 Relation Between Gain and Bandwidth in Feedback Amplifiers 624

9.3 Instability and the Nyquist Criterion 626

9.4 Compensation 633

9.4.1 Theory of Compensation 633

9.4.2 Methods of Compensation 637

9.4.3 Two-Stage MOS Amplifier Compensation 643

9.4.4 Compensation of Single-Stage CMOS Op Amps 650

9.4.5 Nested Miller Compensation 654

9.5 Root-Locus Techniques 664

9.5.1 Root Locus for a Three-Pole Transfer Function 665

9.5.2 Rules for Root-Locus Construction 667

9.5.3 Root Locus for Dominant-Pole Compensation 676

9.5.4 Root Locus for Feedback-Zero Compensation 677

9.6 Slew Rate 681

9.6.1 Origin of Slew-Rate Limitations 681

9.6.2 Methods of Improving Slew-Rate in Two-Stage Op Amps 685

9.6.3 Improving Slew-Rate in Bipolar Op Amps 687

9.6.4 Improving Slew-Rate in MOS Op Amps 688

9.6.5 Effect of Slew-Rate Limitations on Large-Signal Sinusoidal Performance 692

A.9.1 Analysis in Terms of Return-Ratio Parameters 693

A.9.2 Roots of a Quadratic Equation 694

**CHAPTER 10  
Nonlinear Analog Circuits 704**

10.1 Introduction 704

10.2 Analog Multipliers Employing the Bipolar Transistor 704

10.2.1 The Emitter-Coupled Pair as a Simple Multiplier 704

10.2.2 The dc Analysis of the Gilbert Multiplier Cell 706

- 10.2.3 The Gilbert Cell as an Analog Multiplier 708
  - 10.2.4 A Complete Analog Multiplier 711
  - 10.2.5 The Gilbert Multiplier Cell as a Balanced Modulator and Phase Detector 712
  - 10.3 Phase-Locked Loops (PLL) 716
    - 10.3.1 Phase-Locked Loop Concepts 716
    - 10.3.2 The Phase-Locked Loop in the Locked Condition 718
    - 10.3.3 Integrated-Circuit Phase-Locked Loops 727
  - 10.4 Nonlinear Function Synthesis 731
- CHAPTER 11**  
**Noise in Integrated Circuits 736**
- 11.1 Introduction 736
  - 11.2 Sources of Noise 736
    - 11.2.1 Shot Noise 736
    - 11.2.2 Thermal Noise 740
    - 11.2.3 Flicker Noise ( $1/f$  Noise) 741
    - 11.2.4 Burst Noise (*Popcorn Noise*) 742
    - 11.2.5 Avalanche Noise 743
  - 11.3 Noise Models of Integrated-Circuit Components 744
    - 11.3.1 Junction Diode 744
    - 11.3.2 Bipolar Transistor 745
    - 11.3.3 MOS Transistor 746
    - 11.3.4 Resistors 747
    - 11.3.5 Capacitors and Inductors 747
  - 11.4 Circuit Noise Calculations 748
    - 11.4.1 Bipolar Transistor Noise Performance 750
    - 11.4.2 Equivalent Input Noise and the Minimum Detectable Signal 754
  - 11.5 Equivalent Input Noise Generators 756
    - 11.5.1 Bipolar Transistor Noise Generators 757
    - 11.5.2 MOS Transistor Noise Generators 762
  - 11.6 Effect of Feedback on Noise Performance 764
    - 11.6.1 Effect of Ideal Feedback on Noise Performance 764
    - 11.6.2 Effect of Practical Feedback on Noise Performance 765
  - 11.7 Noise Performance of Other Transistor Configurations 771
    - 11.7.1 Common-Base Stage Noise Performance 771
    - 11.7.2 Emitter-Follower Noise Performance 773
    - 11.7.3 Differential-Pair Noise Performance 773
  - 11.8 Noise in Operational Amplifiers 776
  - 11.9 Noise Bandwidth 782
  - 11.10 Noise Figure and Noise Temperature 786
    - 11.10.1 Noise Figure 786
    - 11.10.2 Noise Temperature 790
- CHAPTER 12**  
**Fully Differential Operational Amplifiers 796**
- 12.1 Introduction 796
  - 12.2 Properties of Fully Differential Amplifiers 796
  - 12.3 Small-Signal Models for Balanced Differential Amplifiers 799
  - 12.4 Common-Mode Feedback 804
    - 12.4.1 Common-Mode Feedback at Low Frequencies 805
    - 12.4.2 Stability and Compensation Considerations in a CMFB Loop 810
  - 12.5 CMFB Circuits 811
    - 12.5.1 CMFB Using Resistive Divider and Amplifier 812
    - 12.5.2 CMFB Using Two Differential Pairs 816
    - 12.5.3 CMFB Using Transistors in the Triode Region 819
    - 12.5.4 Switched-Capacitor CMFB 821
  - 12.6 Fully Differential Op Amps 823
    - 12.6.1 A Fully Differential Two-Stage Op Amp 823
    - 12.6.2 Fully Differential Telescopic Cascode Op Amp 833

12.6.3 Fully Differential Folded-Cascode Op Amp	834	12.9 Analysis of a CMOS Fully Differential Folded-Cascode Op Amp	845
12.6.4 A Differential Op Amp with Two Differential Input Stages	835	12.9.1 DC Biasing	848
12.6.5 Neutralization	835	12.9.2 Low-Frequency Analysis	850
12.7 Unbalanced Fully Differential Circuits	838	12.9.3 Frequency and Time Responses in a Feedback Application	856
12.8 Bandwidth of the CMFB Loop	844	<b>Index</b>	871

### Symbol Convention

Unless otherwise stated, the following symbol convention is used in this book. *Bias* or *dc* quantities, such as transistor collector current  $I_C$  and collector-emitter voltage  $V_{CE}$ , are represented by uppercase symbols with uppercase subscripts. Small-signal quantities, such as the incremental change in transistor collector current  $i_c$ , are represented by lowercase symbols with lowercase subscripts. Elements such as transconductance  $g_m$  in small-signal equivalent circuits are represented in the same way. Finally, quantities such as *total* collector current  $I_c$ , which represent the sum of the bias quantity *and* the signal quantity, are represented by an uppercase symbol with a lowercase subscript.

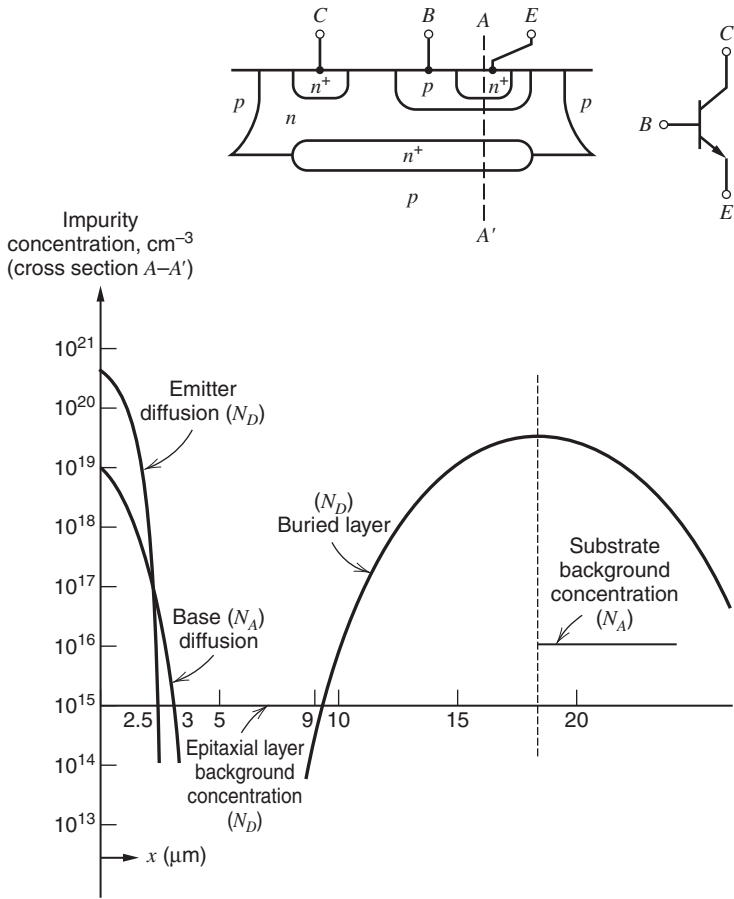


**Figure 2.17** Typical impurity concentration for a monolithic *npn* transistor in a high-voltage, deep-diffused process.

## 2.4 Advanced Bipolar Integrated-Circuit Fabrication

A large fraction of bipolar analog integrated circuits currently manufactured uses the basic technology described in the previous section, or variations thereof. The fabrication sequence is relatively simple and low in cost. However, many of the circuit applications of commercial importance have demanded steadily increasing frequency response capability, which translates directly to a need for transistors of higher frequency-response capability in the technology. The higher speed requirement dictates a device structure with thinner base width to reduce base transit time and smaller dimensions overall to reduce parasitic capacitances. The smaller device dimensions require that the width of the junction depletion layers within the structure be reduced in proportion, which in turn requires the use of lower circuit operating voltages and higher impurity concentrations in the device structure. To meet this need, a class of bipolar fabrication technologies has evolved that, compared to the high-voltage process sequence described in the last section, use much thinner and more heavily doped epitaxial layers, selectively oxidized regions for isolation instead of diffused junctions, and a polysilicon layer as the source of dopant for the emitter. Because of the growing importance of this class of bipolar process, the sequence for such a process is described in this section.

The starting point for the process is similar to that for the conventional process, with a mask and implant step resulting in the formation of a heavily-doped  $n^+$  buried layer in a  $p$ -type

# Current Mirrors, Active Loads, and References

## 4.1 Introduction

Current mirrors made by using active devices have come to be widely used in analog integrated circuits both as biasing elements and as load devices for amplifier stages. The use of current mirrors in biasing can result in superior insensitivity of circuit performance to variations in power supply and temperature. Current mirrors are frequently more economical than resistors in terms of the die area required to provide bias current of a certain value, particularly when the required value of bias current is small. When used as a load element in transistor amplifiers, the high incremental resistance of the current mirror results in high voltage gain at low power-supply voltages.

The first section of this chapter describes the general properties of current mirrors and compares various bipolar and MOS mirrors to each other using these properties. The next section deals with the use of current mirrors as load elements in amplifier stages. The last section shows how current mirrors are used to construct references that are insensitive to variations in supply and temperature. Finally, the appendix analyzes the effects of device mismatch.

## 4.2 Current Mirrors

### 4.2.1 General Properties

A current mirror is an element with at least three terminals, as shown in Fig. 4.1. The common terminal is connected to a power supply, and the input current source is connected to the input terminal. Ideally, the output current is equal to the input current multiplied by a desired current gain. If the gain is unity, the input current is reflected to the output, leading to the name *current mirror*. Under ideal conditions, the current-mirror gain is independent of input frequency, and the output current is independent of the voltage between the output and common terminals. Furthermore, the voltage between the input and common terminals is ideally zero because this condition allows the entire supply voltage to appear across the input current source, simplifying its transistor-level design. More than one input and/or output terminals are sometimes used.

In practice, real transistor-level current mirrors suffer many deviations from this ideal behavior. For example, the gain of a real current mirror is never independent of the input frequency. The topic of frequency response is covered in Chapter 7, and mainly dc and low-frequency ac signals are considered in the rest of this chapter. Deviations from ideality that will be considered in this chapter are listed below.

1. One of the most important deviations from ideality is the variation of the current-mirror output current with changes in voltage at the output terminal. This effect is characterized

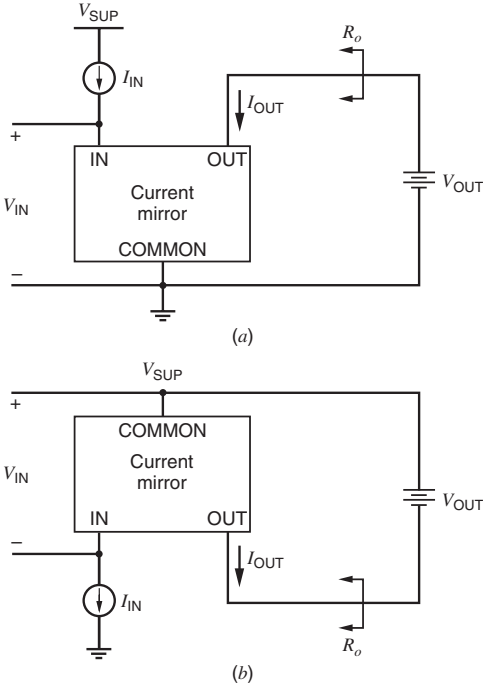


**Figure 4.1** Current-mirror block diagrams referenced to (a) ground and (b) the positive supply.

by the small-signal output resistance,  $R_o$ , of the current mirror. A Norton-equivalent model of the output of the current mirror includes  $R_o$  in parallel with a current source controlled by the input current. The output resistance directly affects the performance of many circuits that use current mirrors. For example, the common-mode rejection ratio of the differential amplifier depends directly on this resistance, as does the gain of the active-load circuits. Increasing the output resistance reduces the dependence of the output current on the output voltage and is therefore desirable. Generally speaking, the output resistance increases in practical circuits when the output current decreases. Unfortunately, decreasing the output current also decreases the maximum operating speed. Therefore, when comparing the output resistance of two current mirrors, they should be compared at identical output currents.

2. Another important error source is the gain error, which is the deviation of the gain of a current mirror from its ideal value. The gain error is separated into two parts: (1) the systematic gain error and (2) the random gain error. The systematic gain error,  $\epsilon$ , is the gain error that arises even when all matched elements in the mirror are perfectly matched and will be calculated for each of the current mirrors presented in this section. The random gain error is the gain error caused by unintended mismatches between matched elements.
3. When the input current source is connected to the input terminal of a real current mirror, it creates a positive voltage drop,  $V_{IN}$ , that reduces the voltage available across the input current source. Minimizing  $V_{IN}$  is important because it simplifies the design of the input current source, especially in low-supply applications. To reduce  $V_{IN}$ , current mirrors sometimes have more than one input terminal. In that case, we will calculate an input voltage for each input terminal. An example is the MOS high-swing cascode current mirror considered in Section 4.2.5.

4. A positive output voltage,  $V_{OUT}$ , is required in practice to make the output current depend mainly on the input current. This characteristic is summarized by the minimum voltage across the output branch,  $V_{OUT(\min)}$ , that allows the output device(s) to operate in the active region. Minimizing  $V_{OUT(\min)}$  maximizes the range of output voltages for which the current-mirror output resistance is almost constant, which is important in applications where current mirrors are used as active loads in amplifiers (especially with low power-supply voltages). This topic is covered in Section 4.3. When current mirrors have more than one output terminal, each output must be biased above its  $V_{OUT(\min)}$  to make the corresponding output current depend mainly on the input current.

In later sections, the performance of various current mirrors will be compared to each other through these four parameters:  $R_o$ ,  $\epsilon$ ,  $V_{IN}$ , and  $V_{OUT(\min)}$ .

## 4.2.2 Simple Current Mirror

### 4.2.2.1 Bipolar

The simplest form of a current mirror consists of two transistors. Fig. 4.2 shows a bipolar version of this mirror. Transistor  $Q_1$  is diode connected, forcing its collector-base voltage to zero. In this mode, the collector-base junction is off in the sense that no injection takes place there, and  $Q_1$  operates in the forward-active region. Assume that  $Q_2$  also operates in the forward-active region and that both transistors have infinite output resistance. Then  $I_{OUT}$  is controlled by  $V_{BE2}$ , which is equal to  $V_{BE1}$  by KVL. A KVL equation is at the heart of the operation of all current mirrors. Neglecting junction leakage currents,

$$V_{BE2} = V_T \ln \frac{I_{C2}}{I_{S2}} = V_{BE1} = V_T \ln \frac{I_{C1}}{I_{S1}} \quad (4.1)$$

where  $V_T = kT/q$  is the thermal voltage and  $I_{S1}$  and  $I_{S2}$  are the transistor saturation currents. From (4.1),

$$I_{C2} = \frac{I_{S2}}{I_{S1}} I_{C1} \quad (4.2)$$

If the transistors are identical,  $I_{S1} = I_{S2}$  and (4.2) shows that the current flowing in the collector of  $Q_1$  is mirrored to the collector of  $Q_2$ . KCL at the collector of  $Q_1$  yields

$$I_{IN} - I_{C1} - \frac{I_{C1}}{\beta_F} - \frac{I_{C2}}{\beta_F} = 0 \quad (4.3)$$

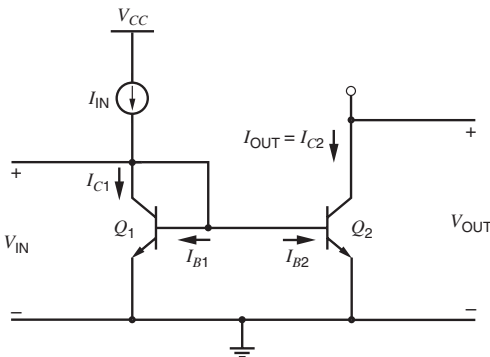


**Figure 4.2** A simple bipolar current mirror.

Therefore, with identical transistors,

$$I_{OUT} = I_{C2} = I_{C1} = \frac{I_{IN}}{1 + \frac{2}{\beta_F}} \tag{4.4}$$

If  $\beta_F$  is large, the base currents are small and

$$I_{OUT} = I_{C1} \simeq I_{IN} \tag{4.5}$$

Thus for identical devices  $Q_1$  and  $Q_2$ , the gain of the current mirror is approximately unity. This result holds for both dc and low-frequency ac currents. Above the 3-dB frequency of the mirror, however, the base current increases noticeably because the impedance of the base-emitter capacitance decreases, reducing the gain of the current mirror. Frequency response is discussed in Chapter 7. The rest of this section considers dc currents only.

In practice, the devices need not be identical. Then from (4.2) and (4.3),

$$I_{OUT} = \frac{I_{S2}}{I_{S1}} I_{C1} = \left( \frac{I_{S2}}{I_{S1}} I_{IN} \right) \left( \frac{1}{1 + \frac{1 + (I_{S2}/I_{S1})}{\beta_F}} \right) \tag{4.6}$$

When  $I_{S2} = I_{S1}$ , (4.6) is the same as (4.4). Since the saturation current of a bipolar transistor is proportional to its emitter area, the first term in (4.6) shows that the gain of the current mirror can be larger or smaller than unity because the emitter areas can be ratioed. If the desired current-mirror gain is a rational number,  $M/N$ , the area ratio is usually set by connecting  $M$  identical devices called *units* in parallel to form  $Q_2$  and  $N$  units in parallel to form  $Q_1$  to minimize mismatch arising from lithographic effects in forming the emitter regions. However, area ratios greater than about five to one consume a large die area dominated by the area of the larger of the two devices. Thus other methods described in later sections are preferred for the generation of large current ratios. The last term in (4.6) accounts for error introduced by finite  $\beta_F$ . Increasing  $I_{S2}/I_{S1}$  increases the magnitude of this error by increasing the base current of  $Q_2$  compared to that of  $Q_1$ .

In writing (4.1) and (4.2), we assumed that the collector currents of the transistors are independent of their collector-emitter voltages. If a transistor is biased in the forward-active region, its collector current actually increases slowly with increasing collector-emitter voltage. Fig. 4.3 shows an output characteristic for  $Q_2$ . The output resistance of the current mirror at any given operating point is the reciprocal of the slope of the output characteristic at that point. In the forward-active region,

$$R_o = r_{o2} = \frac{V_A}{I_{C2}} \tag{4.7}$$

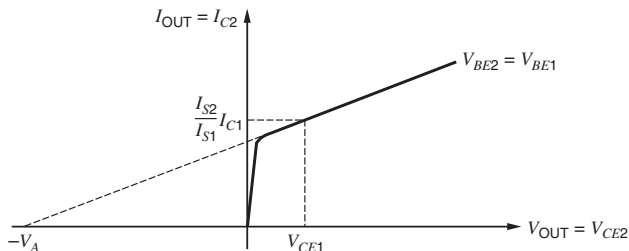


Figure 4.3 n-p-n output characteristic.

The point where  $V_{CE2} = V_{CE1}$  and  $V_{BE2} = V_{BE1}$  is labeled on the characteristic. Because the collector current is controlled by the base-emitter and collector-emitter voltages,  $I_{C2} = (I_{S2}/I_{S1})I_{C1}$  at this point. If the slope of the characteristic in saturation is constant, the variation in  $I_{C2}$  for changes in  $V_{CE2}$  can be predicted by a straight line that goes through the labeled point. As described in Chapter 1, extrapolation of the output characteristic in the forward-active region back to the  $V_{CE2}$  axis gives an intercept at  $-V_A$ , where  $V_A$  is the Early voltage. If  $V_A \gg V_{CE1}$ , the slope of the straight line is about equal to  $(I_{S2}/I_{S1})(I_{C1}/V_A)$ . Therefore,

$$I_{OUT} = \frac{I_{S2}}{I_{S1}} I_{C1} \left( 1 + \frac{V_{CE2} - V_{CE1}}{V_A} \right) = \frac{I_{S2}}{I_{S1}} I_{IN} \left( 1 + \frac{V_{CE2} - V_{CE1}}{V_A} \right) \frac{1}{1 + \frac{1 + (I_{S2}/I_{S1})}{\beta_F}} \quad (4.8)$$

Since the ideal gain of the current mirror is  $I_{S2}/I_{S1}$ , the systematic gain error,  $\epsilon$ , of the current mirror can be calculated from (4.8).

$$\epsilon = \left( \frac{1 + \frac{V_{CE2} - V_{CE1}}{V_A}}{1 + \frac{1 + (I_{S2}/I_{S1})}{\beta_F}} \right) - 1 \simeq \frac{V_{CE2} - V_{CE1}}{V_A} - \frac{1 + (I_{S2}/I_{S1})}{\beta_F} \quad (4.9)$$

The first term in (4.9) stems from finite output resistance and the second term from finite  $\beta_F$ . If  $V_{CE2} > V_{CE1}$ , the polarities of the two terms are opposite. Since the two terms are independent, however, cancellation is unlikely in practice. The first term dominates when the difference in the collector-emitter voltages and  $\beta_F$  are large. For example, with identical transistors and  $V_A = 130$  V, if the collector-emitter voltage of  $Q_1$  is held at  $V_{BE(\text{on})}$ , and if the collector-emitter voltage of  $Q_2$  is 30 V, then the systematic gain error  $(30 - 0.6)/130 - 2/200 \simeq 0.22$ . Thus for a circuit operating at a power-supply voltage of 30 V, the current-mirror currents can differ by more than 20 percent from those values calculated by assuming that the transistor output resistance and  $\beta_F$  are infinite. Although the first term in (4.9) stems from finite output resistance, it does not depend on  $r_{o2}$  directly but instead on the collector-emitter and Early voltages. The Early voltage is independent of the bias current, and

$$V_{IN} = V_{CE1} = V_{BE1} = V_{BE(\text{on})} \quad (4.10)$$

Since  $V_{BE(\text{on})}$  is proportional to the natural logarithm of the collector current,  $V_{IN}$  changes little with changes in bias current. Therefore, changing the bias current in a current mirror changes systematic gain error mainly through changes in  $V_{CE2}$ .

Finally, the minimum output voltage required to keep  $Q_2$  in the forward-active region is

$$V_{OUT(\text{min})} = V_{CE2(\text{sat})} \quad (4.11)$$

#### 4.2.2.2 MOS

Figure 4.4 shows an MOS version of the simple current mirror. The drain-gate voltage of  $M_1$  is zero; therefore, the channel does not exist at the drain, and the transistor operates in the saturation or active region if the threshold is positive. Although the principle of operation for MOS transistors does not involve forward biasing any diodes,  $M_1$  is said to be *diode connected* in an analogy to the bipolar case. Assume that  $M_2$  also operates in the active region and that both transistors have infinite output resistance. Then  $I_{D2}$  is controlled by  $V_{GS2}$ , which is equal to  $V_{GS1}$  by KVL. A KVL equation is at the heart of the operation of all current mirrors. As described in Section 1.5.3, the gate-source voltage of a given MOS transistor is usually

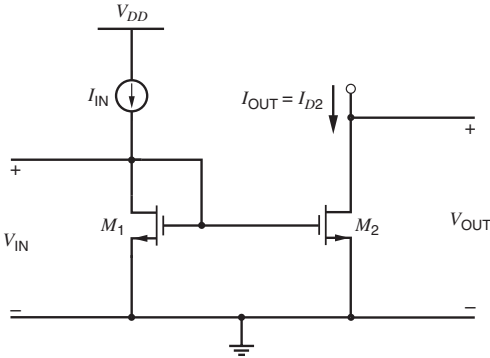


Figure 4.4 A simple MOS current mirror.

separated into two parts: the threshold  $V_t$  and the overdrive  $V_{ov}$ . Assuming square-law behavior as in (1.157), the overdrive for  $M_2$  is

$$V_{ov2} = V_{GS2} - V_t = \sqrt{\frac{2I_{D2}}{k'(W/L)_2}} \tag{4.12}$$

Since the transconductance parameter  $k'$  is proportional to mobility, and since mobility falls with increasing temperature, the overdrive rises with temperature. In contrast, Section 1.5.4 shows that the threshold falls with increasing temperature. From KVL and (1.157),

$$V_{GS2} = V_t + \sqrt{\frac{2I_{D2}}{k'(W/L)_2}} = V_{GS1} = V_t + \sqrt{\frac{2I_{D1}}{k'(W/L)_1}} \tag{4.13}$$

Equation 4.13 shows that the overdrive of  $M_2$  is equal to that of  $M_1$ .

$$V_{ov2} = V_{ov1} = V_{ov} \tag{4.14}$$

If the transistors are identical,  $(W/L)_2 = (W/L)_1$ , and therefore

$$I_{OUT} = I_{D2} = I_{D1} \tag{4.15}$$

Equation 4.15 shows that the current that flows in the drain of  $M_1$  is mirrored to the drain of  $M_2$ . Since  $\beta_F \rightarrow \infty$  for MOS transistors, (4.15) and KCL at the drain of  $M_1$  yield

$$I_{OUT} = I_{D1} = I_{IN} \tag{4.16}$$

Thus for identical devices operating in the active region with infinite output resistance, the gain of the current mirror is unity. This result holds when the gate currents are zero; that is, (4.16) is at least approximately correct for dc and low-frequency ac currents. As the input frequency increases, however, the gate currents of  $M_1$  and  $M_2$  increase because each transistor has a nonzero gate-source capacitance. The part of the input current that flows into the gate leads does not flow into the drain of  $M_1$  and is not mirrored to  $M_2$ ; therefore, the gain of the current mirror decreases as the frequency of the input current increases. The rest of this section considers dc currents only.

In practice, the devices need not be identical. Then from (4.13) and (4.16),

$$I_{OUT} = \frac{(W/L)_2}{(W/L)_1} I_{D1} = \frac{(W/L)_2}{(W/L)_1} I_{IN} \tag{4.17}$$

Equation 4.17 shows that the gain of the current mirror can be larger or smaller than unity because the transistor sizes can be ratioed. To ratio the transistor sizes, either the widths or the lengths can be made unequal in principle. In practice, however, the lengths of  $M_1$  and  $M_2$  are rarely made unequal. The lengths that enter into (4.17) are the effective channel lengths given by (2.35). Equation 2.35 shows that the effective channel length of a given transistor differs from its drawn length by offset terms stemming from the depletion region at the drain and lateral diffusion at the drain and source. Since the offset terms are independent of the drawn length, a ratio of two effective channel lengths is equal to the drawn ratio only if the drawn lengths are identical. As a result, a ratio of unequal channel lengths depends on process parameters that may not be well controlled in practice. Similarly, Section 2.9.1 shows that the effective width of a given transistor differs from the drawn width because of lateral oxidation resulting in a *bird's beak*. Therefore, a ratio of unequal channel widths will also be process dependent. In many applications, however, the shortest channel length allowed in a given technology is selected for most transistors to maximize speed and minimize area. In contrast, the drawn channel widths are usually many times larger than the minimum dimensions allowed in a given technology. Therefore, to minimize the effect of the offset terms when the current-mirror gain is designed to differ from unity, the widths are ratioed rather than the lengths in most practical cases. If the desired current-mirror gain is a rational number,  $M/N$ , the ratio is usually set by connecting  $M$  identical devices called *units* in parallel to form  $M_2$  and  $N$  units in parallel to form  $M_1$  to minimize mismatch arising from lithographic effects in forming the gate regions. As in the bipolar case, ratios greater than about five to one consume a large die area dominated by the area of the larger of the two devices. Thus other methods described in later sections are preferred for the generation of large current ratios.

In writing (4.13) and (4.15), we assumed that the drain currents of the transistors are independent of their drain-source voltages. If a transistor is biased in the active region, its drain current actually increases slowly with increasing drain-source voltage. Figure 4.5 shows an output characteristic for  $M_2$ . The output resistance of the current mirror at any given operating point is the reciprocal of the slope of the output characteristic at that point. In the active region,

$$R_o = r_{o2} = \frac{V_A}{I_{D2}} = \frac{1}{\lambda I_{D2}} \quad (4.18)$$

The point where  $V_{DS2} = V_{DS1}$  and  $V_{GS2} = V_{GS1}$  is labeled on the characteristic. Because the drain current is controlled by the gate-source and drain-source voltages,  $I_{D2} = [(W/L)_2/(W/L)_1]I_{D1}$  at this point. If the slope of the characteristic in saturation is constant, the variation in  $I_{D2}$  for changes in  $V_{DS2}$  can be predicted by a straight line that goes through the

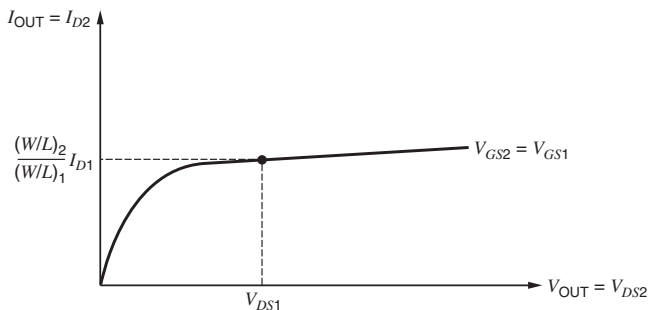


Figure 4.5 Output characteristic of simple MOS current mirror.

labeled point. As described in Chapter 1, extrapolation of the output characteristic in the active region back to the  $V_{DS2}$  axis gives an intercept at  $-V_A = -1/\lambda$ , where  $V_A$  is the Early voltage. If  $V_A \gg V_{DS1}$ , the slope of the straight line is about equal to  $[(W/L)_2/(W/L)_1][I_{D1}/V_A]$ . Therefore,

$$I_{OUT} = \frac{(W/L)_2}{(W/L)_1} I_{IN} \left( 1 + \frac{V_{DS2} - V_{DS1}}{V_A} \right) \tag{4.19}$$

Since the ideal gain of the current mirror is  $(W/L)_2/(W/L)_1$ , the systematic gain error,  $\epsilon$ , of the current mirror can be calculated from (4.19).

$$\epsilon = \frac{V_{DS2} - V_{DS1}}{V_A} \tag{4.20}$$

For example, if the drain-source voltage of  $M_1$  is held at 1.2 V, and if the drain-source voltage of  $M_2$  is 5 V, then the systematic gain error is  $(5 - 1.2)/10 \simeq 0.38$  with  $V_A = 10$  V. Thus for a circuit operating at a power-supply voltage of 5 V, the current-mirror currents can differ by more than 35 percent from those values calculated by assuming that the transistor output resistance is infinite. Although  $\epsilon$  stems from finite output resistance, it does not depend on  $r_{o2}$  directly but instead on the drain-source and Early voltages. Since the Early voltage is independent of the bias current, this observation shows that changing the input bias current in a current mirror changes systematic gain error mainly through changes to the drain-source voltages.

For the simple MOS current mirror, the input voltage is

$$V_{IN} = V_{GS1} = V_t + V_{ov1} = V_t + V_{ov} \tag{4.21}$$

With square-law behavior, the overdrive in (4.21) is proportional to the square root of the input current. In contrast, (4.10) shows that the entire  $V_{IN}$  in a simple bipolar mirror is proportional to the natural logarithm of the input current. Therefore, for a given change in the input current, the variation in  $V_{IN}$  in a simple MOS current mirror is generally larger than in its bipolar counterpart.

Finally, the minimum output voltage required to keep  $M_2$  in the active region is

$$V_{OUT(\min)} = V_{ov2} = V_{ov} = \sqrt{\frac{2I_{OUT}}{k'(W/L)_2}} \tag{4.22}$$

Equation 4.22 predicts that  $V_{OUT(\min)}$  depends on the transistor geometry and can be made arbitrarily small in a simple MOS mirror, unlike in the bipolar case. However, if the overdrive predicted by (4.22) is less than  $2nV_T$ , where  $n$  is defined in (1.247) and  $V_T$  is a thermal voltage, the result is invalid except to indicate that the transistors operate in weak inversion. At room temperature with  $n = 1.5$ ,  $2nV_T \simeq 78$  mV. If the transistors operate in weak inversion,

$$V_{OUT(\min)} \simeq 3V_T \tag{4.23}$$

as shown in Fig. 1.43.<sup>1</sup>

## 4.2.3 Simple Current Mirror with Beta Helper

### 4.2.3.1 Bipolar

In addition to the variation in output current due to finite output resistance, the second term in (4.9) shows that the collector current  $I_{C2}$  differs from the input current because of finite  $\beta_F$ . To reduce this source of error, an additional transistor can be added, as shown in Fig. 4.6. If  $Q_1$  and  $Q_3$  are identical, the emitter current of transistor  $Q_2$  is

$$I_{E2} = -\frac{I_{C1}}{\beta_F} - \frac{I_{C3}}{\beta_F} = -\frac{2}{\beta_F} I_{C1} \tag{4.24}$$

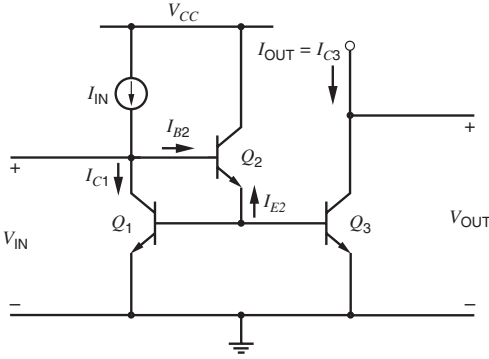


**Figure 4.6** Simple current mirror with beta helper.

where  $I_E$ ,  $I_C$ , and  $I_B$  are defined as positive when flowing into the transistor, and where we have neglected the effects of finite output resistance. The base current of transistor  $Q_2$  is equal to

$$I_{B2} = -\frac{I_{E2}}{\beta_F + 1} = \frac{2}{\beta_F(\beta_F + 1)} I_{C1} \quad (4.25)$$

Finally, KCL at the collector of  $Q_1$  gives

$$I_{IN} - I_{C1} - \frac{2}{\beta_F(\beta_F + 1)} I_{C1} = 0 \quad (4.26)$$

Since  $I_{C1}$  and  $I_{C3}$  are equal when  $Q_1$  and  $Q_3$  are identical,

$$I_{OUT} = I_{C3} = \frac{I_{IN}}{1 + \frac{2}{\beta_F(\beta_F + 1)}} \simeq I_{IN} \left( 1 - \frac{2}{\beta_F(\beta_F + 1)} \right) \quad (4.27)$$

Equation 4.27 shows that the systematic gain error from finite  $\beta_F$  has been reduced by a factor of  $[\beta_F + 1]$ , which is the current gain of emitter follower  $Q_2$ . As a result,  $Q_2$  is often referred to as a *beta helper*.

Although the beta helper has little effect on the output resistance and the minimum output voltage of the current mirror, it increases the input voltage by the base-emitter voltage of  $Q_2$ :

$$V_{IN} = V_{BE1(\text{on})} + V_{BE2(\text{on})} \quad (4.28)$$

If multiple emitter followers are cascaded to further reduce the gain error arising from finite  $\beta_F$ ,  $V_{IN}$  increases by an extra base-emitter voltage for each additional emitter follower, posing one limit to the use of cascaded emitter followers.

Current mirrors often use a beta helper when they are constructed with *pnp* transistors because the value of  $\beta_F$  for *pnp* transistors is usually less than for *nnp* transistors. Another application of the beta-helper configuration is in current mirrors with multiple outputs. An example with two independent outputs is shown in Fig. 4.7. At first, ignore  $Q_2$  and imagine that  $Q_1$  is simply diode connected. Also, let  $R_1 = R_3 = R_4 = 0$  here. (The effects of nonzero resistances will be considered in Section 4.2.4.) Then the gain from the input to each output is primarily determined by the area ratios  $I_{S3}/I_{S1}$  and  $I_{S4}/I_{S1}$ . Because the bases of three instead of two transistors are connected together, the total base current is increased here, which increases the gain error from the input to either output arising from finite  $\beta_F$ . Furthermore, the

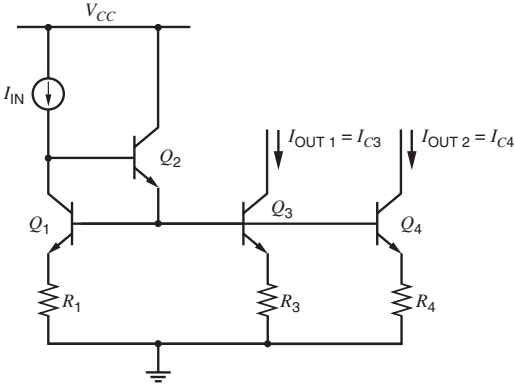


**Figure 4.7** Simple current mirror with beta helper, multiple outputs, and emitter degeneration.

gain errors worsen as the number of independent outputs increases. Since the beta helper,  $Q_2$ , reduces the gain error from the input to each output by a factor of  $[\beta_F + 1]$ , it is often used in bipolar current mirrors with multiple outputs.

**4.2.3.2 MOS**

Since  $\beta_F \rightarrow \infty$  for an MOS transistor, beta helpers are not used in simple MOS current mirrors to reduce the systematic gain error. However, a beta-helper configuration can increase the bandwidth of MOS and bipolar current mirrors.

**4.2.4 Simple Current Mirror with Degeneration**

**4.2.4.1 Bipolar**

The performance of the simple bipolar transistor current mirror of Fig. 4.6 can be improved by the addition of emitter degeneration as shown in Fig. 4.7 for a current mirror with two independent outputs. The purpose of the emitter resistors is twofold. First, Appendix A.4.1 shows that the matching between  $I_{IN}$  and outputs  $I_{C3}$  and  $I_{C4}$  can be greatly improved by using emitter degeneration. Second, as shown in Section 3.3.8, the use of emitter degeneration boosts the output resistance of each output of the current mirror. Transistors  $Q_1$  and  $Q_2$  combine to present a very low resistance at the bases of  $Q_3$  and  $Q_4$ . Therefore, from (3.99), the small-signal output resistance seen at the collectors of  $Q_3$  and  $Q_4$  is

$$R_o \simeq r_o(1 + g_m R_E) \tag{4.29}$$

if  $r_\pi \gg R_E$ . Taking  $Q_3$  as an example and using  $g_{m3} = I_{C3}/V_T$ , we find

$$R_o \simeq r_{o3} \left( 1 + \frac{I_{C3} R_3}{V_T} \right) \tag{4.30}$$

This increase in the output resistance for a given output current also decreases the component of systematic gain error that stems from finite output resistance by the same factor. From (4.9) and (4.30) with infinite  $\beta_F$ ,

$$\epsilon \simeq \frac{V_{CE2} - V_{CE1}}{V_A \left( 1 + \frac{I_{C3} R_3}{V_T} \right)} \tag{4.31}$$

The quantity  $I_{C3}R_3$  is just the dc voltage drop across  $R_3$ . If this quantity is 260 mV, for example, then  $R_o$  is about  $10r_o$  at room temperature, and  $\epsilon$  is reduced by a factor of about eleven. Unfortunately, this improvement in  $R_o$  is limited by corresponding increases in the input and minimum output voltages of the mirror:

$$V_{IN} \simeq V_{BE1(\text{on})} + V_{BE2(\text{on})} + I_{IN}R_1 \quad (4.32)$$

and

$$V_{OUT(\text{min})} = V_{CE3(\text{sat})} + I_{C3}R_3 \quad (4.33)$$

The emitter areas of  $Q_1$ ,  $Q_3$ , and  $Q_4$  may be matched or ratioed. For example, if we want  $I_{OUT1} = I_{IN}$  and  $I_{OUT2} = 2I_{IN}$ , we would make  $Q_3$  identical to  $Q_1$ , and  $Q_4$  consist of two copies of  $Q_1$  connected in parallel so that  $I_{S4} = 2I_{S1}$ . In addition, we could make  $R_3 = R_1$ , and  $R_4$  consist of two copies of  $R_1$  connected in parallel so that  $R_4 = R_1/2$ . Note that all the dc voltage drops across  $R_1$ ,  $R_3$ , and  $R_4$  would then be equal. Using KVL around the loop including  $Q_1$  and  $Q_4$  and neglecting base currents, we find

$$I_{C1}R_1 + V_T \ln \frac{I_{C1}}{I_{S1}} = I_{C4}R_4 + V_T \ln \frac{I_{C4}}{I_{S4}} \quad (4.34)$$

from which

$$I_{OUT2} = I_{C4} = \frac{1}{R_4} \left( I_{IN}R_1 + V_T \ln \frac{I_{IN} I_{S4}}{I_{C4} I_{S1}} \right) \quad (4.35)$$

Since  $I_{S4} = 2I_{S1}$ , the solution to (4.35) is

$$I_{OUT2} = \frac{R_1}{R_4} I_{IN} = 2I_{IN} \quad (4.36)$$

because the last term in (4.35) goes to zero. If we make the voltage drops  $I_{IN}R_1$  and  $I_{C4}R_4$  much greater than  $V_T$ , the current-mirror gain to the  $Q_4$  output is determined primarily by the resistor ratio  $R_4/R_1$ , and only to a secondary extent by the emitter area ratio, because the natural log term in (4.35) varies slowly with its argument.

#### 4.2.4.2 MOS

Source degeneration is rarely used in MOS current mirrors because, in effect, MOS transistors are inherently controlled resistors. Thus, matching in MOS current mirrors is improved simply by increasing the gate areas of the transistors.<sup>2,3,4</sup> Furthermore, the output resistance can be increased by increasing the channel length. To increase the output resistance while keeping the current and  $V_{GS} - V_t$  constant, the  $W/L$  ratio must be held constant. Therefore, the channel width must be increased as much as the length, and the price paid for the improved output resistance is that increased chip area is consumed by the current mirror.

### 4.2.5 Cascode Current Mirror

#### 4.2.5.1 Bipolar

Section 3.4.2 shows that the cascode connection achieves a very high output resistance. Since this is a desirable characteristic for a current mirror, exploring the use of cascodes for high-performance current mirrors is natural. A bipolar-transistor current mirror based on the cascode connection is shown in Fig. 4.8. Transistors  $Q_3$  and  $Q_1$  form a simple current mirror, and emitter resistances can be added to improve the matching. Transistor  $Q_2$  acts as the common-base part of the cascode and transfers the collector current of  $Q_1$  to the output while presenting a high

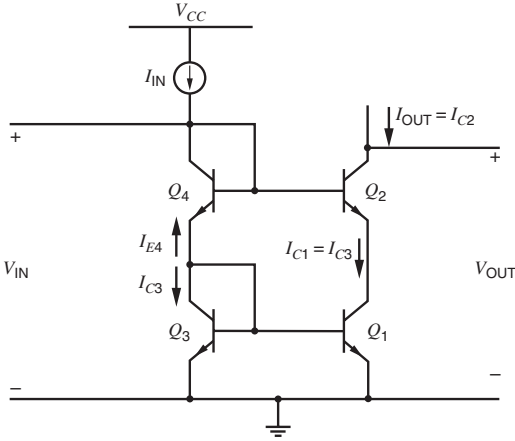


Figure 4.8 Cascode current mirror with bipolar transistors.

output resistance. Transistor  $Q_4$  acts as a diode level shifter and biases the base of  $Q_2$  so that  $Q_1$  operates in the forward-active region with  $V_{CE1} \simeq V_{CE3} = V_{BE3(\text{on})}$ . If we assume that the small-signal resistances of diodes  $Q_3$  and  $Q_4$  are small, a direct application of (3.98) with  $R_E = r_{o1}$  concludes that

$$R_o = r_{o2} \left( 1 + \frac{g_{m2}r_{o1}}{1 + \frac{g_{m2}r_{o1}}{\beta_0}} \right) \simeq \beta_0 r_{o2} \tag{4.37}$$

because  $g_{m2}r_{o1} \simeq g_{m1}r_{o1} \gg \beta_0$ . This calculation assumes that almost all of the small-signal current that flows into the collector of  $Q_2$  flows out its base because the small-signal resistance connected to the emitter of  $Q_2$  is much greater than that connected to its base. A key problem with this calculation, however, is that it ignores the effect of the simple current mirror formed by  $Q_3$  and  $Q_1$ . Let  $i_{b2}$  and  $i_{e2}$  represent increases in the base and emitter currents flowing out of  $Q_2$  caused by increasing output voltage. Then the simple mirror forces  $i_{e2} \simeq i_{b2}$ . As a result, the variation in the collector current of  $Q_2$  splits into two equal parts and half flows in  $r_{\pi 2}$ . A small-signal analysis shows that  $R_o$  in (4.37) is reduced by half to

$$R_o \simeq \frac{\beta_0 r_{o2}}{2} \tag{4.38}$$

Thus, the cascode configuration boosts the output resistance by approximately  $\beta_0/2$ . For  $\beta_0 = 100$ ,  $V_A = 130$  V, and  $I_{C2} = 1$  mA,

$$R_o = \frac{\beta_0 V_A}{2 I_{C2}} = \frac{100(130)}{2 \text{ mA}} = 6.5 \text{ M}\Omega \tag{4.39}$$

In this calculation of output resistance, we have neglected the effects of  $r_{\mu}$ . Although this assumption is easy to justify in the case of the simple current mirror, it must be reexamined here because the output resistance is so high. The collector-base resistance  $r_{\mu}$  results from modulation of the base-recombination current as a consequence of the Early effect, as described in Chapter 1. For a transistor whose base current is composed entirely of base-recombination current, the percentage change in base current when  $V_{CE}$  is changed at a constant  $V_{BE}$  would equal that of the collector current, and  $r_{\mu}$  would be equal to  $\beta_0 r_o$ . In this case, the effect of

$r_\mu$  would be to reduce the output resistance of the cascode current mirror given in (4.38) by a factor of 1.5.

In actual integrated-circuit *nnp* transistors, however, only a small percentage of the base current results from recombination in the base. Since only this component is modulated by the Early effect, the observed values of  $r_\mu$  are a factor of 10 or more larger than  $\beta_0 r_o$ . Therefore,  $r_\mu$  has a negligible effect here with *nnp* transistors. On the other hand, for lateral *pnp* transistors, the feedback resistance  $r_\mu$  is much smaller than for *nnp* transistors because most of the base current results from base-region recombination. The actual value of this resistance depends on a number of process and device-geometry variables, but observed values range from 2 to 5 times  $\beta_0 r_o$ . Therefore, for a cascode current mirror constructed with lateral *pnp* transistors, the effect of  $r_\mu$  on the output resistance can be significant. Furthermore, when considering current mirrors that give output resistances higher than  $\beta_0 r_o$ , the effects of  $r_\mu$  must be considered.

In the cascode current mirror, the base of  $Q_1$  is connected to a low-resistance point because  $Q_3$  is diode connected. As a result, feedback from  $r_{\mu 1}$  is greatly attenuated and has negligible effect on the output resistance. On the other hand, if the resistance from the base of  $Q_1$  to ground is increased while all other parameters are held constant, local feedback from  $r_{\mu 1}$  significantly affects the base-emitter voltage of  $Q_1$  and reduces the output resistance. In the limit where the resistance from the base of  $Q_1$  to ground becomes infinite,  $Q_1$  acts as if it were diode connected. Local feedback is considered in Chapter 8.

The input voltage of the cascode current mirror is

$$V_{IN} = V_{BE3} + V_{BE4} = 2V_{BE(on)} \quad (4.40)$$

Although  $V_{IN}$  is higher here than in (4.10) for a simple current mirror, the increase becomes a limitation only if the power-supply voltage is reduced to nearly two diode drops.

The minimum output voltage for which the output resistance is given by (4.38) must allow both  $Q_1$  and  $Q_2$  to be biased in the forward-active region. Since  $V_{CE1} \simeq V_{CE3} = V_{BE(on)}$ ,

$$V_{OUT(min)} = V_{CE1} + V_{CE2(sat)} \simeq V_{BE(on)} + V_{CE2(sat)} \quad (4.41)$$

Comparing (4.41) and (4.11) shows that the minimum output voltage for a cascode current mirror is higher than for a simple current mirror by a diode drop. This increase poses an important limitation on the minimum supply voltage when the current mirror is used as an active load for an amplifier.

Since  $V_{CE1} \simeq V_{CE3}$ ,  $I_{C1} \simeq I_{C3}$ , and the systematic gain error arising from finite transistor output resistance is almost zero. A key limitation of the cascode current mirror, however, is that the systematic gain error arising from finite  $\beta_F$  is worse than for a simple current mirror. From KCL at the collector of  $Q_3$ ,

$$-I_{E4} = I_{C3} + \frac{2I_{C3}}{\beta_F} \quad (4.42)$$

From KCL at the collector of  $Q_4$ ,

$$I_{IN} = -I_{E4} + \frac{I_{C2}}{\beta_F} \quad (4.43)$$

The collector current of  $Q_2$  is

$$I_{C2} = \frac{\beta_F}{\beta_F + 1} I_{C3} \quad (4.44)$$

Substituting (4.42) and (4.44) into (4.43) gives

$$I_{IN} = I_{C3} + \frac{2I_{C3}}{\beta_F} + \frac{I_{C3}}{\beta_F + 1} \quad (4.45)$$

Rearranging (4.45) to find  $I_{C3}$  and substituting back into (4.44) gives

$$I_{OUT} = I_{C2} = \left( \frac{\beta_F}{\beta_F + 1} \right) \left( \frac{I_{IN}}{1 + \frac{2}{\beta_F} + \frac{1}{\beta_F + 1}} \right) \quad (4.46)$$

Equation 4.46 can be rearranged to give

$$I_{OUT} = I_{IN} \left( 1 - \frac{4\beta_F + 2}{\beta_F^2 + 4\beta_F + 2} \right) \quad (4.47)$$

Equation 4.47 shows that the systematic gain error is

$$\epsilon = - \frac{4\beta_F + 2}{\beta_F^2 + 4\beta_F + 2} \quad (4.48)$$

When  $\beta_F \gg 1$ , (4.48) simplifies to

$$\epsilon \simeq - \frac{4}{\beta_F + 4} \quad (4.49)$$

In contrast, the systematic gain error stemming from finite  $\beta_F$  in a simple current mirror with identical transistors is about  $-2/\beta_F$ , which is less in magnitude than (4.49) predicts for a cascode current mirror if  $\beta_F > 4$ . This limitation of a cascode current mirror is overcome by the Wilson current mirror described in Section 4.2.6.

#### 4.2.5.2 MOS

The cascode current mirror is widely used in MOS technology, where it does not suffer from finite  $\beta_F$  effects. Figure 4.9 shows the simplest form. From (3.107), the small-signal output resistance is

$$R_o = r_{o2}[1 + (g_{m2} + g_{mb2})r_{o1}] + r_{o1} \quad (4.50)$$

As shown in the previous section, the bipolar cascode current mirror cannot realize an output resistance larger than  $\beta_0 r_o/2$  because  $\beta_0$  is finite and nonzero small-signal base current flows in the cascode transistor. In contrast, the MOS cascode is capable of realizing arbitrarily high output resistance by increasing the number of stacked cascode devices because  $\beta_0 \rightarrow \infty$  for MOS transistors. However, the MOS substrate leakage current described in Section 1.9 can create a resistive shunt to ground from the output node, which can dominate the output resistance for  $V_{OUT} > V_{OUT(\min)}$ .<sup>5</sup>

#### ■ EXAMPLE

Find the output resistance of the double-cascode current mirror shown in Fig. 4.10. Assume all the transistors operate in the active region with  $I_D = 10 \mu\text{A}$ ,  $V_A = 50 \text{ V}$ , and  $g_m r_o = 50$ . Neglect body effect.

The output resistance of each transistor is

$$r_o = \frac{V_A}{I_D} = \frac{50 \text{ V}}{10 \mu\text{A}} = 5 \text{ M}\Omega$$

From (4.50), looking into the drain of  $M_2$ :

$$R_{o2} = r_{o2}(1 + g_{m2}r_{o1}) + r_{o1} \quad (4.51)$$

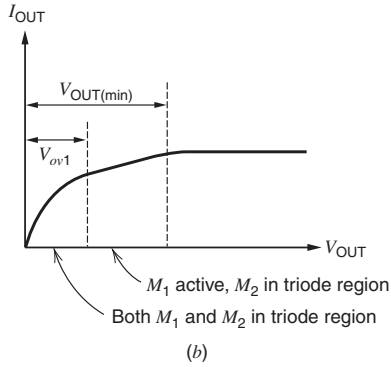
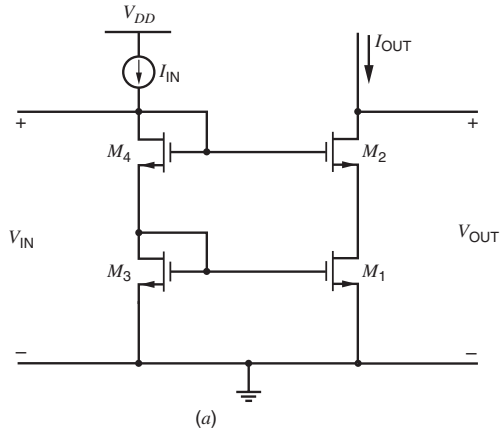


Figure 4.9 (a) Cascode current mirror using MOS transistors. (b) I-V characteristic.

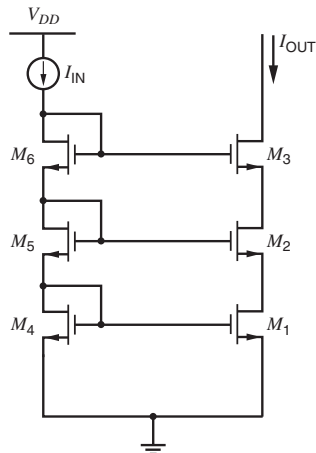


Figure 4.10 Example of a double-cascode current mirror.

Similarly, looking into the drain of  $M_3$ :

$$R_o = r_{o3}[1 + g_{m3}R_{o2}] + R_{o2} \quad (4.52)$$

Each cascode stage increases the output resistance by a factor of about  $(1 + g_m r_o)$ . Therefore,

$$R_o \simeq r_o(1 + g_m r_o)^2 \simeq 5(51)^2 \text{ M}\Omega \simeq 13 \text{ G}\Omega \quad (4.53)$$

With such a large output resistance, other parasitic leakage paths, such as the substrate leakage path, could be comparable to this resistance in practice.

From KVL in Fig. 4.9,

$$V_{DS1} = V_{GS3} + V_{GS4} - V_{GS2} \quad (4.54)$$

Since  $V_{DS3} = V_{GS3}$ , (4.54) shows that  $V_{DS1} = V_{DS3}$  when  $V_{GS2} = V_{GS4}$ . Under this condition, the systematic gain error of the cascode current mirror is zero because  $M_1$  and  $M_3$  are identically biased, and because  $\beta_F \rightarrow \infty$  for MOS transistors. In practice,  $V_{GS2}$  is not exactly equal to  $V_{GS4}$  even with perfect matching unless  $V_{OUT} = V_{IN}$  because of channel-length modulation. As a result,  $V_{DS1} \simeq V_{DS3}$  and

$$\epsilon \simeq 0 \quad (4.55)$$

The input voltage of the MOS cascode current mirror in Fig. 4.9 is

$$\begin{aligned} V_{IN} &= V_{GS3} + V_{GS4} \\ &= V_{t3} + V_{ov3} + V_{t4} + V_{ov4} \end{aligned} \quad (4.56)$$

The input voltage here includes two gate-source drops, each composed of threshold and overdrive components. Ignoring the body effect and assuming the transistors all have equal overdrives,

$$V_{IN} = 2V_t + 2V_{ov} \quad (4.57)$$

Also, adding extra cascode levels increases the input voltage by another threshold and another overdrive component for each additional cascode. Furthermore, the body effect increases the threshold of all transistors with  $V_{SB} > 0$ . Together, these facts increase the difficulty of designing the input current source for low power-supply voltages.

When  $M_1$  and  $M_2$  both operate in the active region,  $V_{DS1} \simeq V_{DS3} = V_{GS3}$ . For  $M_2$  to operate in the active region,  $V_{DS2} > V_{ov2}$  is required. Therefore, the minimum output voltage for which  $M_1$  and  $M_2$  operate in the active region is

$$\begin{aligned} V_{OUT(\min)} &= V_{DS1} + V_{ov2} \\ &\simeq V_{GS3} + V_{ov2} = V_t + V_{ov3} + V_{ov2} \end{aligned} \quad (4.58)$$

If the transistors all have equal overdrives,

$$V_{OUT(\min)} \simeq V_t + 2V_{ov} \quad (4.59)$$

On the other hand,  $M_2$  operates in the triode region if  $V_{OUT} < V_{OUT(\min)}$ , and both  $M_1$  and  $M_2$  operate in the triode region if  $V_{OUT} < V_{ov1}$ . These results are shown graphically in Fig. 4.9b.

Although the overdrive term in (4.59) can be made small by using large values of  $W$  for a given current, the threshold term represents a significant loss of voltage swing when the current mirror is used as an active load in an amplifier. The threshold term in (4.59) stems from the biasing of the drain-source voltage of  $M_1$  so that

$$V_{DS1} = V_{IN} - V_{GS2} \quad (4.60)$$

Ignoring the body effect and assuming that  $M_1$ - $M_4$  all operate in the active region with equal overdrives,

$$V_{DS1} = V_t + V_{ov} \tag{4.61}$$

Therefore, the drain-source voltage of  $M_1$  is a threshold larger than necessary to operate  $M_1$  in the active region. To reduce  $V_{DS1}$ , the voltage from the gate of  $M_2$  to ground can be level shifted down by a threshold as shown in Fig. 4.11a. In practice, a source follower is used to implement the level shift, as shown in Fig. 4.11b.<sup>6</sup> Transistor  $M_5$  acts as the source follower and is biased by the output of the simple current mirror  $M_3$  and  $M_6$ . Because the gate-source voltage of  $M_5$  is greater than its threshold by the overdrive, however, the drain-source voltage of  $M_1$  would be zero with equal thresholds and overdrives on all transistors. To bias  $M_1$  at the

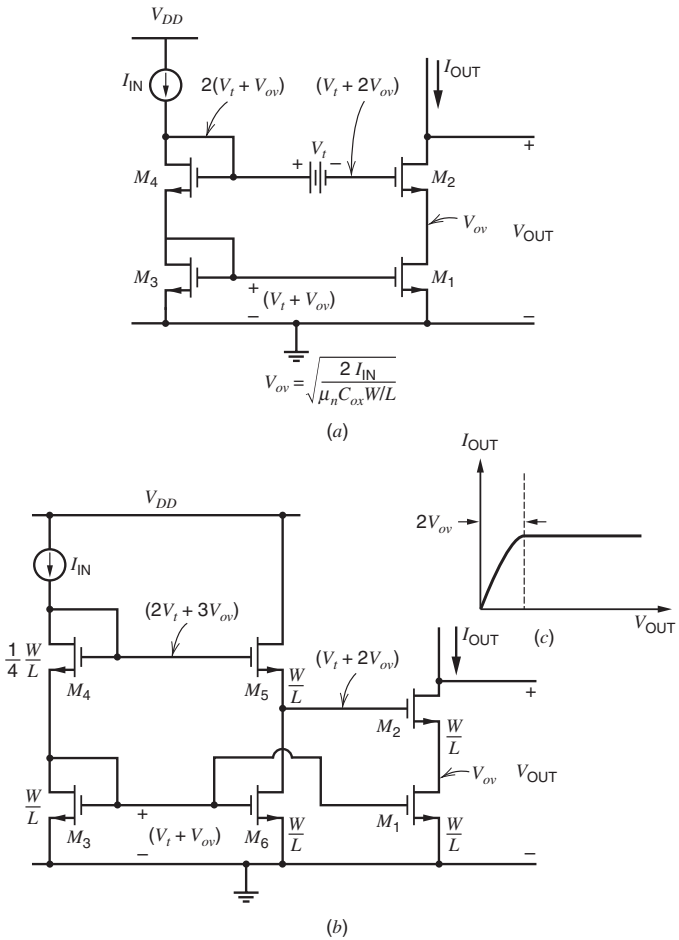


**Figure 4.11** (a) MOS cascode current mirror with improved biasing for maximum voltage swing. (b) Practical implementation. (c) I-V characteristic.

boundary between the active and triode regions,

$$V_{DS1} = V_{ov} \quad (4.62)$$

is required. Therefore, the overdrive on  $M_4$  is doubled by reducing its  $W/L$  by a factor of four to satisfy (4.62). As a result, the threshold term in (4.59) is eliminated and

$$V_{OUT(\min)} \simeq 2V_{ov} \quad (4.63)$$

Because the minimum output voltage does not contain a threshold component, the range of output voltages for which  $M_1$  and  $M_2$  both operate in the active region is significantly improved. Therefore, the current mirror in Fig. 4.11 places much less restriction on the range of output voltages that can be achieved in an amplifier using this current mirror as an active load than the mirror in Fig. 4.9. For this reason, the mirror in Fig. 4.11 is called a *high-swing* cascode current mirror. This type of level shifting to reduce  $V_{OUT(\min)}$  can also be applied to bipolar circuits.

The output resistance of the high-swing cascode current mirror is the same as in (4.50) when both  $M_1$  and  $M_2$  operate in the active region. However, the input voltage and the systematic gain error are worsened compared to the cascode current mirror without level shift. The input voltage is still given by (4.56), but the overdrive component of the gate-source voltage of  $M_4$  has increased by a factor of two because its  $W/L$  has been reduced by a factor of four. Therefore,

$$V_{IN} = 2V_t + 3V_{ov} \quad (4.64)$$

Since  $M_3$  and  $M_1$  form a simple current mirror with unequal drain-source voltages, the systematic gain error is

$$\epsilon = \frac{V_{DS1} - V_{DS3}}{V_A} \simeq \frac{V_{ov1} - (V_t + V_{ov1})}{V_A} = -\frac{V_t}{V_A} \quad (4.65)$$

The negative sign in (4.65) shows that  $I_{OUT} < I_{IN}$ . For example, if  $I_{IN} = 100 \mu\text{A}$ ,  $V_t = 1 \text{ V}$ , and  $V_A = 10 \text{ V}$ ,  $\epsilon \simeq -0.1$ , which means that  $I_{OUT} \simeq 90 \mu\text{A}$ .

In practice,  $(W/L)_4 < (1/4)(W/L)$  is usually selected for two reasons. First, MOS transistors display an indistinct transition from the triode to active regions. Therefore, increasing the drain-source voltage of  $M_1$  by a few hundred millivolts above  $V_{ov1}$  is usually required to realize the incremental output resistance predicted by (4.50). Second, although the body effect was not considered in this analysis, it tends to reduce the drain-source voltage on  $M_1$ , which is determined by the following KVL loop

$$V_{DS1} = V_{GS3} + V_{GS4} - V_{GS5} - V_{GS2} \quad (4.66)$$

Each of the gate-source voltage terms in (4.66) contains a threshold component. Since the source-body voltage of  $M_5$  is higher than that of  $M_4$ ,  $V_{t5} > V_{t4}$ . Also,  $V_{t2} > V_{t3}$  because the source-body voltage of  $M_2$  is higher than that of  $M_3$ . Simulations with high-accuracy models are usually required to find the optimum  $(W/L)_4$ .

One drawback of the current mirror in Fig. 4.11 is that the input current is mirrored to a new branch to do the level shift. Combining the input branches eliminates the possibility of mismatch between the two branch currents and may reduce the power dissipation. In a single combined input branch, some element must provide a voltage drop equal to the desired difference between the gate voltages of  $M_1$  and  $M_2$ . To bias  $M_1$  at the edge of the active region, the required voltages from the gates  $M_1$  and  $M_2$  to ground are  $V_t + V_{ov}$  and  $V_t + 2V_{ov}$ , respectively. Therefore, the desired difference in the gate voltages is  $V_{ov}$ . This voltage difference can be developed across the drain to the source of a transistor deliberately operated in the triode region, as shown in Fig. 4.12a.<sup>7</sup> Since  $M_6$  is diode connected, it operates

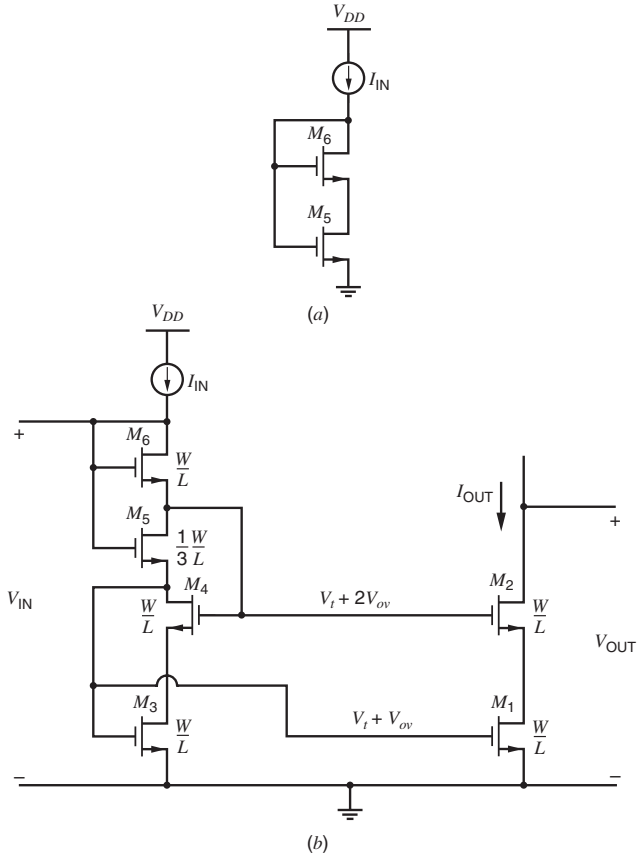


**Figure 4.12** (a) Circuit that forces  $M_5$  to operate in the triode region. (b) Sooch cascode current mirror using the circuit in (a).

in the active region as long as the input current and threshold are positive. However, since the gate-source voltage of  $M_6$  is equal to the gate-drain voltage of  $M_5$ , a channel exists at the drain of  $M_5$  when it exists at the source of  $M_6$ . In other words,  $M_6$  forces  $M_5$  to operate in the triode region.

To use the circuit in Fig. 4.12a in a current mirror, we would like to choose the aspect ratios of the transistors so that the drain-source voltage of  $M_5$  is  $V_{ov}$ . Since  $M_6$  operates in the active region,

$$I_{IN} = \frac{k'}{2} \left( \frac{W}{L} \right)_6 (V_{GS6} - V_T)^2 \tag{4.67}$$

Since  $M_5$  operates in the triode region,

$$I_{IN} = \frac{k'}{2} \left( \frac{W}{L} \right)_5 \left( 2(V_{GS5} - V_T)V_{DS5} - (V_{DS5})^2 \right) \tag{4.68}$$

The goal is to set

$$V_{DS5} = V_{ov} \quad (4.69)$$

when

$$V_{GS6} = V_t + V_{ov} \quad (4.70)$$

From (4.69) and (4.70),

$$V_{GS5} = V_{GS6} + V_{DS5} = V_t + 2V_{ov} \quad (4.71)$$

Substituting (4.68) - (4.71) into (4.67) gives

$$\frac{k'}{2} \left( \frac{W}{L} \right)_6 (V_{ov})^2 = \frac{k'}{2} \left( \frac{W}{L} \right)_5 \left( 2(2V_{ov})V_{ov} - (V_{ov})^2 \right) \quad (4.72)$$

Equation 4.72 can be simplified to

$$\left( \frac{W}{L} \right)_5 = \frac{1}{3} \left( \frac{W}{L} \right)_6 \quad (4.73)$$

The circuit of Fig. 4.12a is used in the current mirror of Fig. 4.12b,<sup>7</sup> which is called the *Sooch* cascode current mirror after its inventor. At first, ignore transistor  $M_4$  and assume that  $M_3$  is simply diode connected. The difference between the voltages to ground from the gates of  $M_1$  and  $M_2$  is set by the drain-source voltage of  $M_5$ . By choosing equal aspect ratios for all devices except  $M_5$ , whose aspect ratio is given by (4.73), the drain-source voltage of  $M_5$  is  $V_{ov}$  and  $M_1$  is biased at the edge of the active region. The output resistance, minimum output voltage, input voltage, and systematic gain error are the same as in (4.50), (4.63), (4.64), and (4.65) respectively.

Now we will consider the effect of transistor  $M_4$ . The purpose of  $M_4$  is to set the drain-source voltage of  $M_3$  equal to that of  $M_1$ . Without  $M_4$ , these drain-source voltages differ by a threshold, causing nonzero systematic gain error. With  $M_4$ ,

$$V_{DS3} = V_{G2} - V_{GS4} \quad (4.74)$$

where

$$V_{G2} = V_{GS3} + V_{DS5} \quad (4.75)$$

Ignoring channel-length modulation,

$$V_{G2} = (V_t + V_{ov}) + V_{ov} = V_t + 2V_{ov} \quad (4.76)$$

Ignoring the body effect and assuming that  $M_4$  operates in the active region,

$$V_{GS4} = V_t + V_{ov} \quad (4.77)$$

Then substituting (4.76) and (4.77) into (4.74) gives

$$V_{DS3} = V_{ov} \quad (4.78)$$

If  $M_2$  also operates in the active region under these conditions,  $V_{DS3} = V_{DS1}$ . As a result, the systematic gain error is

$$\epsilon = 0 \quad (4.79)$$

Therefore, the purpose of  $M_4$  is to equalize the drain-source voltages of  $M_3$  and  $M_1$  to reduce the systematic gain error.



Since the mirror in Fig. 4.13 has two input branches, an input voltage can be calculated for each:

$$V_{IN1} = V_{DS5} + V_{GS6} = V_t + 2V_{ov} \tag{4.82}$$

$$V_{IN2} = V_{GS3} = V_t + V_{ov} \tag{4.83}$$

Both  $V_{IN1}$  and  $V_{IN2}$  are less than the input voltage given in (4.64) for Fig. 4.12b by more than a threshold, allowing the input current sources to operate properly with power-supply voltages greater than about 2 V, assuming thresholds of about 1 V.

Finally, in Fig. 4.13, the drain-source voltage of  $M_5$  is only used to bias the source of  $M_6$ . Therefore,  $M_5$  and  $M_6$  can be collapsed into one diode-connected transistor whose source is grounded. Call this replacement transistor  $M_7$ . The aspect ratio of  $M_7$  should be a factor of four smaller than the aspect ratios of  $M_1$ - $M_4$  to maintain the bias conditions as in Fig. 4.13. In practice, the aspect ratio of  $M_7$  is further reduced to bias  $M_1$  past the edge of the active region and to overcome a mismatch in the thresholds of  $M_7$  and  $M_2$  caused by body effect.

### 4.2.6 Wilson Current Mirror

#### 4.2.6.1 Bipolar

The main limitation of the bipolar cascode current mirror is that the systematic gain error stemming from finite  $\beta_F$  was large, as given in (4.49). To overcome this limitation, the Wilson current mirror can be used as shown in Fig. 4.14a.<sup>8</sup> This circuit uses negative feedback through  $Q_1$ , activating  $Q_3$  to reduce the base-current error and raise the output resistance. (See Chapter 8.)

From a qualitative standpoint, the difference between the input current and  $I_{C3}$  flows into the base of  $Q_2$ . This base current is multiplied by  $(\beta_F + 1)$  and flows in the diode-connected transistor  $Q_1$ , which causes current of the same magnitude to flow in  $Q_3$ . A feedback path is thus formed that regulates  $I_{C3}$  so that it is nearly equal to the input current, reducing the systematic gain error caused by finite  $\beta_F$ . Similarly, when the output voltage increases, the collector current of  $Q_2$  also increases, in turn increasing the collector current of  $Q_1$ . As a result, the collector current of  $Q_3$  increases, which reduces the base current of  $Q_2$ . The decrease in the base current of  $Q_2$  caused by negative feedback reduces the original change in the collector current of  $Q_2$  and increases the output resistance.

To find the output resistance of the Wilson current mirror when all transistors operate in the active region, we will analyze the small-signal model shown in Fig. 4.14b, in which a

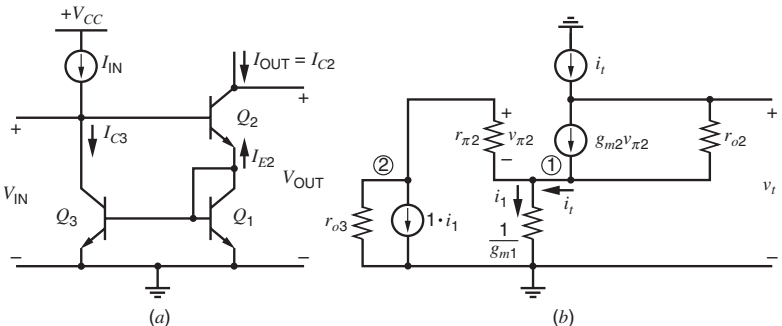


Figure 4.14 (a) Bipolar Wilson current mirror. (b) Small-signal model.

test current source  $i_t$  is applied at the output. Transistors  $Q_1$  and  $Q_3$  form a simple current mirror. Since  $Q_1$  is diode connected, the small-signal resistance from the base of  $Q_1$  to ground is  $(1/g_{m1})||r_{\pi1}||r_{\pi3}||r_{o1}$ . Assume that an unknown current  $i_1$  flows in this resistance. When  $g_{m1}r_{\pi1} \gg 1$ ,  $g_{m1}r_{\pi3} \gg 1$ , and  $g_{m1}r_{o1} \gg 1$ , this resistance is approximately equal to  $1/g_{m1}$ . Transistor  $Q_3$  could be modeled as a voltage-controlled current source of value  $g_{m3}v_{\pi3}$  in parallel with  $r_{o3}$ . Since  $v_{\pi3} = v_{\pi1} \simeq i_1/g_{m1}$ , the voltage-controlled current source in the model for  $Q_3$  can be replaced by a current-controlled current source of value  $(g_{m3}/g_{m1})(i_1) = 1(i_1)$ , as shown in Fig. 4.14b. This model represents the behavior of the simple current mirror directly: The input current  $i_1$  is mirrored to the output by the current-controlled current source.

Using this model, the resulting voltage  $v_t$  is

$$v_t = \frac{i_1}{g_{m1}} + (i_t - g_{m2}v_{\pi2})r_{o2} \quad (4.84)$$

To find the relationship between  $i_1$  and  $v_{\pi2}$ , note that the voltage across  $r_{o3}$  is  $(i_1/g_{m1} + v_{\pi2})$  and use KCL at node ② in Fig. 4.14b to show that

$$\frac{v_{\pi2}}{r_{\pi2}} + i_1 + \frac{g_{m1}}{r_{o3}}(i_1/g_{m1} + v_{\pi2}) = 0 \quad (4.85)$$

Rearranging (4.85) gives

$$v_{\pi2} = -i_1 r_{\pi2} \left( \frac{1 + \frac{1}{g_{m1}r_{o3}}}{1 + \frac{r_{\pi2}}{r_{o3}}} \right) \quad (4.86)$$

To find the relationship between  $i_1$  and  $i_t$ , use KCL at node ① in Fig. 4.14b to show that

$$i_t = i_1 - \frac{v_{\pi2}}{r_{\pi2}} \quad (4.87)$$

Substituting (4.86) into (4.87) and rearranging gives

$$i_1 = \frac{i_t}{1 + \left( \frac{1 + \frac{1}{g_{m1}r_{o3}}}{1 + \frac{r_{\pi2}}{r_{o3}}} \right)} \quad (4.88)$$

Substituting (4.88) into (4.86) and rearranging gives

$$v_{\pi2} = -i_t r_{\pi2} \left( \frac{1 + \frac{1}{g_{m1}r_{o3}}}{2 + \frac{r_{\pi2}}{r_{o3}} + \frac{1}{g_{m1}r_{o3}}} \right) \quad (4.89)$$

Substituting (4.88) and (4.89) into (4.84) and rearranging gives

$$R_o = \frac{v_t}{i_t} = \frac{1}{g_{m1} \left[ 1 + \left( \frac{1 + \frac{1}{g_{m1}r_{o3}}}{1 + \frac{r_{\pi2}}{r_{o3}}} \right) \right]} + r_{o2} + \frac{g_{m2}r_{\pi2}r_{o2} \left( 1 + \frac{1}{g_{m1}r_{o3}} \right)}{2 + \frac{r_{\pi2}}{r_{o3}} + \frac{1}{g_{m1}r_{o3}}} \quad (4.90)$$

If  $r_{o3} \rightarrow \infty$ , the small-signal current that flows in the collector of  $Q_3$  is equal to  $i_1$  and (4.90) reduces to

$$R_o = \frac{1}{g_{m1}(2)} + r_{o2} + \frac{g_{m2}r_{\pi2}r_{o2}}{2} \simeq \frac{\beta_0 r_{o2}}{2} \quad (4.91)$$

This result is the same as (4.38) for the cascode current mirror. In the cascode current mirror, the small-signal current that flows in the base of  $Q_2$  is mirrored through  $Q_3$  to  $Q_1$  so that the small-signal base and emitter currents leaving  $Q_2$  are approximately equal. On the other hand, in the Wilson current mirror, the small-signal current that flows in the emitter of  $Q_2$  is mirrored through  $Q_1$  to  $Q_3$  and then flows in the base of  $Q_2$ . Although the cause and effect relationship here is opposite of that in a cascode current mirror, the output resistance is unchanged because the small-signal base and emitter currents leaving  $Q_2$  are still forced to be equal. Therefore, the small-signal collector current of  $Q_2$  that flows because of changes in the output voltage still splits into two equal parts with half flowing in  $r_{\pi2}$ .

For the purpose of dc analysis, we assume that  $V_A \rightarrow \infty$  and that the transistors are identical. Then the input voltage is

$$V_{IN} = V_{CE3} = V_{BE1} + V_{BE2} = 2V_{BE(\text{on})} \quad (4.92)$$

which is the same as in (4.40) for a cascode current mirror. Also, the minimum output voltage for which both transistors in the output branch operate in the forward-active region is

$$V_{OUT(\text{min})} = V_{CE1} + V_{CE2(\text{sat})} = V_{BE(\text{on})} + V_{CE2(\text{sat})} \quad (4.93)$$

The result in (4.93) is the same as in (4.41) for a cascode current mirror.

To find the systematic gain error, start with KCL at the collector of  $Q_1$  to show that

$$-I_{E2} = I_{C1} + I_{B1} + I_{B3} = I_{C1} \left( 1 + \frac{1}{\beta_F} \right) + \frac{I_{C3}}{\beta_F} \quad (4.94)$$

Since we assumed that the transistors are identical and  $V_A \rightarrow \infty$ ,

$$I_{C3} = I_{C1} \quad (4.95)$$

Substituting (4.95) into (4.94) gives

$$-I_{E2} = I_{C1} \left( 1 + \frac{2}{\beta_F} \right) \quad (4.96)$$

Using (4.96), the collector current of  $Q_2$  is then

$$I_{C2} = -I_{E2} \left( \frac{\beta_F}{1 + \beta_F} \right) = I_{C1} \left( 1 + \frac{2}{\beta_F} \right) \left( \frac{\beta_F}{1 + \beta_F} \right) \quad (4.97)$$

Rearranging (4.97) we obtain

$$I_{C1} = I_{C2} \left[ \frac{1}{\left( 1 + \frac{2}{\beta_F} \right) \left( \frac{\beta_F}{1 + \beta_F} \right)} \right] \quad (4.98)$$

From KCL at the base of  $Q_2$ ,

$$I_{C3} = I_{IN} - \frac{I_{C2}}{\beta_F} \quad (4.99)$$

Inserting (4.98) and (4.99) into (4.95), we find that

$$I_{OUT} = I_{C2} = I_{IN} \left( 1 - \frac{2}{\beta_F^2 + 2\beta_F + 2} \right) = \frac{I_{IN}}{1 + \frac{2}{\beta_F(\beta_F + 2)}} \quad (4.100)$$

In the configuration shown in Fig. 4.14a, the systematic gain error arising from finite output resistance is not zero because  $Q_3$  and  $Q_1$  operate with collector-emitter voltages that differ by the base-emitter voltage of  $Q_2$ . With finite  $V_A$  and finite  $\beta_F$ ,

$$\begin{aligned} I_{OUT} &\simeq I_{IN} \left( 1 - \frac{2}{\beta_F^2 + 2\beta_F + 2} \right) \left( 1 + \frac{V_{CE1} - V_{CE3}}{V_A} \right) \\ &\simeq I_{IN} \left( 1 - \frac{2}{\beta_F^2 + 2\beta_F + 2} \right) \left( 1 - \frac{V_{BE2}}{V_A} \right) \end{aligned} \quad (4.101)$$

Therefore, the systematic gain error is

$$\epsilon \simeq - \left( \frac{2}{\beta_F^2 + 2\beta_F + 2} + \frac{V_{BE2}}{V_A} \right) \quad (4.102)$$

Comparing (4.102) to (4.49) shows two key points. First, the systematic gain error arising from finite  $\beta_F$  in a Wilson current mirror is much less than in a cascode current mirror. Second, the systematic gain error arising from finite output resistance is worse in the Wilson current mirror shown in Fig. 4.14a than in the cascode current mirror shown in Fig. 4.9. However, this limitation is not fundamental because it can be overcome by introducing a new diode-connected transistor between the collector of  $Q_3$  and the base of  $Q_2$  to equalize the collector-emitter voltages of  $Q_3$  and  $Q_1$ .

#### 4.2.6.2 MOS

Wilson current mirrors are also used in MOS technology, as shown in Fig. 4.15. Ignoring  $M_4$ , the circuit operation is essentially identical to the bipolar case with  $\beta_F \rightarrow \infty$ . One way to calculate the output resistance is to let  $r_{\pi 2} \rightarrow \infty$  in (4.90), which gives

$$R_o = \frac{1}{g_{m1}} + r_{o2} + g_{m2}r_{o2} \left( 1 + \frac{1}{g_{m1}r_{o3}} \right) r_{o3} \simeq (1 + g_{m2}r_{o3})r_{o2} \quad (4.103)$$

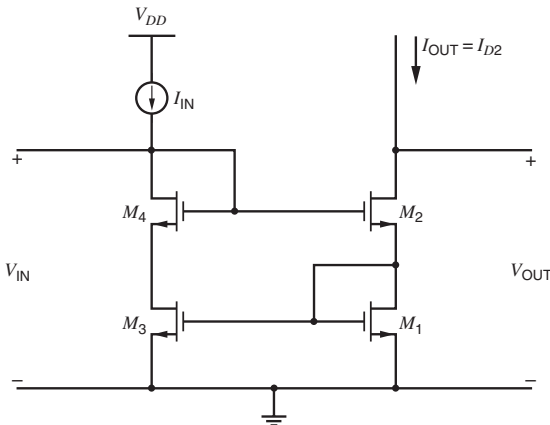


**Figure 4.15** Improved MOS Wilson current mirror with an additional device such that the drain voltages of  $M_1$  and  $M_3$  are equal.

Since the calculation in (4.103) is based on the small-signal model for the bipolar Wilson current mirror in Fig. 4.14*b*, it ignores the body effect in transistor  $M_2$ . Repeating the analysis with a body-effect generator in parallel with  $r_{o2}$  gives

$$R_o \simeq (2 + g_{m2}r_{o3})r_{o2} \quad (4.104)$$

The body effect on  $M_2$  has little effect on (4.104) because  $M_1$  is diode connected and therefore the voltage from the source of  $M_2$  to ground is almost constant.

Although  $\beta_F \rightarrow \infty$  for MOS transistors, the systematic gain error is not zero without  $M_4$  because the drain-source voltage of  $M_3$  differs from that of  $M_1$  by the gate-source voltage of  $M_2$ . Therefore, without  $M_4$ ,

$$\epsilon = \frac{V_{DS1} - V_{DS3}}{V_A} = -\frac{V_{GS2}}{V_A} \quad (4.105)$$

Transistor  $M_4$  is inserted in series with  $M_3$  to equalize the drain-source voltages of  $M_3$  and  $M_1$  so that

$$\epsilon \simeq 0 \quad (4.106)$$

With  $M_4$ , the output resistance is still given by (4.104) if all transistors operate in the active region. Also, insertion of  $M_4$  does not change either the minimum output voltage for which (4.104) applies or the input voltage. Ignoring body effect and assuming equal overdrives on all transistors, the minimum output voltage is

$$V_{\text{OUT}(\min)} = V_{GS1} + V_{ov2} = V_t + 2V_{ov} \quad (4.107)$$

Under the same conditions, the input voltage is

$$V_{\text{IN}} = V_{GS1} + V_{GS2} = 2V_t + 2V_{ov} \quad (4.108)$$

## 4.3 Active Loads

### 4.3.1 Motivation

In differential amplifiers of the type described in Chapter 3, resistors are used as the load elements. For example, consider the differential amplifier shown in Fig. 3.45. For this circuit, the differential-mode (dm) voltage gain is

$$A_{dm} = -g_m R_C \quad (4.109)$$

Large gain is often desirable because it allows negative feedback to make the gain with feedback insensitive to variations in the parameters that determine the gain without feedback. This topic is covered in Chapter 8. In Chapter 9, we will show that the required gain should be obtained in as few stages as possible to minimize potential problems with instability. Therefore, maximizing the gain of each stage is important.

Multiplying the numerator and denominator of (4.109) by  $I$  gives

$$A_{dm} = -\frac{I(R_C)}{I/g_m} \quad (4.110)$$

With bipolar transistors, let  $I$  represent the collector current  $I_C$  of each transistor in the differential pair. From (1.91), (4.110) can be rewritten as

$$A_{dm} = -\frac{I_C R_C}{V_T} \quad (4.111)$$

To achieve large voltage gain, (4.111) shows that the  $I_D R_C$  product must be made large, which in turn requires a large power-supply voltage. Furthermore, large values of resistance are required when low current is used to limit the power dissipation. As a result, the required die area for the resistors can be large.

A similar situation occurs in MOS amplifiers with resistive loads. Let  $I$  represent the drain current  $I_D$  of each transistor in the differential pair, and let the resistive loads be  $R_D$ . From (1.157) and (1.180), (4.110) can be rewritten as

$$A_{dm} = -\frac{I_D R_D}{(V_{GS} - V_t)/2} = -\frac{2I_D R_D}{V_{ov}} \quad (4.112)$$

Equation 4.112 shows that the  $I_D R_D$  product must be increased to increase the gain with constant overdrive. As a result, a large power supply is usually required for large gain, and large resistance is usually required to limit power dissipation. Also, since the overdrive is usually much larger than the thermal voltage, comparing (4.111) and (4.112) shows that the gain of an MOS differential pair is usually much less than the gain of its bipolar counterpart with equal resistive drops. This result stems from the observation that bipolar transistors provide much more transconductance for a given current than MOS transistors provide.

If the power-supply voltage is only slightly larger than the drop on the resistors, the range of common-mode input voltages for which the input transistors would operate in the active region would be severely restricted in both bipolar and MOS amplifiers. To overcome this problem and provide large gain without large power-supply voltages or resistances, the  $r_o$  of a transistor can be used as a load element.<sup>9</sup> Since the load element in such a circuit is a transistor instead of a resistor, the load element is said to be *active* instead of *passive*.

### 4.3.2 Common-Emitter-Common-Source Amplifier with Complementary Load

A common-emitter amplifier with *pnp* current-mirror load is shown in Fig. 4.16a. The common-source counterpart with a *p*-channel MOS current-mirror load is shown in Fig. 4.16b. In both cases, there are two output variables: the output voltage,  $V_{out}$ , and the output current,  $I_{out}$ . The relationship between these variables is governed by both the input transistor and the load transistor. From the standpoint of the input transistor  $T_1$ ,

$$I_{out} = I_{c1} \quad \text{or} \quad I_{out} = I_{d1} \quad (4.113)$$

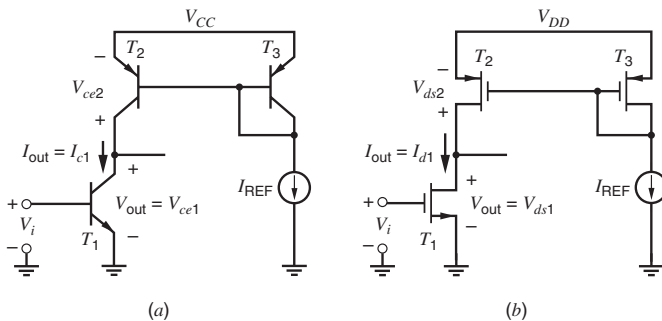


**Figure 4.16** (a) Common-emitter amplifier with active load. (b) Common-source amplifier with active load.

and

$$V_{out} = V_{ce1} \quad \text{or} \quad V_{out} = V_{ds1} \tag{4.114}$$

Equations 4.113 and 4.114 show that the output  $I$ - $V$  characteristics of  $T_1$  can be used directly in the analysis of the relationship between the output variables. Since the input voltage is the base-emitter voltage of  $T_1$  in Fig. 4.16a and the gate-source voltage of  $T_1$  in Fig. 4.16b, the input voltage is the parameter that determines the particular curve in the family of output characteristics under consideration at any point, as shown in Fig. 4.17a.

In contrast, the base-emitter or gate-source voltage of the load transistor  $T_2$  is fixed by diode-connected transistor  $T_3$ . Therefore, only one curve in the family of output  $I$ - $V$  characteristics needs to be considered for the load transistor, as shown in Fig. 4.17b. From the standpoint of the load transistor,

$$I_{out} = -I_{c2} \quad \text{or} \quad I_{out} = -I_{d2} \tag{4.115}$$

and

$$V_{out} = V_{CC} + V_{ce2} \quad \text{or} \quad V_{out} = V_{DD} + V_{ds2} \tag{4.116}$$

Equation 4.115 shows that the output characteristic of the load transistor should be mirrored along the horizontal axis to plot in the same quadrant as the output characteristics of the input

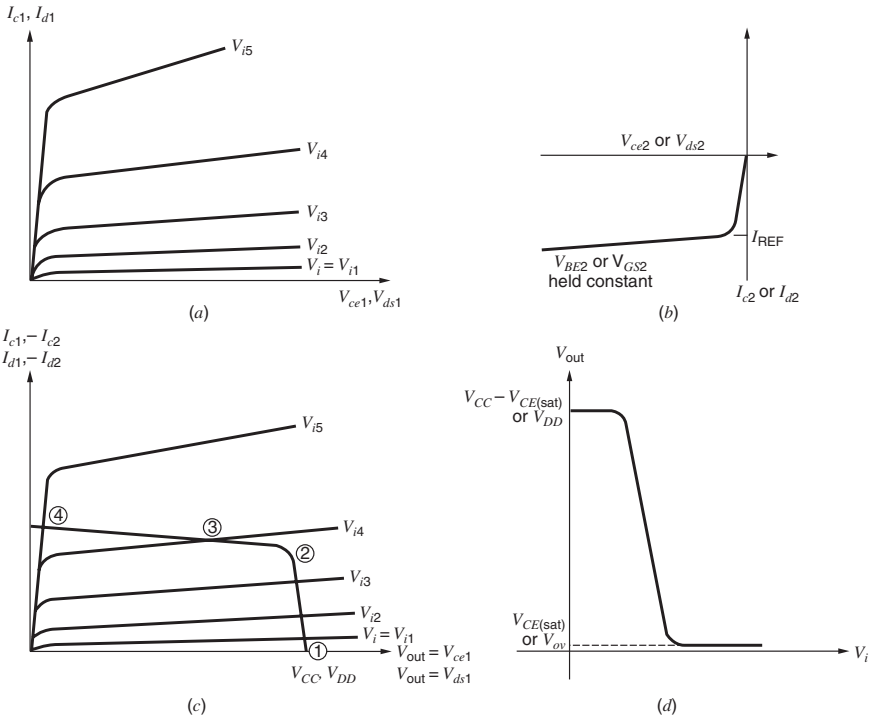


**Figure 4.17** (a)  $I$ - $V$  characteristics of the input transistor. (b)  $I$ - $V$  characteristic of the active load. (c)  $I$ - $V$  characteristics with load characteristic superimposed. (d) dc transfer characteristic of common-emitter or common-source amplifier with current-mirror load.

transistor. Equation 4.116 shows that the load curve should be shifted to the right by an amount equal to the power-supply voltage.

We now consider the dc transfer characteristic of the circuits. Initially, assume that  $V_i = 0$ . Then the input transistor is turned off, and the load is saturated in the bipolar case and linear in the MOS case, corresponding to point ① in Fig. 4.17c. As  $V_i$  is increased, the input transistor eventually begins to conduct current but the load remains saturated or linear until point ② is reached. Here the load enters the active region and a small further increase in  $V_i$  moves the operating point through point ③ to point ④, where the input transistor saturates in the bipolar case or enters the linear region in the MOS case. The change in  $V_i$  required to move from point ② to point ④ is small because the slopes of the output  $I$ - $V$  characteristics in the active region are small for both transistors. The transfer curve ( $V_{out}$  as a function of  $V_i$ ) is sketched in Fig. 4.17d.

A key point of this analysis is that the slope of the output characteristic is not constant, which is important because the slope is the gain of the amplifier. Since the gain of the amplifier depends on the input voltage, the amplifier is nonlinear in general, causing distortion to appear in the amplifier output. For low  $V_i$ , the output is high and the gain is low because the load transistor does not operate in the active region. Similarly, for large  $V_i$ , the output is low and the gain is low because the input transistor does not operate in the active region. To minimize distortion while providing gain, the amplifier should be operated in the intermediate region of  $V_i$ , where all transistors operate in the active region. The range of outputs for which all transistors operate in the active region should be maximized to use the power-supply voltage to the maximum extent. The active loads in Fig. 4.16 maintain high incremental output resistance as long as the drop across the load is more than  $V_{OUT(min)}$  of the current mirror, which is  $|V_{CE2(sat)}|$  in the bipolar case and  $|V_{ov2}|$  in the MOS case here. Therefore, minimizing  $V_{OUT(min)}$  of the mirror maximizes the range of outputs over which the amplifier provides high and nearly constant gain. In contrast, an ideal passive load requires a large voltage drop to give high gain, as shown in (4.111) and (4.112). As a result, the range of outputs for which the gain is high and nearly constant is much less than with an active load.

The gain at any output voltage can be found by finding the slope in Fig. 4.17d. In general, this procedure requires writing equations for the various curves in all of Fig. 4.17. Although this process is required to study the nonlinear behavior of the circuits, it is so complicated analytically that it is difficult to carry out for more than just a couple of transistors at a time. Furthermore, after completing such a large-signal analysis, the results are often so complicated that the effects of the key parameters are difficult to understand, increasing the difficulty of designing with these results. Since we are ultimately interested in being able to analyze and design circuits with a large number of transistors, we will concentrate on the small-signal analysis, which is much simpler to carry out and interpret than the large-signal analysis. Unfortunately, the small-signal analysis provides no information about nonlinearity because it assumes that all transistor parameters are constant.

The primary characteristics of interest in the small-signal analysis here are the voltage gain and output resistance when both devices operate in the active region. The small-signal equivalent circuit is shown in Fig. 4.18. It is drawn for the bipolar case but applies for the MOS case as well when  $r_{\pi 1} \rightarrow \infty$  and  $r_{\pi 2} \rightarrow \infty$  because  $\beta_0 \rightarrow \infty$ . Since  $I_{REF}$  in Fig. 4.16 is assumed constant, the large-signal base-emitter or gate-source voltage of the load transistor is constant. Therefore, the small-signal base-emitter or gate-source voltage of the load transistor,  $v_2$ , is zero. As a result, the small-signal voltage-controlled current  $g_{m2}v_2 = 0$ . To find the output resistance of the amplifier, we set the input to zero. Therefore,  $v_1 = 0$  and  $g_{m1}v_1 = 0$ , and the output resistance is

$$R_o = r_{o1} || r_{o2} \quad (4.117)$$

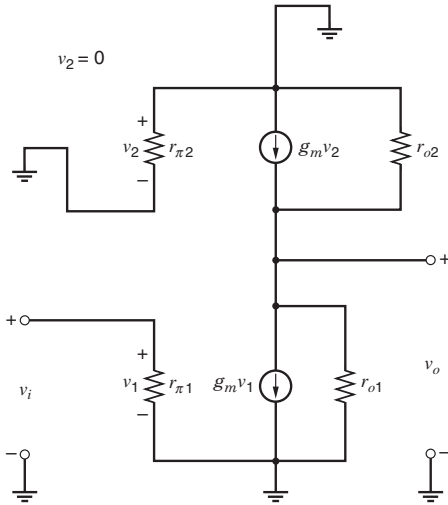


Figure 4.18 Small-signal equivalent circuit for common-emitter amplifier with active load.

Equation 4.117 together with (1.112) and (1.194) show that the output resistance is inversely proportional to the current in both the bipolar and MOS cases.

Since  $v_2 = 0$ ,  $g_{m1}v_1$  flows in  $r_{o1}||r_{o2}$  and

$$A_v = -g_{m1}(r_{o1}||r_{o2}) \tag{4.118}$$

Substituting (1.91) and (1.112) into (4.118) gives for the bipolar case,

$$A_v = -\frac{1}{\frac{V_T}{V_{A1}} + \frac{V_T}{V_{A2}}} \tag{4.119}$$

Equation 4.119 shows that the gain is independent of the current in the bipolar case because the transconductance is proportional to the current while the output resistance is inversely proportional to the current. Typical values for this voltage gain are in the 1000 to 2000 range. Therefore, the actively loaded bipolar stage provides very high voltage gain.

In contrast, (1.180) shows that the transconductance is proportional to the square root of the current in the MOS case assuming square-law operation. Therefore, the gain in (4.118) is inversely proportional to the square root of the current. With channel lengths less than 1  $\mu\text{m}$ , however, the drain current is almost linearly related to the gate-source voltage, as shown in (1.224). Therefore, the transconductance is almost constant, and the gain is inversely proportional to the current with very short channel lengths. Furthermore, typical values for the voltage gain in the MOS case are between 10 and 100, which is much less than with bipolar transistors.

### 4.3.3 Common-Emitter-Common-Source Amplifier with Depletion Load

Actively loaded gain stages using MOS transistors can be realized in processes that include only  $n$ -channel or only  $p$ -channel transistors if depletion devices are available. A depletion transistor is useful as a load element because it behaves like a current source when the transistor operates in the active region with the gate shorted to the source.

The  $I$ - $V$  characteristic of an  $n$ -channel MOS depletion-load transistor is illustrated in Fig. 4.19. Neglecting body effect, the device exhibits a very high output resistance (equal to the device  $r_o$ ) as long as the device operates in the active region. When the body effect is included, the resistance seen across the device drops to approximately  $1/g_{mb}$ . A complete gain stage is shown in Fig. 4.20 together with its dc transfer characteristic. The small-signal equivalent model when both transistors operate in the active region is shown in Fig. 4.21. From this circuit, we find that the gain is

$$\frac{v_o}{v_i} = -g_{m1} \left( r_{o1} || r_{o2} || \frac{1}{g_{mb2}} \right) \approx -\frac{g_{m1}}{g_{mb2}} \quad (4.120)$$

For a common-source amplifier with a depletion load, rearranging (4.120) and using (1.180) and (1.200) gives

$$\frac{v_o}{v_i} \approx -\frac{g_{m1}}{\frac{g_{mb2}}{g_{m2}}} = -\frac{1}{\chi} \sqrt{\frac{(W/L)_1}{(W/L)_2}} \quad (4.121)$$

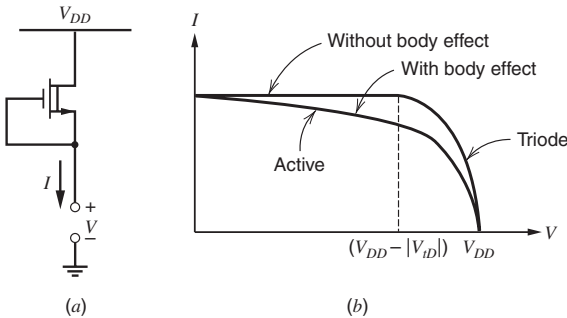


**Figure 4.19** (a)  $n$ -channel depletion-mode load transistor. (b)  $I$ - $V$  characteristic.

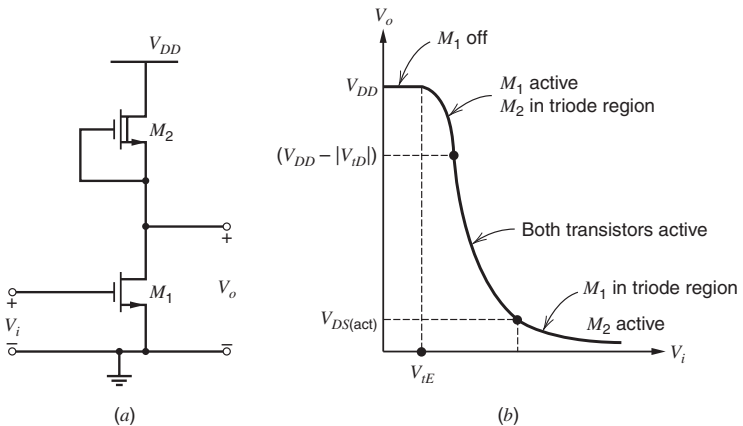


**Figure 4.20** (a) Common-source amplifier with depletion-mode transistor load. (b) dc transfer characteristic.

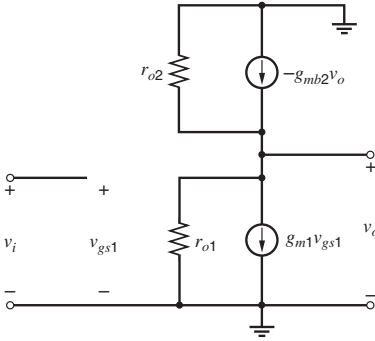


**Figure 4.21** Small-signal equivalent circuit of the common-source amplifier with depletion load, including the body effect in the load and the channel-length modulation in the load and the common-source device.

From (1.196) and (1.141),

$$\frac{1}{\chi} = 2\sqrt{2\phi_f}C_{ox}\sqrt{\frac{1 + V_{SB}/(2\phi_f)}{2q\epsilon N_A}} \tag{4.122}$$

Since  $\chi$  depends on  $V_o = V_{SB}$ , the incremental voltage gain varies with output voltage, giving the slope variation shown in the active region of Fig. 4.20b.

Equation 4.120 applies for either a common-emitter or common-source driver with a depletion MOS load. If this circuit is implemented in a *p*-well CMOS technology,  $M_2$  can be built in an isolated well, which can be connected to the source of  $M_2$ . Since this connection sets the source-body voltage in the load transistor to zero, it eliminates the body effect. Setting  $g_{mb2} = 0$  in (4.120) gives

$$\frac{v_o}{v_i} = -g_{m1}(r_{o1} || r_{o2}) \tag{4.123}$$

Although the gain predicted in (4.123) is much higher than in (4.120), this connection reduces the bandwidth of the amplifier because it adds extra capacitance (from the well of  $M_2$  to the substrate of the integrated circuit) to the amplifier output node.

### 4.3.4 Common-Emitter-Common-Source Amplifier with Diode-Connected Load

In this section, we examine the common-emitter/source amplifier with diode-connected load as shown in MOS form in Fig. 4.22. Since the load is diode connected, the load resistance is no more than the reciprocal of the transconductance of the load. As a result, the gain of this circuit is low, and it is often used in wideband amplifiers that require low gain.

For input voltages that are less than one threshold voltage, transistor  $M_1$  is off and no current flows in the circuit. When the input voltage exceeds a threshold, transistor  $M_1$  turns on, and the circuit provides amplification. Assume that both transistors operate in the active region. From (1.157), the drain currents of  $M_1$  and  $M_2$  are

$$I_1 = \frac{k'}{2} \left(\frac{W}{L}\right)_1 (V_{gs1} - V_{t1})^2 \tag{4.124}$$

and

$$I_2 = \frac{k'}{2} \left(\frac{W}{L}\right)_2 (V_{gs2} - V_{t2})^2 \tag{4.125}$$

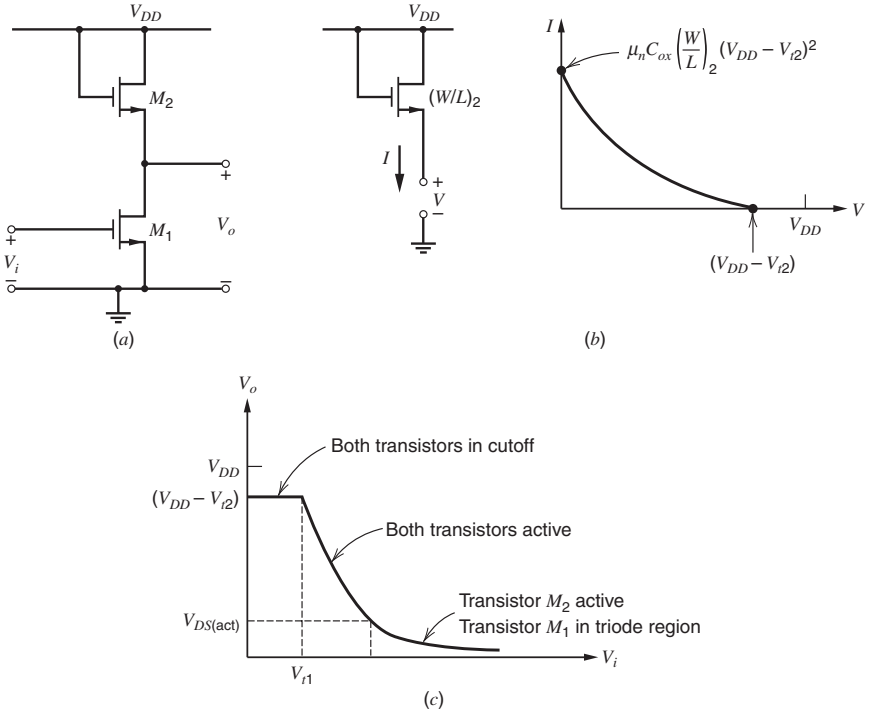


**Figure 4.22** (a) Common-source amplifier with enhancement-mode load. (b)  $I$ - $V$  characteristic of load transistor. (c) Transfer characteristic of the circuit.

From KVL in Fig. 4.22,

$$V_o = V_{DD} - V_{gs2} \tag{4.126}$$

Solving (4.125) for  $V_{gs2}$  and substituting into (4.126) gives

$$V_o = V_{DD} - V_{t2} - \sqrt{\frac{2I_2}{k'(W/L)_2}} \tag{4.127}$$

Since  $I_2 = I_1$ , (4.127) can be rewritten as

$$V_o = V_{DD} - V_{t2} - \sqrt{\frac{2I_1}{k'(W/L)_2}} \tag{4.128}$$

Substituting (4.124) into (4.128) with  $V_{gs1} = V_i$  gives

$$V_o = V_{DD} - V_{t2} - \sqrt{\frac{(W/L)_1}{(W/L)_2}} (V_i - V_{t1}) \tag{4.129}$$

Equation 4.129 shows that the slope of the transfer characteristic is the square root of the aspect ratios, assuming that the thresholds are constant. Since the slope of the transfer characteristic is the gain of the amplifier, the gain is constant and the amplifier is linear for a wide range

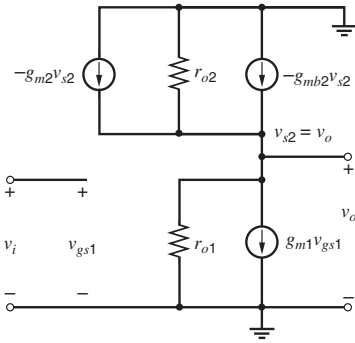


**Figure 4.23** Small-signal equivalent circuit for the common-source amplifier with enhancement-mode load, including output resistance and body effect in the load.

of inputs if the thresholds are constant. This amplifier is useful in implementing broadband, low-gain amplifiers with high linearity.

Equation 4.129 holds when both transistors operate in the active region and when channel-length modulation and body effect are negligible. In practice, the requirement that both transistors operate in the active region leads to an important performance limitation in enhancement-load inverters. The load device remains in the active region only if the drain-source voltage of the load is at least a threshold voltage. For output voltages more positive than  $V_{DD} - V_{t2}$ , the load transistor enters the cutoff region and carries no current. Therefore, the amplifier is incapable of producing an output more positive than one threshold voltage below the positive supply. Also, in practice, channel-length modulation and body effect reduce the gain as shown in the following small-signal analysis.

The small-signal voltage gain can be determined by using the small-signal equivalent circuit of Fig. 4.23, in which both the body effect and the output resistance of the two transistors have been included. From KCL at the output node,

$$g_{m1}v_i + \frac{v_o}{r_{o1}} + \frac{v_o}{r_{o2}} + g_{m2}v_o + g_{mb2}v_o = 0 \tag{4.130}$$

Rearranging (4.130) gives

$$\begin{aligned} \frac{v_o}{v_i} &= -g_{m1} \left( \frac{1}{g_{m2}} \parallel \frac{1}{g_{mb2}} \parallel r_{o1} \parallel r_{o2} \right) \\ &= -\frac{g_{m1}}{g_{m2}} \left( \frac{1}{1 + \frac{g_{mb2}}{g_{m2}} + \frac{1}{g_{m2}r_{o1}} + \frac{1}{g_{m2}r_{o2}}} \right) \end{aligned} \tag{4.131}$$

If  $g_{m2}/g_{mb2} \gg 1$ ,  $g_{m2}r_{o1} \gg 1$ , and  $g_{m2}r_{o2} \gg 1$ ,

$$\frac{v_o}{v_i} \simeq -\frac{g_{m1}}{g_{m2}} = -\sqrt{\frac{(W/L)_1}{(W/L)_2}} \tag{4.132}$$

as in (4.129). For practical device geometries, this relationship limits the maximum voltage gain to values on the order of 10 to 20.

The bipolar counterpart of the circuit in Fig. 4.22 is a common-emitter amplifier with a diode-connected load. The magnitude of its gain would be approximately equal to the ratio of the transconductances, which would be unity. However, the current that would flow in this circuit would be extremely large for inputs greater than  $V_{be(on)}$  because the collector current in a bipolar transistor is an exponential function of its base-emitter voltage. To limit the current

but maintain unity gain, equal-value resistors can be placed in series with the emitter of each transistor. Alternatively, the input transistors can be replaced by a differential pair, where the current is limited by the tail current source. In this case, emitter degeneration is used in the differential pair to increase the range of inputs for which all transistors operate in the active region, as in Fig. 3.49. In contrast, source degeneration is rarely used in MOS differential pairs because their transconductance and linear range can be controlled through the device aspect ratios.

### 4.3.5 Differential Pair with Current-Mirror Load

#### 4.3.5.1 Large-Signal Analysis

A straightforward application of the active-load concept to the differential pair would yield the circuit shown in Fig. 4.24a. Assume at first that all  $n$ -channel transistors are identical

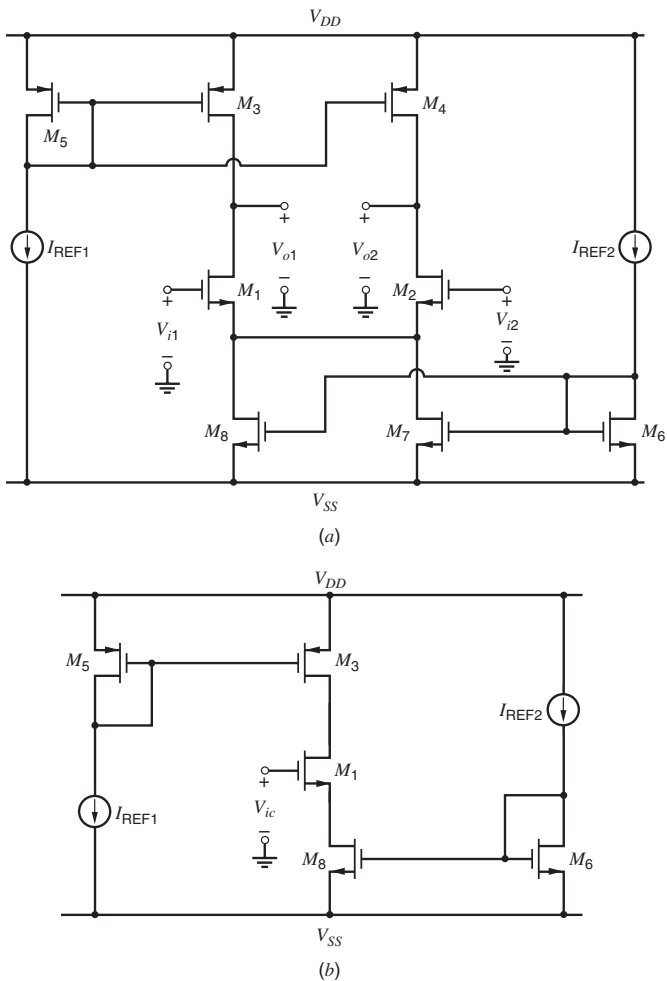


**Figure 4.24** (a) Differential pair with active load. (b) Common-mode half circuit for differential pair with active load.

and that all  $p$ -channel transistors are identical. Then the differential-mode half circuit for this differential pair is just a common-source amplifier with an active-load, as in Fig. 4.16*b*. Thus the differential-mode voltage gain is large when all the transistors are biased in the active region. The circuit as it stands, however, has the drawback that the quiescent value of the common-mode output voltage is very sensitive to changes in the drain currents of  $M_3$ ,  $M_4$ ,  $M_7$ , and  $M_8$ . As a result, some transistors may operate in or near the triode region, reducing the differential gain or the range of outputs for which the differential gain is high.

This fact is illustrated by the dc common-mode half-circuit shown in Fig. 4.24*b*. In the common-mode half circuit, the combination of  $M_1$ ,  $M_6$ , and  $M_8$  form a cascode current mirror, which is connected to the simple current mirror formed by  $M_3$  and  $M_5$ . If all transistors operate in the active region,  $M_3$  pushes down a current about equal to  $I_{REF1}$ , and  $M_8$  pulls down a current about equal to  $I_{REF2}$ . KCL requires that the current in  $M_3$  must be equal to the current in  $M_8$ . If  $I_{REF2} = I_{REF1}$ , KCL can be satisfied while all transistors operate in the active region. In practice, however,  $I_{REF2}$  is not exactly equal to  $I_{REF1}$ , and the current mirrors contain nonzero mismatch, causing changes in the common-mode output to satisfy KCL. Since the output resistance of each current mirror is high, the required change in the common-mode output voltage can be large even for a small mismatch in reference currents or transistors, and one or more transistors can easily move into or near the triode region. For example, suppose that the current pushed down by  $M_3$  when it operates in the active region is more than the current pulled down by  $M_8$  when it operates in the active region. Then the common-mode output voltage must rise to reduce the current in  $M_3$ . If the common-mode output voltage rises within  $V_{ov3}$  of  $V_{DD}$ ,  $M_3$  operates in the triode region. Furthermore, even if all the transistors continue to be biased in the active region, any change in the common-mode output voltage from its desired value reduces the range of outputs for which the differential gain is high.

Since  $M_1$  and  $M_2$  act as cascodes for  $M_7$  and  $M_8$ , shifts in the common-mode input voltage have little effect on the common-mode output unless the inputs become low enough that  $M_7$  and  $M_8$  are forced to operate in the triode region. Therefore, feedback to the inputs of the circuit in Fig. 4.24*a* is not usually adequate to overcome the common-mode bias problem. Instead, this problem is usually overcome in practice through the use of a separate common-mode feedback circuit, which either adjusts the sum of the currents in  $M_3$  and  $M_4$  to be equal to the sum of the currents in  $M_7$  and  $M_8$  or vice versa for a given common-mode output voltage. This topic is covered in Chapter 12.

An alternative approach that avoids the need for common-mode feedback is shown in Fig. 4.25. For simplicity in the bipolar circuit shown in Fig. 4.25*a*, assume that  $\beta_F \rightarrow \infty$ . The circuit in Fig. 4.25*b* is the MOS counterpart of the bipolar circuit in Fig. 4.25*a* because each  $nnp$  and  $pnp$  transistor has been replaced by  $n$ -channel and  $p$ -channel MOS transistors, respectively. Then under ideal conditions in both the bipolar and MOS circuits, the active load is a current mirror that forces the current in its output transistor  $T_4$  to equal the current in its input transistor  $T_3$ . Since the sum of the currents in both transistors of the active load must equal  $I_{TAIL}$  by KCL,  $I_{TAIL}/2$  flows in each side of the active load. Therefore, these circuits eliminate the common-mode bias problem by allowing the currents in the active load to be set by the tail current source. Furthermore, these circuits each provide a single output with much better rejection of common-mode input signals than a standard resistively loaded differential pair with the output taken off one side only. Although these circuits can be analyzed from a large-signal standpoint, we will concentrate on the small-signal analysis for simplicity.

#### 4.3.5.2 Small-Signal Analysis

We will analyze the low-frequency small-signal behavior of the bipolar circuit shown in Fig. 4.25*a* because these results cover both the bipolar and MOS cases by letting  $\beta_0 \rightarrow \infty$  and  $r_\pi \rightarrow \infty$ . Key parameters of interest in this circuit include the small-signal

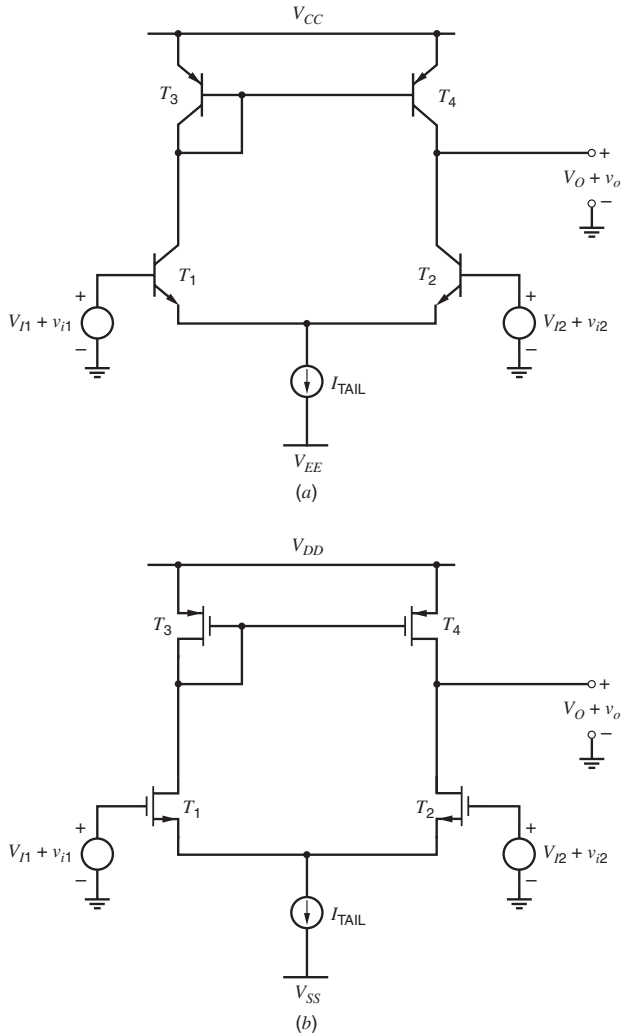


**Figure 4.25** (a) Emitter-coupled pair with current-mirror load. (b) Source-coupled pair with current-mirror load (MOS counterpart).

transconductance and output resistance. (The product of these two quantities gives the small-signal voltage gain with no load.) Since only one transistor in the active load is diode connected, the circuit is not symmetrical and a half-circuit approach is not useful. Therefore, we will analyze the small-signal model of this circuit directly. Assume that all transistors operate in the active region with  $r_{\mu} \rightarrow \infty$  and  $r_b = 0$ . Let  $r_{tail}$  represent the output resistance of the tail current source  $I_{TAIL}$ . The resulting small-signal circuit is shown in Fig. 4.26a.

Since  $T_3$  and  $T_4$  form a current mirror, we expect the mirror output current to be approximately equal to the mirror input current. Therefore, we will write

$$g_{m4}v_3 = i_3(1 - \epsilon_m) \tag{4.133}$$

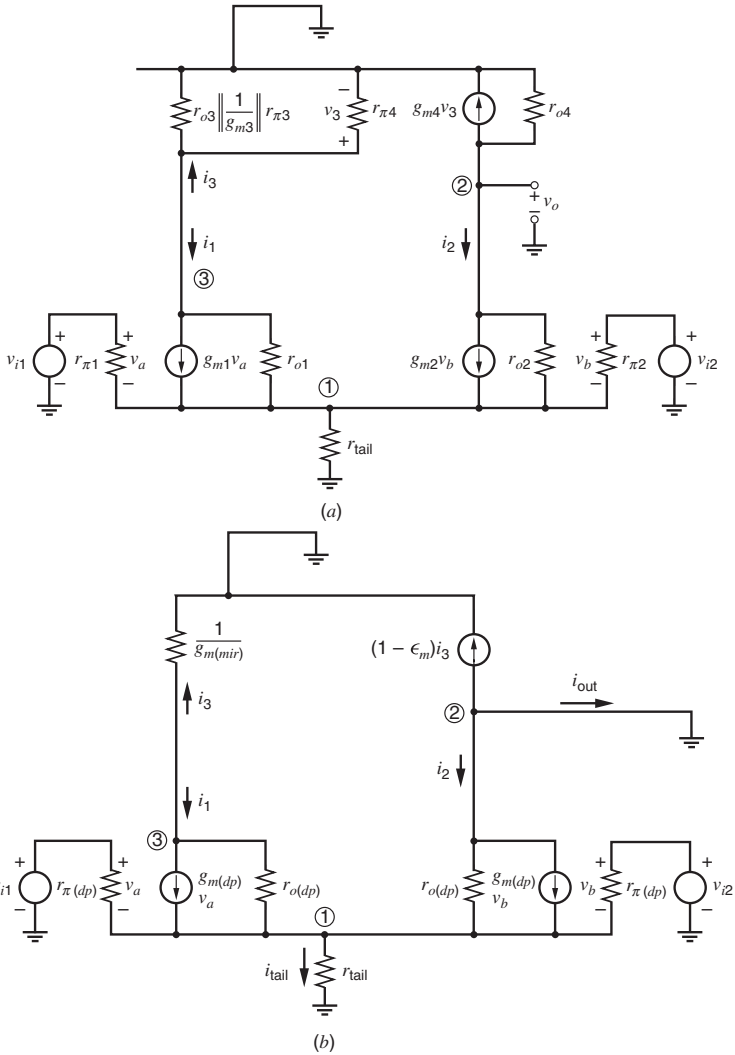


**Figure 4.26** (a) Small-signal equivalent circuit, differential pair with current-mirror load. (b) Simplified drawing of small-signal model of differential pair with current-mirror load.

where  $\epsilon_m$  is the systematic gain error of the current mirror calculated from small-signal parameters. Let  $r_3$  represent the total resistance connected between the base or gate of  $T_3$  and the power supply. Then  $r_3$  is the parallel combination of  $1/g_{m3}$ ,  $r_{\pi 3}$ ,  $r_{\pi 4}$ , and  $r_{o3}$ . Under the simplifying assumptions that  $\beta_0 \gg 1$  and  $g_m r_o \gg 1$ , this parallel combination is approximately equal to  $1/g_{m3}$ . Then the drop across  $r_{\pi 4}$  is

$$v_3 = i_3 r_3 \simeq \frac{i_3}{g_{m3}} \tag{4.134}$$

We will also assume that the two transistors in the differential pair match perfectly and operate with equal dc currents, as do the two transistors in the current-mirror load. Then  $g_{m(dp)} = g_{m1}$

$= g_{m2}, g_{m(mir)} = g_{m3} = g_{m4}, r_{\pi(dp)} = r_{\pi1} = r_{\pi2}, r_{\pi(mir)} = r_{\pi3} = r_{\pi4}, r_{o(dp)} = r_{o1} = r_{o2},$  and  $r_{o(mir)} = r_{o3} = r_{o4}$ . From (4.134), the resulting voltage-controlled current  $g_{m4}v_3$  is

$$g_{m4}v_3 = g_{m(mir)}v_3 \simeq g_{m(mir)} \frac{i_3}{g_{m(mir)}} = i_3 \quad (4.135)$$

Equations 4.133 and 4.135 show that  $\epsilon_m \simeq 0$  and thus the active load acts as a current mirror in a small-signal sense, as expected. Using (4.133), the small-signal circuit is redrawn in Fig. 4.26*b* with the output grounded to find the transconductance. Note that  $r_{o4}$  is omitted because it is attached to a small-signal ground on both ends.

From KCL at node ①,

$$(v_{i1} - v_1 + v_{i2} - v_1) \left( \frac{1}{r_{\pi(dp)}} + g_{m(dp)} \right) + \frac{v_3 - v_1}{r_{o(dp)}} - \frac{v_1}{r_{o(dp)} || r_{tail}} = 0 \quad (4.136)$$

where  $v_1$  and  $v_3$  are the voltages to ground from nodes ① and ③. To complete an exact small-signal analysis, KCL equations could also be written at nodes ② and ③, and these KCL equations plus (4.136) could be solved simultaneously. However, this procedure is complicated algebraically and leads to an equation that is difficult to interpret. To simplify the analysis, we will assume at first that  $r_{tail} \rightarrow \infty$  and  $r_{o(dp)} \rightarrow \infty$  since the transistors are primarily controlled by their base-emitter or gate-source voltages. Then from (4.136)

$$v_1 = \frac{v_{i1} + v_{i2}}{2} = v_{ic} \quad (4.137)$$

where  $v_{ic}$  is the common-mode component of the input. Let  $v_{id} = v_{i1} - v_{i2}$  represent the differential-mode component of the input. Then  $v_{i1} = v_{ic} + v_{id}/2$  and  $v_{i2} = v_{ic} - v_{id}/2$ , and the small-signal collector or drain currents

$$i_1 = g_{m(dp)}(v_{i1} - v_1) = \frac{g_{m(dp)}v_{id}}{2} \quad (4.138)$$

and

$$i_2 = g_{m(dp)}(v_{i2} - v_1) = -\frac{g_{m(dp)}v_{id}}{2} \quad (4.139)$$

With a resistive load and a single-ended output, only  $i_2$  flows in the output. Therefore, the transconductance for a differential-mode (dm) input with a passive load is

$$G_m[dm] = \left. \frac{i_{out}}{v_{id}} \right|_{v_{out}=0} = -\frac{i_2}{v_{id}} = \frac{g_{m(dp)}}{2} \quad (4.140)$$

On the other hand, with the active loads in Fig. 4.25, not only  $i_2$  but also most of  $i_3$  flows in the output because of the action of the current mirror, as shown by (4.135). Therefore, the output current in Fig. 4.26*b* is

$$i_{out} = -(1 - \epsilon_m)i_3 - i_2 \quad (4.141)$$

Assume at first that the current mirror is ideal so that  $\epsilon_m = 0$ . Then since  $i_3 = -i_1$ , substituting (4.138) and (4.139) in (4.141) gives

$$i_{out} = g_{m(dp)}v_{id} \quad (4.142)$$

Therefore, with an active load,

$$G_m[dm] = \left. \frac{i_{out}}{v_{id}} \right|_{v_{out}=0} = g_{m(dp)} \quad (4.143)$$

Equation 4.143 applies for both the bipolar and MOS amplifiers shown in Fig. 4.25. Comparing (4.140) and (4.143) shows that the current-mirror load doubles the differential transconductance

compared to the passive-load case. This result stems from the fact that the current mirror creates a second signal path to the output. (The first path is through the differential pair.) Although frequency response is not analyzed in this chapter, note that the two signal paths usually have different frequency responses, which is often important in high-speed applications.

The key assumptions that led to (4.142) and (4.143) are that the current mirror is ideal so  $\epsilon_m = 0$  and that  $r_{tail} \rightarrow \infty$  and  $r_{o(dp)} \rightarrow \infty$ . Under these assumptions, the output current is independent of the common-mode input. In practice, none of these assumptions is exactly true, and the output current depends on the common-mode input. However, this dependence is small because the active load greatly enhances the common-mode rejection ratio of this stage, as shown in Section 4.3.5.3.

Another important parameter of the differential pair with active load is the output resistance. The output resistance is calculated using the circuit of Fig. 4.27, in which a test voltage source  $v_t$  is applied at the output while the inputs are connected to small-signal ground. The resulting current  $i_t$  has four components. The current in  $r_{o4}$  is

$$i_{t1} = \frac{v_t}{r_{o4}} \tag{4.144}$$

The resistance in the emitter or source lead of  $T_2$  is  $r_{tail}$  in parallel with the resistance seen looking into the emitter or source of  $T_1$ , which is approximately  $1/g_{m1}$ . Thus, using (3.99) for a transistor with degeneration, we find that the effective output resistance looking into the collector or drain of  $T_2$  is

$$R_{o2} \simeq r_{o2} \left( 1 + g_{m2} \frac{1}{g_{m1}} \right) = 2r_{o2} \tag{4.145}$$

Hence

$$i_{t2} + i_{t4} \simeq \frac{v_t}{2r_{o2}} \tag{4.146}$$

If  $r_{tail} \gg 1/g_{m1}$ , this current flows into the emitter or source of  $T_1$ , and is mirrored to the output with a gain of approximately unity to produce

$$i_{t3} \simeq i_{t2} + i_{t4} \simeq \frac{v_t}{2r_{o2}} \tag{4.147}$$

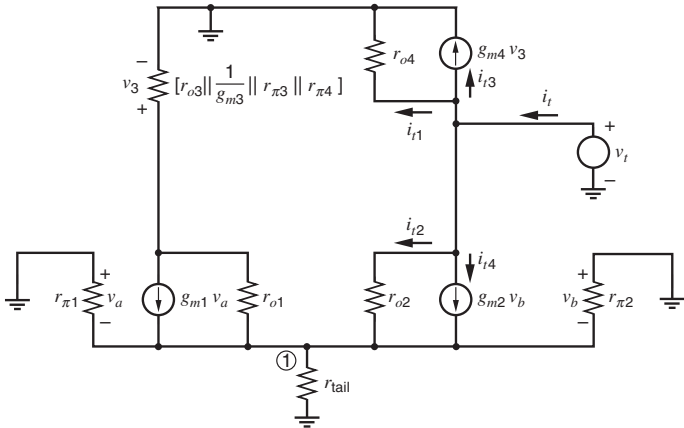


**Figure 4.27** Circuit for calculation of the output resistance of the differential pair with current-mirror load.

Thus

$$i_t = i_{t1} + i_{t2} + i_{t3} + i_{t4} \simeq v_t \left( \frac{1}{r_{o4}} + \frac{1}{r_{o2}} \right) \tag{4.148}$$

Since  $r_{o2} = r_{o(dp)}$  and  $r_{o4} = r_{o(mir)}$ ,

$$R_o = \frac{v_t}{i_t} \bigg|_{v_{i1}=0, v_{i2}=0} \simeq \frac{1}{\frac{1}{r_{o(dp)}} + \frac{1}{r_{o(mir)}}} = r_{o(dp)} || r_{o(mir)} \tag{4.149}$$

The result in (4.149) applies for both the bipolar and MOS amplifiers shown in Fig. 4.25. In multistage bipolar amplifiers, the low-frequency gain of the loaded circuit is likely to be reduced by the input resistance of the next stage because the output resistance is high. In contrast, low-frequency loading is probably not an issue in multistage MOS amplifiers because the next stage has infinite input resistance if the input is the gate of an MOS transistor.

Finally, although the source-coupled pair has infinite input resistance, the emitter-coupled pair has finite input resistance because  $\beta_0$  is finite. If the effects of the  $r_o$  of  $T_2$  and  $T_4$  are neglected, the differential input resistance of the actively loaded emitter-coupled pair is simply  $2r_{\pi(dp)}$  as in the resistively loaded case. In practice, however, the asymmetry of the circuit together with the high voltage gain cause feedback to occur through the output resistance of  $T_2$  to node ①. This feedback causes the input resistance to differ slightly from  $2r_{\pi(dp)}$ .

In summary, the actively loaded differential pair is capable of providing differential-to-single-ended conversion, that is, the conversion from a differential voltage to a voltage referenced to the ground potential. The high output resistance of the circuit requires that the next stage must have high input resistance if the large gain is to be realized. A small-signal two-port equivalent circuit for the stage is shown in Fig. 4.28.

### 4.3.5.3 Common-Mode Rejection Ratio

In addition to providing high voltage gain, the circuits in Fig. 4.25 provide conversion from a differential input signal to an output signal that is referenced to ground. Such a conversion is required in all differential-input, single-ended output amplifiers.

The simplest differential-to-single-ended converter is a resistively loaded differential pair in which the output is taken from only one side, as shown in Fig. 4.29a. In this case,  $A_{dm} > 0$ ,  $A_{cm} < 0$ , and the output is

$$v_o = -\frac{v_{od}}{2} + v_{oc} = -\frac{A_{dm}v_{id}}{2} + A_{cm}v_{ic} \tag{4.150}$$

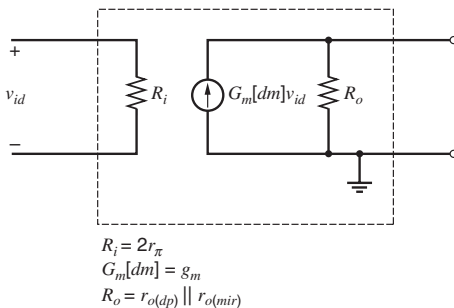


**Figure 4.28** Two-port representation of small-signal properties of differential pair with current-mirror load. The effects of asymmetrical input resistance have been neglected.

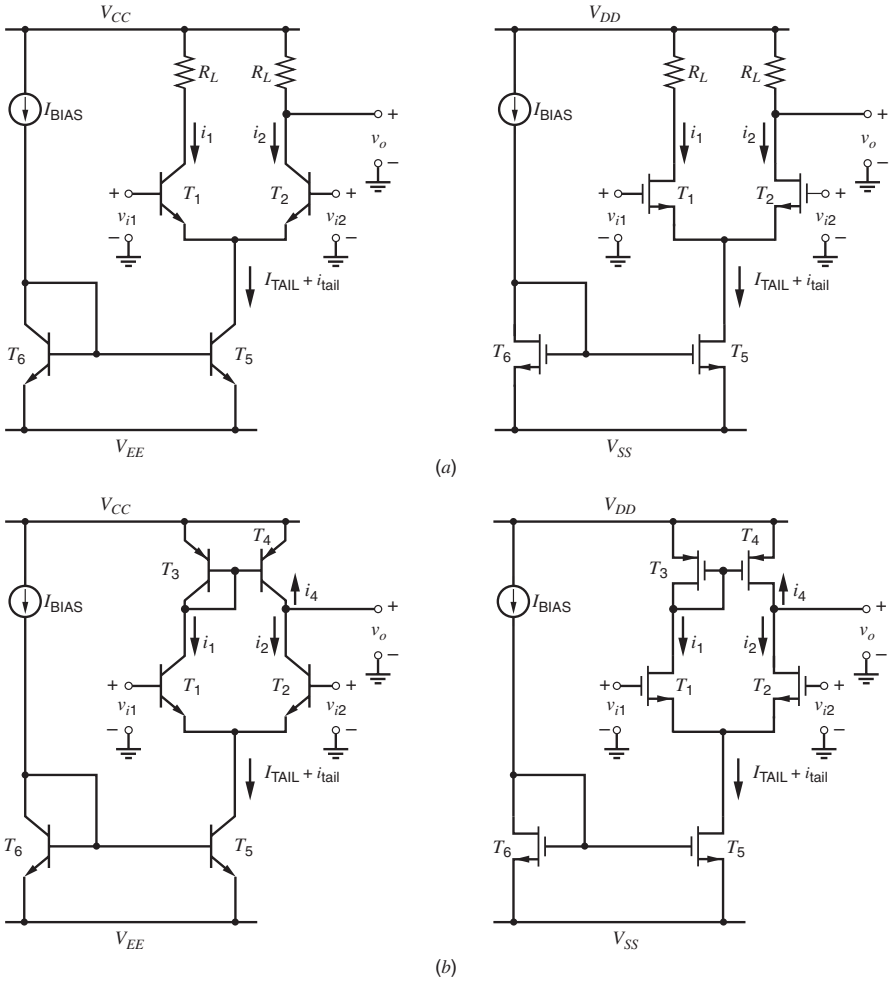


**Figure 4.29** Differential-to-single-ended conversion using (a) resistively loaded differential pairs and (b) actively loaded differential pairs.

$$v_o = -\frac{A_{dm}}{2} \left( v_{id} - \frac{2A_{cm}}{A_{dm}} v_{ic} \right) = -\frac{A_{dm}}{2} \left( v_{id} + 2 \left| \frac{A_{cm}}{A_{dm}} \right| v_{ic} \right) \quad (4.151)$$

$$= -\frac{A_{dm}}{2} \left( v_{id} + \frac{2v_{ic}}{CMRR} \right) \quad (4.152)$$

Thus, common-mode signals at the input will cause changes in the output voltage. The common-mode rejection ratio (CMRR) is

$$CMRR = \left| \frac{A_{dm}}{A_{cm}} \right| = \left| \frac{G_m[dm]R_o}{G_m[cm]R_o} \right| = \left| \frac{G_m[dm]}{G_m[cm]} \right| \quad (4.153)$$

where the common-mode (cm) transconductance is

$$G_m[cm] = \left. \frac{i_{out}}{v_{ic}} \right|_{v_{out}=0} \quad (4.154)$$

Since the circuits in Fig. 4.29a are symmetrical, a common-mode half circuit can be used to find  $G_m[cm]$ . The common-mode half circuit is a common-emitter/source amplifier with degeneration. From (3.93) and (3.104),

$$G_m[cm] = -\frac{i_2}{v_{ic}} \simeq -\frac{g_m(dp)}{1 + g_m(dp)(2r_{tail})} \quad (4.155)$$

where  $g_m(dp) = g_{m1} = g_{m2}$  and  $r_{tail}$  represents the output resistance of the tail current source  $T_5$ . The negative sign appears in (4.155) because the output current is defined as positive when it flows from the output terminal into the small-signal ground to be consistent with the differential case, as in Fig. 4.26b. Equation 4.155 applies for both the bipolar and MOS cases if the base current is ignored in the bipolar case, the body effect is ignored in the MOS case, and  $r_{o1}$  and  $r_{o2}$  are ignored in both cases. Substituting (4.140) and (4.155) into (4.153) gives

$$CMRR = \frac{1 + 2g_m(dp)r_{tail}}{2} \simeq g_m(dp)r_{tail} = g_{m1}r_{o5} \quad (4.156)$$

Equation 4.156 shows that the common-mode rejection ratio here is about half that in (3.193) because the outputs in Fig. 4.29 are taken only from one side of each differential pair instead of from both sides, reducing the differential-mode gain by a factor of two. The result in (4.156) applies for both the bipolar and MOS amplifiers shown in Fig. 4.29a. Because  $g_m r_o$  is much higher for bipolar transistors than MOS transistors, the CMRR of a bipolar differential pair with resistive load is much higher than that of its MOS counterpart.

On the other hand, the active-load stages shown in Fig 4.29b have common-mode rejection ratios much superior to those of the corresponding circuits in Fig. 4.29a. Assume that the outputs in Fig. 4.29b are connected to small-signal ground to allow calculation of the common-mode transconductance. The small-signal model is the same as shown in Fig. 4.26b with  $v_{i1} = v_{i2} = v_{ic}$ . For simplicity, let  $\beta_0 \rightarrow \infty$  and  $r_\pi \rightarrow \infty$  at first. As with a resistive load, changes in the common-mode input will cause changes in the tail bias current  $i_{tail}$  because the output resistance of  $T_5$  is finite. If we assume that the currents in the differential-pair transistors are controlled only by the base-emitter or gate-source voltages, the change in the current in  $T_1$  and  $T_2$  is

$$i_1 = i_2 = \frac{i_{tail}}{2} \quad (4.157)$$

If  $\epsilon_m = 0$ , the gain of the current mirror is unity. Then substituting (4.157) into (4.141) with  $i_3 = -i_1$  gives

$$i_{out} = -i_3 - i_2 = i_1 - i_2 = 0 \quad (4.158)$$

As a result,

$$G_m[cm] = \left. \frac{i_{out}}{v_{ic}} \right|_{v_{out}=0} = 0 \quad (4.159)$$

Therefore,

$$CMRR \rightarrow \infty \quad (4.160)$$

The common-mode rejection ratio in (4.160) is infinite because the change in the current in  $T_4$  cancels that in  $T_2$  even when  $r_{tail}$  is finite under these assumptions.

The key assumptions that led to (4.160) are that  $r_{o(dp)} \rightarrow \infty$  so  $i_1 = i_2$  and that the current mirror is ideal so  $\epsilon_m = 0$ . In practice, the currents in the differential-pair transistors are not

only controlled by their base-emitter or gate-source voltages, but also to some extent by their collector-emitter or drain-source voltages. As a result,  $i_1$  is not exactly equal to  $i_2$  because of finite  $r_{o(dp)}$  in  $T_1$  and  $T_2$ . Furthermore, the gain of the current mirror is not exactly unity, which means that  $\epsilon_m$  is not exactly zero in practice because of finite  $r_{o(mir)}$  in  $T_3$  and  $T_4$ . Finite  $\beta_0$  also affects the systematic gain error of the current mirror when bipolar transistors are used. For these reasons, the common-mode rejection ratio is finite in practice. However, the use of the active load greatly improves the common-mode rejection ratio compared to the resistive load case, as we will show next.

Suppose that

$$i_1 = i_2(1 - \epsilon_d) \quad (4.161)$$

where  $\epsilon_d$  can be thought of as the gain error in the differential pair. Substituting (4.161) into (4.141) with  $i_3 = -i_1$  gives

$$i_{out} = i_1(1 - \epsilon_m) - i_2 = i_2((1 - \epsilon_d)(1 - \epsilon_m) - 1) \quad (4.162)$$

Rearranging (4.162) gives

$$i_{out} = -i_2(\epsilon_d + \epsilon_m - \epsilon_d\epsilon_m) \quad (4.163)$$

If  $\epsilon_d \ll 1$  and  $\epsilon_m \ll 1$ , the product term  $\epsilon_d\epsilon_m$  is a second-order error and can be neglected. Therefore,

$$i_{out} \simeq -i_2(\epsilon_d + \epsilon_m) \quad (4.164)$$

Substituting (4.164) into (4.154) gives

$$G_m[cm] \simeq -\left(\frac{i_2}{v_{ic}}\right)(\epsilon_d + \epsilon_m) \quad (4.165)$$

Equation 4.165 applies for the active-load circuits shown in Fig. 4.29b; however, the first term has approximately the same value as in the passive-load case. Therefore, we will substitute (4.155) into (4.165), which gives

$$G_m[cm] \simeq -\left(\frac{g_m(dp)}{1 + g_m(dp)(2r_{tail})}\right)(\epsilon_d + \epsilon_m) \quad (4.166)$$

Substituting (4.166) and (4.143) into (4.153) gives

$$CMRR = \left|\frac{G_m[dm]}{G_m[cm]}\right| \simeq \frac{1 + 2g_m(dp)r_{tail}}{(\epsilon_d + \epsilon_m)} \quad (4.167)$$

Comparing (4.167) and (4.156) shows that the active load improves the common-mode rejection ratio by a factor of  $2/(\epsilon_d + \epsilon_m)$ . The factor of 2 in the numerator of this expression stems from the increase in the differential transconductance, and the denominator stems from the decrease in the common-mode transconductance.

To find  $\epsilon_d$ , we will refer to Fig. 4.26b with  $v_{i1} = v_{i2} = v_{ic}$ . First, we write

$$i_1 = g_m(dp)(v_{ic} - v_1) + \frac{v_3 - v_1}{r_{o(dp)}} \quad (4.168)$$

and

$$i_2 = g_m(dp)(v_{ic} - v_1) - \frac{v_1}{r_{o(dp)}} \quad (4.169)$$

Substituting (4.134) and  $i_3 = -i_1$  into (4.168) gives

$$i_1 \simeq g_m(dp)(v_{ic} - v_1) - \frac{v_1}{r_{o(dp)}} - \frac{i_1}{g_m(mir)r_{o(dp)}} \quad (4.170)$$

Equation 4.170 can be rearranged to give

$$\left( \frac{1 + g_m(\text{mir})r_{o(dp)}}{g_m(\text{mir})r_{o(dp)}} \right) i_1 \simeq g_m(dp)(v_{ic} - v_1) - \frac{v_1}{r_{o(dp)}} \quad (4.171)$$

Substituting (4.169) into (4.171) gives

$$i_1 \simeq \left( \frac{g_m(\text{mir})r_{o(dp)}}{1 + g_m(\text{mir})r_{o(dp)}} \right) i_2 \quad (4.172)$$

Substituting (4.161) into (4.172) gives

$$\epsilon_d \simeq \frac{1}{1 + g_m(\text{mir})r_{o(dp)}} \quad (4.173)$$

To find  $\epsilon_m$ , we will again refer to Fig. 4.26b with  $v_{i1} = v_{i2} = v_{ic}$ . In writing (4.134), we assumed that  $r_3 \simeq 1/g_{m3}$ . We will now reconsider this assumption and write

$$r_3 = \frac{1}{g_{m3}} ||r_{\pi 3}||r_{\pi 4}||r_{o3} \quad (4.174)$$

We will still assume that the two transistors in the differential pair match perfectly and operate with equal dc currents, as do the two transistors in the active load. Then (4.174) can be rewritten as

$$r_3 = \frac{r_{\pi(\text{mir})}r_{o(\text{mir})}}{r_{\pi(\text{mir})} + 2r_{o(\text{mir})} + g_m(\text{mir})r_{\pi(\text{mir})}r_{o(\text{mir})}} \quad (4.175)$$

Substituting (4.175) into (4.135) gives

$$g_{m4}v_3 = g_{m4}i_3r_3 = \frac{g_m(\text{mir})r_{\pi(\text{mir})}r_{o(\text{mir})}i_3}{r_{\pi(\text{mir})} + 2r_{o(\text{mir})} + g_m(\text{mir})r_{\pi(\text{mir})}r_{o(\text{mir})}} \quad (4.176)$$

Substituting (4.133) into (4.176) gives

$$\epsilon_m = \frac{r_{\pi(\text{mir})} + 2r_{o(\text{mir})}}{r_{\pi(\text{mir})} + 2r_{o(\text{mir})} + g_m(\text{mir})r_{\pi(\text{mir})}r_{o(\text{mir})}} \quad (4.177)$$

For bipolar transistors,  $r_{\pi}$  is usually much less than  $r_o$ ; therefore,

$$\epsilon_m[\text{bip}] = \frac{2 + \frac{r_{\pi(\text{mir})}}{r_{o(\text{mir})}}}{2 + \frac{r_{\pi(\text{mir})}}{r_{o(\text{mir})}} + g_m(\text{mir})r_{\pi(\text{mir})}} \simeq \frac{1}{1 + \frac{g_m(\text{mir})r_{\pi(\text{mir})}}{2}} = \frac{1}{1 + \frac{\beta_0}{2}} \quad (4.178)$$

Since  $r_{\pi} \rightarrow \infty$  for MOS transistors,

$$\epsilon_m[\text{MOS}] = \frac{1}{1 + g_m(\text{mir})r_{o(\text{mir})}} \quad (4.179)$$

For the bipolar circuit in Fig. 4.29b, substituting (4.173) and (4.178) into (4.167) gives

$$\text{CMRR} \simeq \frac{1 + 2g_m(dp)r_{\text{tail}}}{\left( \frac{1}{1 + g_m(\text{mir})r_{o(dp)}} + \frac{1}{1 + \frac{g_m(\text{mir})r_{\pi(\text{mir})}}{2}} \right)} \quad (4.180)$$

If  $(g_m(mir)r_{o(dp)}) \gg 1$  and  $(g_m(mir)r_{\pi(mir)}/2) \gg 1$ , (4.180) can be simplified to give

$$\begin{aligned} \text{CMRR} &\simeq (1 + 2g_m(dp)r_{\text{tail}})g_m(mir) \left( r_{o(dp)} \parallel \frac{r_{\pi(mir)}}{2} \right) \\ &\simeq (2g_m(dp)r_{\text{tail}})g_m(mir) \left( r_{o(dp)} \parallel \frac{r_{\pi(mir)}}{2} \right) \end{aligned} \quad (4.181)$$

Comparing (4.181) and (4.156) shows that the active load increases the common-mode rejection ratio by a factor of about  $2g_m(mir) (r_{o(dp)} \parallel (r_{\pi(mir)}/2))$  for the bipolar circuit in Fig. 4.29b compared to its passive-load counterpart in Fig. 4.29a.

On the other hand, for the MOS circuit in Fig. 4.29b, substituting (4.173) and (4.179) into (4.167) gives

$$\text{CMRR} \simeq \frac{1 + 2g_m(dp)r_{\text{tail}}}{\left( \frac{1}{1 + g_m(mir)r_{o(dp)}} + \frac{1}{1 + g_m(mir)r_{o(mir)}} \right)} \quad (4.182)$$

If  $(g_m(mir)r_{o(dp)}) \gg 1$  and  $(g_m(mir)r_{o(mir)}) \gg 1$ , (4.182) can be simplified to give

$$\begin{aligned} \text{CMRR} &\simeq (1 + 2g_m(dp)r_{\text{tail}})g_m(mir)(r_{o(dp)} \parallel r_{o(mir)}) \\ &\simeq (2g_m(dp)r_{\text{tail}})g_m(mir)(r_{o(dp)} \parallel r_{o(mir)}) \end{aligned} \quad (4.183)$$

Comparing (4.183) and (4.156) shows that the active load increases the common-mode rejection ratio by a factor of about  $2g_m(mir)(r_{o(dp)} \parallel r_{o(mir)})$  for the MOS circuit in Fig. 4.29b compared to its passive-load counterpart in Fig. 4.29a.

For these calculations, perfect matching was assumed so that  $g_{m1} = g_{m2}$ ,  $g_{m3} = g_{m4}$ ,  $r_{o1} = r_{o2}$ , and  $r_{o3} = r_{o4}$ . In practice, however, nonzero mismatch occurs. With mismatch in a MOS differential pair using a current-mirror load, the differential-mode transconductance is

$$G_m[dm] \simeq g_{m1-2} \left[ \frac{1 - \left( \frac{\Delta g_{m1-2}}{2g_{m1-2}} \right)^2}{1 + \left( \frac{\Delta g_{m3-4}}{2g_{m3-4}} \right)} \right] \quad (4.184)$$

where  $\Delta g_{m1-2} = g_{m1} - g_{m2}$ ,  $g_{m1-2} = (g_{m1} + g_{m2})/2$ ,  $\Delta g_{m3-4} = g_{m3} - g_{m4}$ , and  $g_{m3-4} = (g_{m3} + g_{m4})/2$ . See Problem 4.18. The approximation in (4.184) is valid to the extent that  $g_m r_o \gg 1$  for each transistor and  $(g_{m1} + g_{m2})r_{\text{tail}} \gg 1$  for the tail current source. Equation 4.184 shows that the mismatch between  $g_{m1}$  and  $g_{m2}$  has only a minor effect on  $G_m[dm]$ . This result stems from the fact that the small-signal voltage across the tail current source,  $v_{\text{tail}}$ , is zero with a purely differential input only when  $g_{m1} = g_{m2}$ , assuming  $r_{o1} \rightarrow \infty$  and  $r_{o2} \rightarrow \infty$ . For example, increasing  $g_{m1}$  compared to  $g_{m2}$  tends to increase the small-signal drain current  $i_1$  if  $v_{gs1}$  is constant. However, this change also increases  $v_{\text{tail}}$ , which reduces  $v_{gs1}$  for a fixed  $v_{id}$ . The combination of these two effects causes  $i_1$  to be insensitive to  $g_{m1} - g_{m2}$ . On the other hand, mismatch between  $g_{m3}$  and  $g_{m4}$  directly modifies the contribution of  $i_1$  through the current mirror to the output current. Therefore, (4.184) shows that  $G_m[dm]$  is most sensitive to the mismatch between  $g_{m3}$  and  $g_{m4}$ .

With mismatch in a MOS differential pair using a current-mirror load, the common-mode transconductance is

$$G_m[cm] \simeq -\frac{1}{2r_{\text{tail}}}(\epsilon_d + \epsilon_m) \quad (4.185)$$

where  $\epsilon_d$  is the gain error in the source-coupled pair with a pure common-mode input defined in (4.161) and  $\epsilon_m$  is the gain error in the current mirror defined in (4.133). From Problem 4.19,

$$\epsilon_d \simeq \frac{1}{g_{m3}r_{o(dp)}} - \frac{\Delta g_{m1-2}}{g_{m1-2}} \left( 1 + \frac{2r_{\text{tail}}}{r_{o(dp)}} \right) - \frac{2r_{\text{tail}}}{r_{o(dp)}} \frac{\Delta r_{o(dp)}}{r_{o(dp)}} \quad (4.186)$$

Each term in (4.186) corresponds to one source of gain error by itself, and interactions between terms are ignored. The first term in (4.186) is consistent with (4.173) when  $g_{m3}r_{o(dp)} \gg 1$  and stems from the observation that the drain of  $T_1$  is not connected to a small-signal ground during the calculation of  $G_m[dm]$ , unlike the drain of  $T_2$ . The second term in (4.186) stems from mismatch between  $g_{m1}$  and  $g_{m2}$  alone. The third term in (4.186) stems from the mismatch between  $r_{o1}$  and  $r_{o2}$  alone. The contribution of this mismatch to  $G_m[cm]$  is significant because the action of the current mirror nearly cancels the contributions of the input  $g_m$  generators to  $G_m[cm]$  under ideal conditions, causing  $G_m[cm] \simeq 0$  in (4.166). In contrast,  $G_m[dm]$  is insensitive to the mismatch between  $r_{o1}$  and  $r_{o2}$  because the dominant contributions to  $G_m[dm]$  arising from the input  $g_m$  generators do not cancel at the output. From Problem 4.19,

$$\epsilon_m = \frac{1}{1 + g_{m3}r_{o3}} + \frac{(g_{m3} - g_{m4})r_{o3}}{1 + g_{m3}r_{o3}} \simeq \frac{1}{g_{m3}r_{o3}} + \frac{\Delta g_{m3-4}}{g_{m3-4}} \quad (4.187)$$

Each term in (4.187) corresponds to one source of gain error by itself, and interactions between terms are ignored. The first term in (4.187), which is consistent with (4.179) when  $g_{m3}r_{o3} \gg 1$ , stems from the observation that the small-signal input resistance of the current mirror is not exactly  $1/g_{m3}$  but  $(1/g_{m3})||r_{o3}$ . The second term in (4.187) stems from mismatch between  $g_{m3}$  and  $g_{m4}$  alone. The CMRR with mismatch is the ratio of  $G_m[dm]$  in (4.184) to  $G_m[cm]$  in (4.185), using (4.186) and (4.187) for  $\epsilon_d$  and  $\epsilon_m$ , respectively. Since the common-mode transconductance is very small without mismatch (as a result of the behavior of the current-mirror load), mismatch usually reduces the CMRR by increasing  $|G_m[cm]|$ .

## 4.4 Voltage and Current References

### 4.4.1 Low-Current Biasing

#### 4.4.1.1 Bipolar Widlar Current Source

In ideal operational amplifiers, the current is zero in each of the two input leads. However, the input current is not zero in real op amps with bipolar input transistors because  $\beta_F$  is finite. Since the op-amp inputs are usually connected to a differential pair, the tail current must usually be very small in such op amps to keep the input current small. Typically, the tail current is on the order of 5  $\mu\text{A}$ . Bias currents of this magnitude are also required in a variety of other applications, especially where minimizing power dissipation is important. The simple current mirrors shown in Fig. 4.30 are usually not optimum for such small currents. For example, using a simple bipolar current mirror as in Fig. 4.30a and assuming a maximum practical emitter area ratio between transistors of ten to one, the mirror would need an input current of 50  $\mu\text{A}$  for an output current of 5  $\mu\text{A}$ . If the power-supply voltage in Fig. 4.30a is 5 V, and if  $V_{BE(\text{on})} = 0.7 \text{ V}$ ,  $R = 86 \text{ k}\Omega$  would be required. Resistors of this magnitude are costly in terms of die area. Currents of such low magnitude can be obtained with moderate values of resistance, however, by modifying the simple current mirror so that the transistors operate with unequal base-emitter voltages. In the Widlar current source of Fig. 4.31a, resistor  $R_2$  is inserted in series with the emitter of  $Q_2$ , and transistors  $Q_1$  and  $Q_2$  operate with unequal base emitter voltages if  $R_2 \neq 0$ .<sup>10,11</sup> This circuit is referred to as a current source rather than a current mirror because the output current in Fig. 4.31a is much less dependent on the input

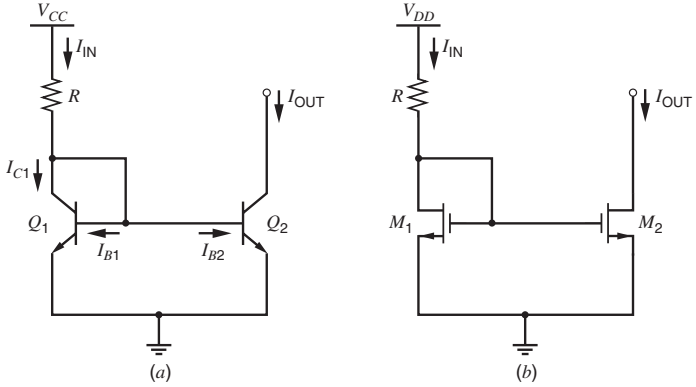


**Figure 4.30** Simple two-transistor current mirrors where the input current is set by the supply voltage and a resistor using (a) bipolar and (b) MOS transistors.

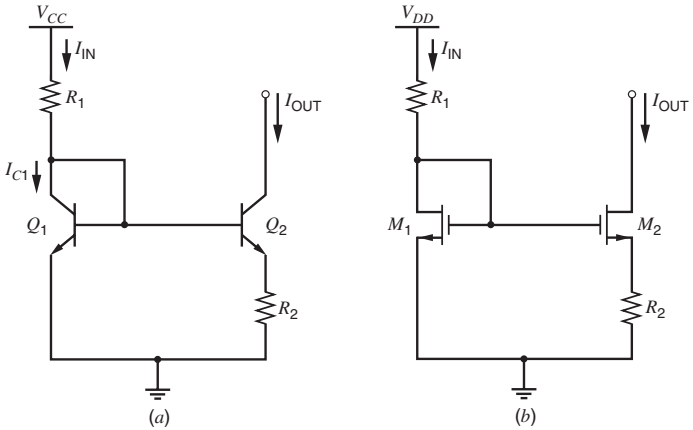


**Figure 4.31** Widlar current sources: (a) bipolar and (b) MOS.

current and the power-supply voltage than in the simple current mirror of Fig. 4.30a, as shown in Section 4.4.2. We will now calculate the output current of the Widlar current source.

If  $I_{IN} > 0$ ,  $Q_1$  operates in the forward-active region because it is diode connected. Assume that  $Q_2$  also operates in the forward active region. KVL around the base-emitter loop gives

$$V_{BE1} - V_{BE2} - \frac{\beta_F + 1}{\beta_F} I_{OUT} R_2 = 0 \tag{4.188}$$

If we assume that  $V_{BE1} = V_{BE2} = V_{BE(on)} = 0.7\text{ V}$  in (4.188), we would predict that  $I_{OUT} = 0$ . Although  $I_{OUT}$  is small in practice, it is greater than zero under the usual bias conditions, which means that the standard assumption about  $V_{BE(on)}$  is invalid here. In contrast, the standard assumption is usually valid in calculating  $I_{IN}$  because small variations in  $V_{BE1}$  have little effect on  $I_{IN}$  if  $V_{CC} \gg V_{BE1}$ . When one base-emitter voltage is subtracted from another, however, small differences between them are important. If  $V_A \rightarrow \infty$ , (4.188) can be rewritten

using (1.35) as

$$V_T \ln \frac{I_{C1}}{I_{S1}} - V_T \ln \frac{I_{OUT}}{I_{S2}} - \frac{\beta_F + 1}{\beta_F} I_{OUT} R_2 = 0 \quad (4.189)$$

If  $\beta_F \rightarrow \infty$ , (4.189) simplifies to

$$V_T \ln \frac{I_{IN}}{I_{S1}} - V_T \ln \frac{I_{OUT}}{I_{S2}} - I_{OUT} R_2 = 0 \quad (4.190)$$

For identical transistors,  $I_{S1}$  and  $I_{S2}$  are equal, and (4.190) becomes

$$V_T \ln \frac{I_{IN}}{I_{OUT}} = I_{OUT} R_2 \quad (4.191)$$

This transcendental equation can be solved by trial and error to find  $I_{OUT}$  if  $R_2$  and  $I_{IN}$  are known, as in typical analysis problems. Because the logarithm function compresses changes in its argument, attention can be focused on the linear term in (4.191), simplifying convergence of the trial-and-error process. In design problems, however, the desired  $I_{IN}$  and  $I_{OUT}$  are usually known, and (4.191) provides the required value of  $R_2$ .

#### ■ EXAMPLE

In the circuit of Fig. 4.31a, determine the proper value of  $R_2$  to give  $I_{OUT} = 5 \mu\text{A}$ . Assume that  $V_{CC} = 5 \text{ V}$ ,  $R_1 = 4.3 \text{ k}\Omega$ ,  $V_{BE(\text{on})} = 0.7 \text{ V}$ , and  $\beta_F \rightarrow \infty$ .

$$I_{IN} = \frac{5 \text{ V} - 0.7 \text{ V}}{4.3 \text{ k}\Omega} = 1 \text{ mA}$$

$$V_T \ln \frac{I_{IN}}{I_{OUT}} = 26 \text{ mV} \ln \left( \frac{1 \text{ mA}}{5 \mu\text{A}} \right) = 137 \text{ mV}$$

Thus from (4.191)

$$I_{OUT} R_2 = 137 \text{ mV}$$

and

$$R_2 = \frac{137 \text{ mV}}{5 \mu\text{A}} = 27.4 \text{ k}\Omega$$

- The total resistance in the circuit is  $31.7 \text{ k}\Omega$ .

#### ■ EXAMPLE

In the circuit of Fig. 4.31a, assume that  $I_{IN} = 1 \text{ mA}$ ,  $R_2 = 5 \text{ k}\Omega$ , and  $\beta_F \rightarrow \infty$ . Find  $I_{OUT}$ . From (4.191),

$$V_T \ln \frac{1 \text{ mA}}{I_{OUT}} - 5 \text{ k}\Omega(I_{OUT}) = 0$$

Try

$$I_{OUT} = 15 \mu\text{A}$$

$$108 \text{ mV} - 75 \text{ mV} \neq 0$$

The linear term  $I_{OUT} R_2$  is too small; therefore,  $I_{OUT} > 15 \mu\text{A}$  should be tried. Try

$$I_{OUT} = 20 \mu\text{A}$$

$$101.7 \text{ mV} - 100 \text{ mV} \simeq 0$$

Therefore, the output current is close to 20  $\mu\text{A}$ . Notice that while the linear term increased by 25 mV from the first to the second trial, the logarithm term decreased by only about 6 mV because the logarithm function compresses changes in its argument.

#### 4.4.1.2 MOS Widlar Current Source

The Widlar configuration can also be used in MOS technology, as shown in Fig. 4.31*b*.

If  $I_{\text{IN}} > 0$ ,  $M_1$  operates in the active region because it is diode connected. Assume that  $M_2$  also operates in the forward active region. KVL around the gate-source loop gives

$$V_{GS1} - V_{GS2} - I_{\text{OUT}}R_2 = 0 \quad (4.192)$$

If we ignore the body effect, the threshold components of the gate-source voltages cancel and (4.192) simplifies to

$$I_{\text{OUT}}R_2 + V_{ov2} - V_{ov1} = 0 \quad (4.193)$$

If the transistors operate in strong inversion and  $V_A \rightarrow \infty$ ,

$$I_{\text{OUT}}R_2 + \sqrt{\frac{2I_{\text{OUT}}}{k'(W/L)_2}} - V_{ov1} = 0 \quad (4.194)$$

This quadratic equation can be solved for  $\sqrt{I_{\text{OUT}}}$ .

$$\sqrt{I_{\text{OUT}}} = \frac{-\sqrt{\frac{2}{k'(W/L)_2}} \pm \sqrt{\frac{2}{k'(W/L)_2} + 4R_2V_{ov1}}}{2R_2} \quad (4.195)$$

where  $V_{ov1} = \sqrt{2I_{\text{IN}}/[k'(W/L)_1]}$ . From (1.157),

$$\sqrt{I_{\text{OUT}}} = \sqrt{\frac{k'(W/L)_2}{2}} (V_{GS2} - V_t) \quad (4.196)$$

Equation 4.196 applies only when  $M_2$  operates in the active region, which means that  $V_{GS2} > V_t$ . As a result,  $\sqrt{I_{\text{OUT}}} > 0$  and the potential solution where the second term in the numerator of (4.195) is subtracted from the first, cannot occur in practice. Therefore,

$$\sqrt{I_{\text{OUT}}} = \frac{-\sqrt{\frac{2}{k'(W/L)_2}} + \sqrt{\frac{2}{k'(W/L)_2} + 4R_2V_{ov1}}}{2R_2} \quad (4.197)$$

Equation 4.197 shows that a closed-form solution for the output current can be written for a Widlar current source that uses MOS transistors operating in strong inversion, unlike the bipolar case where trial and error is required to find  $I_{\text{OUT}}$ .

#### EXAMPLE

In Fig. 4.31*b*, find  $I_{\text{OUT}}$  if  $I_{\text{IN}} = 100 \mu\text{A}$ ,  $R_2 = 4 \text{ k}\Omega$ ,  $k' = 200 \mu\text{A}/\text{V}^2$ , and  $(W/L)_1 = (W/L)_2 = 25$ . Assume the temperature is 27°C and that  $n = 1.5$  in (1.247).

Then  $R_2 = 0.004 \text{ M}\Omega$ ,  $V_{ov1} = \sqrt{200/(200 \times 25)} \text{ V} = 0.2 \text{ V}$ ,

$$\sqrt{I_{\text{OUT}}} = \frac{-\sqrt{\frac{2}{200(25)}} + \sqrt{\frac{2}{200(25)} + 4(0.004)(0.2)}}{2(0.004)} \sqrt{\mu\text{A}} = 5\sqrt{\mu\text{A}}$$

and  $I_{OUT} = 25 \mu\text{A}$ . Also,

$$V_{ov2} = V_{ov1} - I_{OUT}R_2 = 0.2 - 25 \times 0.004 = 0.1 \text{ V} > 2nV_T \simeq 78 \text{ mV}$$

- Therefore, both transistors operate in strong inversion, as assumed.

#### 4.4.1.3 Bipolar Peaking Current Source

The Widlar source described in Section 4.4.1.1 allows currents in the microamp range to be realized with moderate values of resistance. Biasing integrated-circuit stages with currents on the order of nanoamps is often desirable. To reach such low currents with moderate values of resistance, the circuit shown in Fig. 4.32 can be used.<sup>12,13,14</sup> Neglecting base currents, we have

$$V_{BE1} - I_{IN}R = V_{BE2} \quad (4.198)$$

If  $V_A \rightarrow \infty$ , (4.198) can be rewritten using (1.35) as

$$V_T \ln \frac{I_{IN}}{I_{S1}} - V_T \ln \frac{I_{OUT}}{I_{S2}} = I_{IN}R \quad (4.199)$$

If  $Q_1$  and  $Q_2$  are identical, (4.199) can be rewritten as

$$I_{OUT} = I_{IN} \exp\left(-\frac{I_{IN}R}{V_T}\right) \quad (4.200)$$

Equation 4.200 is useful for analysis of a given circuit. For design with identical  $Q_1$  and  $Q_2$ , (4.199) can be rewritten as

$$R = \frac{V_T}{I_{IN}} \ln \frac{I_{IN}}{I_{OUT}} \quad (4.201)$$

For example, for  $I_{IN} = 10 \mu\text{A}$  and  $I_{OUT} = 100 \text{ nA}$ , (4.201) can be used to show that  $R \simeq 12 \text{ k}\Omega$ .

A plot of  $I_{OUT}$  versus  $I_{IN}$  from (4.200) is shown in Fig. 4.33. When the input current is small, the voltage drop on the resistor is small, and  $V_{BE2} \simeq V_{BE1}$  so  $I_{OUT} \simeq I_{IN}$ . As the input current increases,  $V_{BE1}$  increases in proportion to the logarithm of the input current while the drop on the resistor increases linearly with the input current. As a result, increases in the input current eventually cause the base-emitter voltage of  $Q_2$  to decrease. The output current

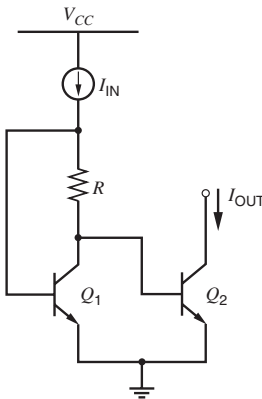
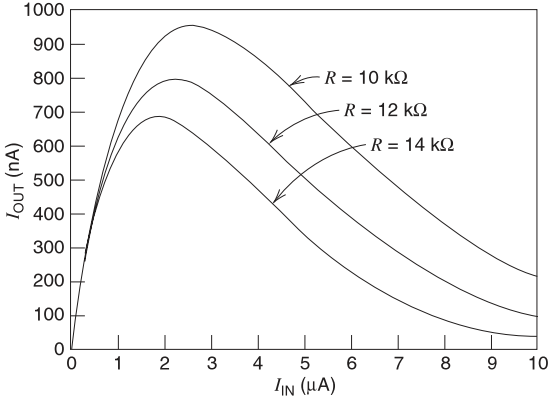


Figure 4.32 Bipolar peaking current source.



**Figure 4.33** Transfer characteristics of the bipolar peaking current source with  $T = 27^{\circ}\text{C}$ .

reaches a maximum when  $V_{BE2}$  is maximum. The name *peaking current source* stems from this behavior, and the location and magnitude of the peak both depend on  $R$ .

**4.4.1.4 MOS Peaking Current Source**

The peaking-current configuration can also be used in MOS technology, as shown in Fig. 4.34. If  $I_{IN}$  is small and positive, the voltage drop on  $R$  is small and  $M_1$  operates in the active region. Assume that  $M_2$  also operates in the active region. KVL around the gate-source loop gives

$$V_{GS1} - I_{IN}R - V_{GS2} = 0 \tag{4.202}$$

Since the sources of  $M_1$  and  $M_2$  are connected together, the thresholds cancel and (4.202) simplifies to

$$V_{ov2} = V_{ov1} - I_{IN}R \tag{4.203}$$

From (1.157),

$$I_{OUT} = \frac{k'(W/L)_2}{2}(V_{ov2})^2 = \frac{k'(W/L)_2}{2}(V_{ov1} - I_{IN}R)^2 \tag{4.204}$$

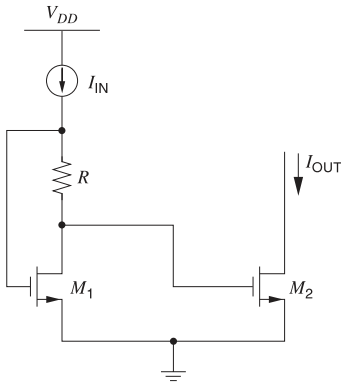


**Figure 4.34** MOS peaking current source.

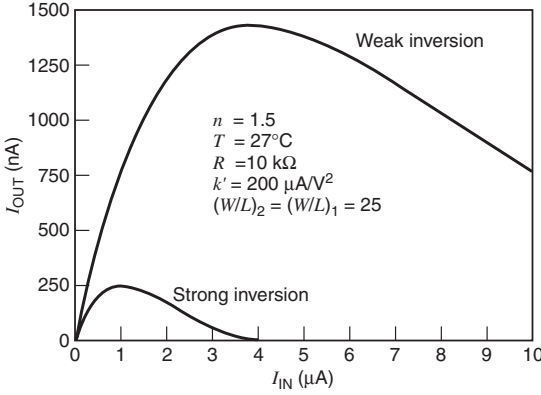


**Figure 4.35** Transfer characteristics of the MOS peaking current source assuming both transistors operate in weak inversion or in strong inversion.

where  $V_{ov1} = \sqrt{2I_{IN}/[k'(W/L)_1]}$ . Equation 4.204 assumes that the transistors operate in strong inversion. In practice, the input current is usually small enough that the overdrive of  $M_1$  is less than  $2nV_T$ , where  $n$  is defined in (1.247) and  $V_T$  is a thermal voltage. Equation 4.203 shows that the overdrive of  $M_2$  is even smaller than that of  $M_1$ . Therefore, both transistors usually operate in weak inversion, where the drain current is an exponential function of the gate-source voltage as shown in (1.252). If  $V_{DS1} > 3V_T$ , applying (1.252) to  $M_1$  and substituting into (4.202) gives

$$V_{GS2} - V_t \simeq nV_T \ln \left( \frac{I_{IN}}{(W/L)_1 I_t} \right) - I_{IN}R \tag{4.205}$$

Then if the transistors are identical and  $V_{DS2} > 3V_T$ , substituting (4.205) into (1.252) gives

$$I_{OUT} \simeq \frac{W}{L} I_t \exp \left( \frac{V_{GS2} - V_t}{nV_T} \right) \simeq I_{IN} \exp \left( -\frac{I_{IN}R}{nV_T} \right) \tag{4.206}$$

where  $I_t$  is given by (1.251) and represents the drain current of  $M_2$  with  $V_{GS2} = V_t$ ,  $W/L = 1$ , and  $V_{DS} \gg V_T$ . Comparing (4.206) with (4.200) shows that the output current in an MOS peaking current source where both transistors operate in weak inversion is the same as in the bipolar case except that  $1.3 \leq n \leq 1.5$  in the MOS case and  $n = 1$  in the bipolar case.

Plots of (4.206) and (4.204) are shown in Fig. 4.35 for  $n = 1.5$ ,  $T = 27^\circ C$ ,  $R = 10 \text{ k}\Omega$ ,  $k' = 200 \text{ }\mu\text{A/V}^2$ , and  $(W/L)_2 = (W/L)_1 = 25$ . In both cases, when the input current is small, the voltage drop on the resistor is small, and  $I_{OUT} \simeq I_{IN}$ . As the input current increases,  $V_{GS1}$  increases more slowly than the drop on the resistor. As a result, increases in the input current eventually cause the gate-source voltage of  $M_2$  to decrease. The output current reaches a maximum when  $V_{GS2}$  is maximum. As in the bipolar case, the name *peaking current source* stems from this behavior, and the location and magnitude of the peak both depend on  $R$ . Because the overdrives on both transistors are usually very small, the strong-inversion equation (4.204) usually underestimates the output current.

### 4.4.2 Supply-Insensitive Biasing

Consider the simple current mirror of Fig. 4.30a, where the input current source has been replaced by a resistor. Ignoring the effects of finite  $\beta_F$  and  $V_A$ , (4.5) shows that the output

current is

$$I_{OUT} \simeq I_{IN} = \frac{V_{CC} - V_{BE(on)}}{R} \quad (4.207)$$

If  $V_{CC} \gg V_{BE(on)}$ , this circuit has the drawback that the output current is proportional to the power-supply voltage. For example, if  $V_{BE(on)} = 0.7$  V, and if this current mirror is used in an operational amplifier that has to function with power-supply voltages ranging from 3 V to 10 V, the bias current would vary over a four-to-one range, and the power dissipation would vary over a thirteen-to-one range.

One measure of this aspect of bias-circuit performance is the fractional change in the bias current that results from a given fractional change in supply voltage. The most useful parameter for describing the variation of the output current with the power-supply voltage is the sensitivity  $S$ . The sensitivity of any circuit variable  $y$  to a parameter  $x$  is defined as follows:

$$S_x^y = \lim_{\Delta x \rightarrow 0} \frac{\Delta y/y}{\Delta x/x} = \frac{x}{y} \frac{\partial y}{\partial x} \quad (4.208)$$

Applying (4.208) to find the sensitivity of the output current to small variations in the power-supply voltage gives

$$S_{V_{SUP}}^{I_{OUT}} = \frac{V_{SUP}}{I_{OUT}} \frac{\partial I_{OUT}}{\partial V_{SUP}} \quad (4.209)$$

The supply voltage  $V_{SUP}$  is usually called  $V_{CC}$  in bipolar circuits and  $V_{DD}$  in MOS circuits. If  $V_{CC} \gg V_{BE(on)}$  in Fig. 4.30a, and if  $V_{DD} \gg V_{GS1}$  in Fig. 4.30b,

$$S_{V_{SUP}}^{I_{OUT}} \simeq 1 \quad (4.210)$$

Equation 4.210 shows that the output currents in the simple current mirrors in Fig. 4.30 depend strongly on the power-supply voltages. Therefore, this configuration should not be used when supply insensitivity is important.

#### 4.4.2.1 Widlar Current Sources

For the case of the bipolar Widlar source in Fig. 4.31a, the output current is given implicitly by (4.191). To determine the sensitivity of  $I_{OUT}$  to the power-supply voltage, this equation is differentiated with respect to  $V_{CC}$ :

$$V_T \frac{\partial}{\partial V_{CC}} \ln \frac{I_{IN}}{I_{OUT}} = R_2 \frac{\partial I_{OUT}}{\partial V_{CC}} \quad (4.211)$$

Differentiating yields

$$V_T \left( \frac{I_{OUT}}{I_{IN}} \right) \left( \frac{1}{I_{OUT}} \frac{\partial I_{IN}}{\partial V_{CC}} - \frac{I_{IN}}{I_{OUT}^2} \frac{\partial I_{OUT}}{\partial V_{CC}} \right) = R_2 \frac{\partial I_{OUT}}{\partial V_{CC}} \quad (4.212)$$

Solving this equation for  $\partial I_{OUT}/\partial V_{CC}$ , we obtain

$$\frac{\partial I_{OUT}}{\partial V_{CC}} = \left( \frac{1}{1 + \frac{I_{OUT} R_2}{V_T}} \right) \frac{I_{OUT}}{I_{IN}} \frac{\partial I_{IN}}{\partial V_{CC}} \quad (4.213)$$

Substituting (4.213) into (4.209) gives

$$S_{V_{CC}}^{I_{OUT}} = \left( \frac{1}{1 + \frac{I_{OUT} R_2}{V_T}} \right) \frac{V_{CC}}{I_{IN}} \frac{\partial I_{IN}}{\partial V_{CC}} = \left( \frac{1}{1 + \frac{I_{OUT} R_2}{V_T}} \right) S_{V_{CC}}^{I_{IN}} \quad (4.214)$$

If  $V_{CC} \gg V_{BE(\text{on})}$ ,  $I_{IN} \simeq V_{CC}/R_1$  and the sensitivity of  $I_{IN}$  to  $V_{CC}$  is approximately unity, as in the simple current mirror of Fig. 4.30a. For the example in Section 4.4.1.1 where  $I_{IN} = 1$  mA,  $I_{OUT} = 5$   $\mu$ A, and  $R_2 = 27.4$  k $\Omega$ , (4.214) gives

$$S_{V_{CC}}^{I_{OUT}} = \frac{V_{CC}}{I_{OUT}} \frac{\partial I_{OUT}}{\partial V_{CC}} \simeq \frac{1}{1 + \frac{137 \text{ mV}}{26 \text{ mV}}} \simeq 0.16 \quad (4.215)$$

Thus for this case, a 10 percent power-supply voltage change results in only 1.6 percent change in  $I_{OUT}$ .

For the case of the MOS Widlar source in Fig. 4.31b, the output current is given by (4.197). Differentiating with respect to  $V_{DD}$  gives

$$\frac{1}{2\sqrt{I_{OUT}}} \frac{\partial I_{OUT}}{\partial V_{DD}} = \frac{1}{4R_2} \frac{1}{\sqrt{\frac{2}{k'(W/L)_2} + 4R_2 V_{ov1}}} 4R_2 \frac{\partial V_{ov1}}{\partial V_{DD}} \quad (4.216)$$

where

$$\frac{\partial V_{ov1}}{\partial V_{DD}} = \sqrt{\frac{2}{k'(W/L)_1}} \frac{1}{2\sqrt{I_{IN}}} \frac{\partial I_{IN}}{\partial V_{DD}} = \frac{V_{ov1}}{2I_{IN}} \frac{\partial I_{IN}}{\partial V_{DD}} \quad (4.217)$$

Substituting (4.216) and (4.217) into (4.209) gives

$$S_{V_{DD}}^{I_{OUT}} = \frac{V_{ov1}}{\sqrt{V_{ov2}^2 + 4I_{OUT}R_2V_{ov1}}} S_{V_{DD}}^{I_{IN}} \quad (4.218)$$

Since  $I_{OUT}$  is usually much less than  $I_{IN}$ ,  $V_{ov2}$  is usually small and  $I_{OUT}R_2 \simeq V_{ov1}$  and (4.218) simplifies to

$$S_{V_{DD}}^{I_{OUT}} \simeq \frac{V_{ov1}}{\sqrt{4V_{ov1}^2}} S_{V_{DD}}^{I_{IN}} = 0.5 S_{V_{DD}}^{I_{IN}} \quad (4.219)$$

If  $V_{DD} \gg V_{GS1}$ ,  $I_{IN} \simeq V_{DD}/R_1$  and the sensitivity of  $I_{IN}$  to  $V_{DD}$  is approximately unity, as in the simple current mirror of Fig. 4.30b. Thus for this case, a 10 percent power-supply voltage change results in a 5 percent change in  $I_{OUT}$ .

#### 4.4.2.2 Current Sources Using Other Voltage Standards

The level of power-supply independence provided by the bipolar and MOS Widlar current sources is not adequate for many types of analog circuits. Much lower sensitivity can be obtained by causing bias currents in the circuit to depend on a voltage standard other than the supply voltage. Bias reference circuits can be classified according to the voltage standard by which the bias currents are established. The most convenient standards are the base-emitter or threshold voltage of a transistor, the thermal voltage, or the breakdown voltage of a reverse-biased  $pn$  junction (a Zener diode). Each of these standards can be used to reduce supply sensitivity, but the drawback of the first three standards is that the reference voltage is quite temperature dependent. Both the base-emitter and threshold voltages have negative temperature coefficients of magnitude 1 to 2 mV/ $^{\circ}$ C, and the thermal voltage has a positive temperature coefficient of  $k/q \simeq 86$   $\mu$ V/ $^{\circ}$ C. The Zener diode has the disadvantage that at least 7 to 10 V of supply voltage are required because standard integrated-circuit processes produce a minimum breakdown voltage of about 6 V across the most highly doped junctions (usually  $npn$  transistor emitter-base junctions). Furthermore,  $pn$  junctions produce large amounts of voltage

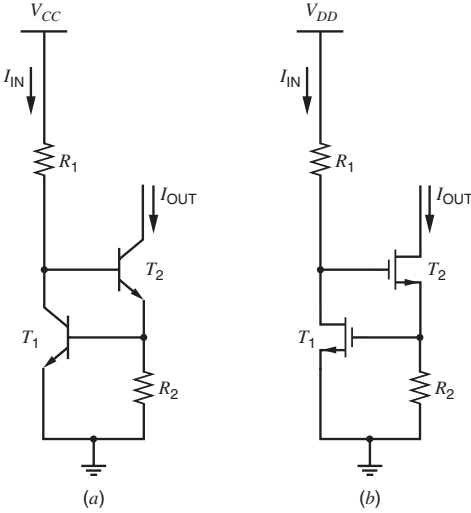


**Figure 4.36** (a) Base-emitter referenced current source. (b) Threshold referenced current source.

noise under the reverse-breakdown conditions encountered in a bias reference circuit. Noise in avalanche breakdown is considered further in Chapter 11.

We now consider bias reference circuits based on the base-emitter or gate-source voltage. The circuit in simplest form in bipolar technology is shown in Fig. 4.36a. This circuit is similar to a Wilson current mirror where the diode-connected transistor is replaced by a resistor. For the input current to flow in \$T\_1\$, transistor \$T\_2\$ must supply enough current into \$R\_2\$ so that the base-emitter voltage of \$T\_1\$ is

$$V_{BE1} = V_T \ln \frac{I_{IN}}{I_{S1}} \tag{4.220}$$

If we neglect base currents, \$I\_{OUT}\$ is equal to the current flowing through \$R\_2\$. Since the voltage drop on \$R\_2\$ is \$V\_{BE1}\$, the output current is proportional to this base-emitter voltage. Thus, neglecting base currents, we have

$$I_{OUT} = \frac{V_{BE1}}{R_2} = \frac{V_T}{R_2} \ln \frac{I_{IN}}{I_{S1}} \tag{4.221}$$

Differentiating (4.221) and substituting into (4.209) gives

$$S_{V_{CC}}^{I_{OUT}} = \frac{V_T}{I_{OUT} R_2} S_{V_{CC}}^{I_{IN}} = \frac{V_T}{V_{BE(ON)}} S_{V_{CC}}^{I_{IN}} \tag{4.222}$$

If \$V\_{CC} \gg 2V\_{BE(ON)}\$, \$I\_{IN} \approx V\_{CC}/R\_1\$ and the sensitivity of \$I\_{IN}\$ to \$V\_{CC}\$ is approximately unity. With \$V\_{BE(ON)} = 0.7\$ V,

$$S_{V_{CC}}^{I_{OUT}} = \frac{0.026 \text{ V}}{0.7 \text{ V}} \approx 0.037 \tag{4.223}$$

Thus for this case, a 10 percent power-supply voltage change results in a 0.37 percent change in \$I\_{OUT}\$. The result is significantly better than for a bipolar Widlar current source.

The MOS counterpart of the base-emitter reference is shown in Fig. 4.36*b*. Here

$$I_{OUT} = \frac{V_{GS1}}{R_2} = \frac{V_t + V_{ov1}}{R_2} = \frac{V_t + \sqrt{\frac{2I_{IN}}{k'(W/L)_1}}}{R_2} \quad (4.224)$$

The case of primary interest is when the overdrive of  $T_1$  is small compared to the threshold voltage. This case can be achieved in practice by choosing sufficiently low input current and large  $(W/L)_1$ . In this case, the output current is determined mainly by the threshold voltage and  $R_2$ . Therefore, this circuit is known as a *threshold-referenced* bias circuit. Differentiating (4.224) with respect to  $V_{DD}$  and substituting into (4.209) gives

$$S_{V_{DD}}^{I_{OUT}} = \frac{V_{ov1}}{2I_{OUT}R_2} S_{V_{DD}}^{I_{IN}} = \frac{V_{ov1}}{2V_{GS1}} S_{V_{DD}}^{I_{IN}} \quad (4.225)$$

For example, if  $V_t = 1$  V,  $V_{ov1} = 0.1$  V, and  $S_{V_{DD}}^{I_{IN}} \simeq 1$

$$S_{V_{DD}}^{I_{OUT}} \simeq \frac{0.1}{2(1.1)} \simeq 0.045 \quad (4.226)$$

These circuits are not fully supply independent because the base-emitter or gate-source voltages of  $T_1$  change slightly with power-supply voltage. This change occurs because the collector or drain current of  $T_1$  is approximately proportional to the supply voltage. The resulting supply sensitivity is often a problem in bias circuits whose input current is derived from a resistor connected to the supply terminal, since this configuration causes the currents in some portion of the circuit to change with the supply voltage.

#### 4.4.2.3 Self-Biasing

Power-supply sensitivity can be greatly reduced by the use of the so-called *bootstrap* bias technique, also referred to as *self-biasing*. Instead of developing the input current by connecting a resistor to the supply, the input current is made to depend directly on the output current of the current source itself. The concept is illustrated in block-diagram form in Fig. 4.37*a*. Assuming that the feedback loop formed by this connection has a stable operating point, the currents flowing in the circuit are much less sensitive to power-supply voltage than in the resistively biased case. The two key variables here are the input current,  $I_{IN}$ , and the output current,  $I_{OUT}$ . The relationship between these variables is governed by both the current source and the current

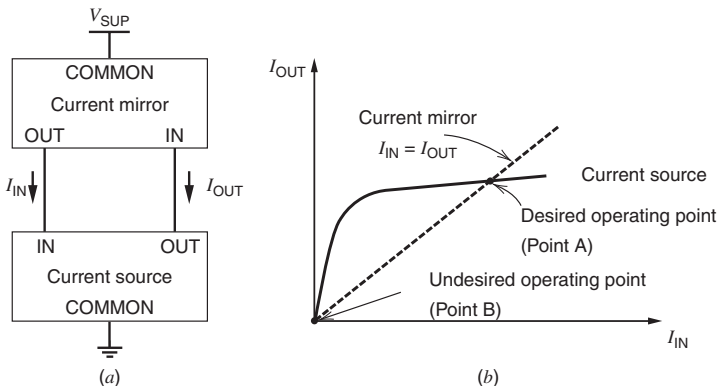


Figure 4.37 (a) Block diagram of a self-biased reference. (b) Determination of operating point.

mirror. From the standpoint of the current source, the output current is almost independent of the input current for a wide range of input currents as shown in Fig. 4.37*b*. From the standpoint of the current mirror,  $I_{IN}$  is set equal to  $I_{OUT}$ , assuming that the gain of the current mirror is unity. The operating point of the circuit must satisfy both constraints and hence is at the intersection of the two characteristics. In the plot of Fig. 4.37*b*, two intersections or potential operating points are shown. Point *A* is the desired operating point, and point *B* is an undesired operating point because  $I_{OUT} = I_{IN} = 0$ .

If the output current in Fig. 4.37*a* increases for any reason, the current mirror increases the input current by the same amount because the gain of the current mirror is assumed to be unity. As a result, the current source increases the output current by an amount that depends on the gain of the current source. Therefore, the loop responds to an initial change in the output current by further changing the output current in a direction that reinforces the initial change. In other words, the connection of a current source and a current mirror as shown in Fig. 4.37*a* forms a positive feedback loop, and the gain around the loop is the gain of the current source. In Chapter 9, we will show that circuits with positive feedback are stable if the gain around the loop is less than unity. At point *A*, the gain around the loop is quite small because the output current of the current source is insensitive to changes in the input current around point *A*. On the other hand, at point *B*, the gain around the feedback loop is deliberately made greater than unity so that the two characteristics shown in Fig. 4.37*b* intersect at a point away from the origin. As a result, this simplified analysis shows that point *B* is an unstable operating point in principle, and the circuit would ideally tend to drive itself out of this state.

In practice, however, point *B* is frequently a stable operating point because the currents in the transistors at this point are very small, often in the picoampere range. At such low current levels, leakage currents and other effects reduce the current gain of both bipolar and MOS transistors, usually causing the gain around the loop to be less than unity. As a result, actual circuits of this type are usually unable to drive themselves out of the zero-current state. Thus, unless precautions are taken, the circuit may operate in the zero-current condition. For these reasons, self-biased circuits often have a stable state in which zero current flows in the circuit even when the power-supply voltage is nonzero. This situation is analogous to a gasoline engine that is not running even though it has a full tank of fuel. An electrical or mechanical device is required to start the engine. Similarly, a start-up circuit is usually required to prevent the self-biased circuit from remaining in the zero-current state.

The application of this technique to the  $V_{BE}$ -referenced current source is illustrated in Fig. 4.38*a*, and the threshold-referenced MOS counterpart is shown in Fig. 4.38*b*. We assume for simplicity that  $V_A \rightarrow \infty$ . The circuit composed of  $T_1$ ,  $T_2$ , and  $R$  dictates that the current  $I_{OUT}$  depends weakly on  $I_{IN}$ , as indicated by (4.221) and (4.224). Second, the current mirror composed of matched transistors  $T_4$  and  $T_5$  dictates that  $I_{IN}$  is equal to  $I_{OUT}$ . The operating point of the circuit must satisfy both constraints and hence is at the intersection of the two characteristics as in Fig. 4.37*b*. Except for the effects of finite output resistance of the transistors, the bias currents are independent of supply voltage. If required, the output resistance of the current source and mirror could be increased by the use of cascode or Wilson configurations in the circuits. The actual bias currents for other circuits are supplied by  $T_6$  and/or  $T_3$ , which are matched to  $T_5$  and  $T_1$ , respectively.

The zero-current state can be avoided by using a start-up circuit to ensure that some current always flows in the transistors in the reference so that the gain around the feedback loop at point *B* in Fig. 4.37*b* does not fall below unity. An additional requirement is that the start-up circuit must not interfere with the normal operation of the reference once the desired operating point is reached. The  $V_{BE}$ -referenced current source with a typical start-up circuit used in bipolar technologies is illustrated in Fig. 4.39*a*. We first assume that the circuit is in the undesired zero-current state. If this were true, the base-emitter voltage of  $T_1$  would be

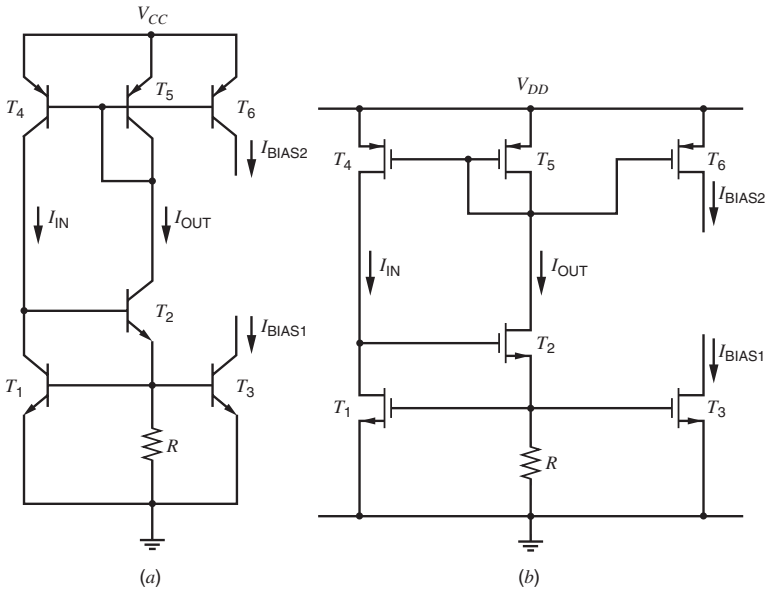


Figure 4.38 (a) Self-biasing  $V_{BE}$  reference. (b) Self-biasing  $V_i$  reference.

zero. The base-emitter voltage  $T_2$  would be tens of millivolts above ground, determined by the leakage currents in the circuit. However, the voltage on the left-hand end of  $D_1$  is four diode drops above ground, so that a voltage of at least three diode drops would appear across  $R_x$ , and a current would flow through  $R_x$  into the  $T_1$ - $T_2$  combination. This action would cause current to flow in  $T_4$  and  $T_5$ , avoiding the zero-current state.

The bias reference circuit then drives itself toward the desired stable state, and we require that the start-up circuit not affect the steady-state current values. This can be accomplished by causing  $R_x$  to be large enough that when the steady-state current is established in  $T_1$ , the voltage drop across  $R_x$  is large enough to reverse bias  $D_1$ . In the steady state, the collector-emitter voltage of  $T_1$  is two diode drops above ground, and the left-hand end of  $D_1$  is four diode drops above ground. Thus if we make  $I_{IN}R_x$  equal to two diode drops,  $D_1$  will have zero voltage across it in the steady state. As a result, the start-up circuit composed of  $R_x$ ,  $D_2$ - $D_5$ , and  $D_1$  is, in effect, disconnected from the circuit for steady-state operation.

Floating diodes are not usually available in MOS technologies. The threshold-referenced current source with a typical start-up circuit used in MOS technologies is illustrated in Fig. 4.39b. If the circuit is in the undesired zero-current state, the gate-source voltage of  $T_1$  would be less than a threshold voltage. As a result,  $T_7$  is off and  $T_8$  operates in the triode region, pulling the gate-source voltage of  $T_9$  up to  $V_{DD}$ . Therefore,  $T_9$  is on and pulls down on the gates of  $T_4$  and  $T_5$ . This action causes current to flow in  $T_4$  and  $T_5$ , avoiding the zero-current state.

In steady state, the gate-source voltage of  $T_7$  rises to  $I_{OUT}R$ , which turns on  $T_7$  and reduces the gate-source voltage of  $T_9$ . In other words,  $T_7$  and  $T_8$  form a CMOS inverter whose output falls when the reference circuit turns on. Since the start-up circuit should not interfere with normal operation of the reference in steady state, the inverter output should fall low enough to turn  $T_9$  off in steady state. Therefore, the gate-source voltage of  $T_9$  must fall below a threshold voltage when the inverter input rises from zero to  $I_{OUT}R$ . In practice,

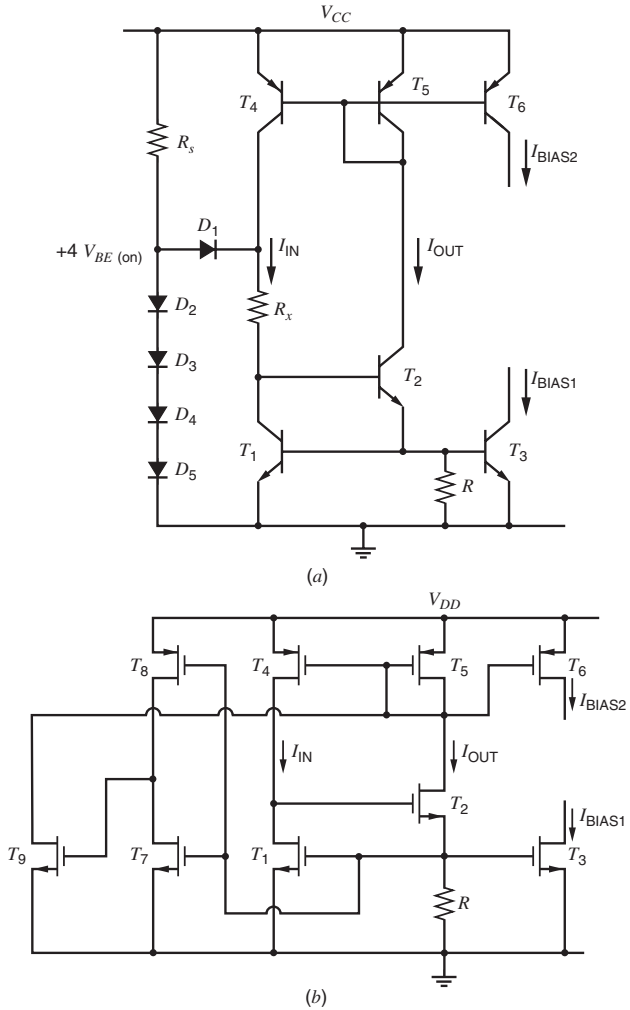


**Figure 4.39** (a) Self-biasing  $V_{BE}$  reference with start-up circuit. (b) Self-biasing  $V_I$  reference with start-up circuit.

this requirement is satisfied by choosing the aspect ratio of  $T_7$  to be much larger than that of  $T_8$ .

Another important aspect of the performance of biasing circuits is their dependence on temperature. This variation is most conveniently expressed in terms of the fractional change in output current per degree centigrade of temperature variation, which we call the fractional temperature coefficient  $TC_F$ :

$$TC_F = \frac{1}{I_{OUT}} \frac{\partial I_{OUT}}{\partial T} \tag{4.227}$$

For the  $V_{BE}$ -referenced circuit of Fig. 4.38a,

$$I_{OUT} = \frac{V_{BE1}}{R} \quad (4.228)$$

$$\frac{\partial I_{OUT}}{\partial T} = \frac{1}{R} \frac{\partial V_{BE1}}{\partial T} - \frac{V_{BE1}}{R^2} \frac{\partial R}{\partial T} \quad (4.229)$$

$$= I_{OUT} \left( \frac{1}{V_{BE1}} \frac{\partial V_{BE1}}{\partial T} - \frac{1}{R} \frac{\partial R}{\partial T} \right) \quad (4.230)$$

Therefore,

$$TC_F = \frac{1}{I_{OUT}} \frac{\partial I_{OUT}}{\partial T} = \frac{1}{V_{BE1}} \frac{\partial V_{BE1}}{\partial T} - \frac{1}{R} \frac{\partial R}{\partial T} \quad (4.231)$$

Thus the temperature dependence of the output current is related to the difference between the resistor temperature coefficient and that of the base-emitter junction. Since the former has a positive and the latter a negative coefficient, the net  $TC_F$  is quite large.

#### EXAMPLE

Design a bias reference as shown in Fig. 4.38a to produce 100  $\mu\text{A}$  output current. Find the  $TC_F$ . Assume that for  $T_1$ ,  $I_S = 10^{-14}$  A. Assume that  $\partial V_{BE}/\partial T = -2\text{mV}/^\circ\text{C}$  and that  $(1/R)(\partial R/\partial T) = +1500\text{ppm}/^\circ\text{C}$ .

The current in  $T_1$  will be equal to  $I_{OUT}$ , so that

$$V_{BE1} = V_T \ln \frac{100\ \mu\text{A}}{10^{-14}\ \text{A}} = 598\ \text{mV}$$

Thus from (4.228),

$$R = \frac{598\ \text{mV}}{0.1\ \text{mA}} = 5.98\ \text{k}\Omega$$

From (4.231),

$$TC_F \simeq \frac{-2\ \text{mV}/^\circ\text{C}}{598\ \text{mV}} - 1.5 \times 10^{-3} \simeq -3.3 \times 10^{-3} - 1.5 \times 10^{-3}$$

and thus

$$TC_F \simeq -4.8 \times 10^{-3}/^\circ\text{C} = -4800\ \text{ppm}/^\circ\text{C}$$

- The term ppm is an abbreviation for parts per million and implies a multiplier of  $10^{-6}$ .

For the threshold-referenced circuit of Fig. 4.38b,

$$I_{OUT} = \frac{V_{GS1}}{R} \simeq \frac{V_t}{R} \quad (4.232)$$

Differentiating (4.232) and substituting into (4.227) gives

$$TC_F = \frac{1}{I_{OUT}} \frac{\partial I_{OUT}}{\partial T} \simeq \frac{1}{V_t} \frac{\partial V_t}{\partial T} - \frac{1}{R} \frac{\partial R}{\partial T} \quad (4.233)$$

Since the threshold voltage of an MOS transistor and the base-emitter voltage of a bipolar transistor both change at about  $-2\text{mV}/^\circ\text{C}$ , (4.233) and (4.231) show that the temperature dependence of the threshold-referenced current source in Fig. 4.38b is about the same as the  $V_{BE}$ -referenced current source in Fig. 4.38a.

$V_{BE}$ -referenced bias circuits are also used in CMOS technology. An example is shown in Fig. 4.40, where the *pnp* transistor is the parasitic device inherent in *p*-substrate CMOS



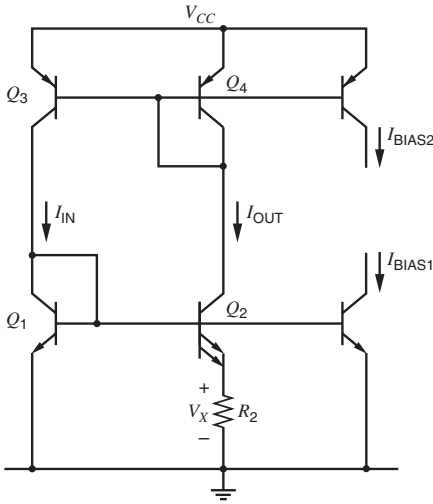


**Figure 4.41** Bias current source using the thermal voltage.

The temperature variation of the output current can be calculated as follows. From (4.237)

$$\begin{aligned} \frac{\partial I_{OUT}}{\partial T} &= (\ln 2) \frac{R_2 \frac{\partial V_T}{\partial T} - V_T \frac{\partial R_2}{\partial T}}{R_2^2} \\ &= \frac{V_T}{R_2} (\ln 2) \left( \frac{1}{V_T} \frac{\partial V_T}{\partial T} - \frac{1}{R_2} \frac{\partial R_2}{\partial T} \right) \end{aligned} \quad (4.238)$$

Substituting (4.237) in (4.238) gives

$$TC_F = \frac{1}{I_{OUT}} \frac{\partial I_{OUT}}{\partial T} = \frac{1}{V_T} \frac{\partial V_T}{\partial T} - \frac{1}{R_2} \frac{\partial R_2}{\partial T} \quad (4.239)$$

This circuit produces much smaller temperature coefficient of the output current than the  $V_{BE}$  reference because the fractional sensitivities of both  $V_T$  and that of a diffused resistor  $R_2$  are positive and tend to cancel in (4.239). We have chosen a transistor area ratio of two to one as an example. In practice, this ratio is often chosen to minimize the total area required for the transistors and for resistor  $R_2$ .

#### EXAMPLE

Design a bias reference of the type shown in Fig. 4.41 to produce an output current of  $100 \mu\text{A}$ . Find the  $TC_F$  of  $I_{OUT}$ . Assume the resistor temperature coefficient  $(1/R)(\partial R/\partial T) = +1500 \text{ ppm}/^\circ\text{C}$ .

From (4.237)

$$R_2 = \frac{V_T (\ln 2)}{I_{OUT}} = \frac{(26 \text{ mV})(\ln 2)}{100 \mu\text{A}} \simeq 180 \Omega$$

From (4.239)

$$\begin{aligned} \frac{1}{I_{OUT}} \frac{\partial I_{OUT}}{\partial T} &= \frac{1}{V_T} \frac{\partial V_T}{\partial T} - 1500 \times 10^{-6} = \frac{1}{V_T} \frac{V_T}{T} - 1500 \times 10^{-6} \\ &= \frac{1}{T} - 1500 \times 10^{-6} \end{aligned}$$

Assuming operation at room temperature,  $T = 300^\circ\text{K}$  and

$$\frac{1}{I_{OUT}} \frac{\partial I_{OUT}}{\partial T} \simeq 3300 \times 10^{-6} - 1500 \times 10^{-6} = 1800 \text{ ppm}/^\circ\text{C}$$

$V_T$ -referenced bias circuits are also commonly used in CMOS technology. A simple example is shown in Fig. 4.42, where bipolar transistors  $Q_1$  and  $Q_2$  are parasitic devices inherent in  $p$ -substrate CMOS technologies. Here the emitter areas of these transistors differ by a factor  $n$ , and the feedback loop forces them to operate at the same bias current. As a result, the difference between the two base-emitter voltages must appear across resistor  $R$ . The resulting current is

$$I_{OUT} = \frac{V_T \ln(n)}{R} \tag{4.240}$$

In the circuit of Fig. 4.42, small differences in the gate-source voltages of  $M_3$  and  $M_4$  result in large variations in the output current because the voltage drop across  $R$  is only on the order of 100 mV. Such gate-source voltage differences can result from device mismatches or from channel-length modulation in  $M_3$  and  $M_4$  because they have different drain-source voltages. Practical implementations of this circuit typically utilize large geometry devices for  $M_3$  and  $M_4$  to minimize offsets and cascode or Wilson current sources to minimize channel-length modulation effects. A typical example of a practical circuit is shown in Fig. 4.43. In general, cascoding is often used to improve the performance of reference circuits in all technologies. The main limitation of the application of cascoding is that it increases the minimum required power-supply voltage to operate all transistors in the active region.

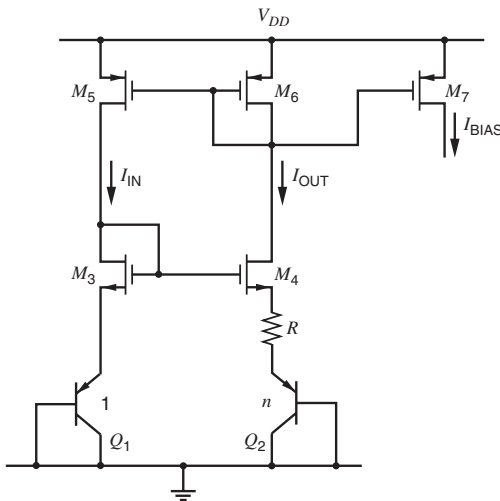


**Figure 4.42** Example of a CMOS  $V_T$ -referenced self-biased circuit.



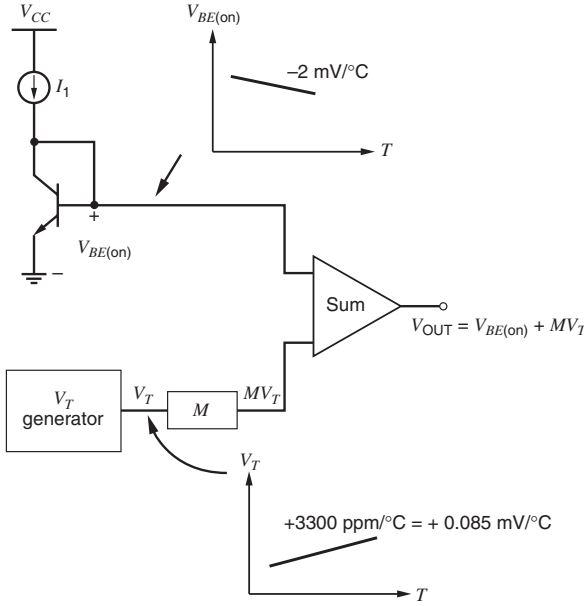


**Figure 4.44** Hypothetical band-gap reference circuit.

As shown in Chapter 1, the saturation current  $I_S$  can be related to the device structure by

$$I_S = \frac{qAn_i^2\bar{D}_n}{Q_B} = Bn_i^2\bar{D}_n = B'n_i^2T\bar{\mu}_n \tag{4.242}$$

where  $n_i$  is the intrinsic minority-carrier concentration,  $Q_B$  is the total base doping per unit area,  $\bar{\mu}_n$  is the average electron mobility in the base,  $A$  is the emitter-base junction area, and  $T$  is the temperature. Here, the constants  $B$  and  $B'$  involve only temperature-independent quantities. The Einstein relation  $\mu_n = (q/kT)D_n$  was used to write  $I_S$  in terms of  $\bar{\mu}_n$  and  $n_i^2$ . The quantities in (4.242) that are temperature dependent are given by<sup>15</sup>

$$\bar{\mu}_n = CT^{-n} \tag{4.243}$$

$$n_i^2 = DT^3 \exp\left(-\frac{V_{G0}}{V_T}\right) \tag{4.244}$$

where  $V_{G0}$  is the band-gap voltage of silicon extrapolated to 0°K. Here again  $C$  and  $D$  are temperature-independent quantities whose exact values are unimportant in the analysis. The exponent  $n$  in the expression for base-region electron mobility  $\bar{\mu}_n$  is dependent on the doping level in the base. Combining (4.241), (4.242), (4.243), and (4.244) yields

$$V_{BE(on)} = V_T \ln\left(I_1 T^{-\gamma} E \exp\frac{V_{G0}}{V_T}\right) \tag{4.245}$$

where  $E$  is another temperature-independent constant and

$$\gamma = 4 - n \tag{4.246}$$

In actual band-gap circuits, the current  $I_1$  is not constant but varies with temperature. We assume for the time being that this temperature variation is known and that it can be written

in the form

$$I_1 = GT^\alpha \quad (4.247)$$

where  $G$  is another temperature-independent constant. Combining (4.245) and (4.247) gives

$$V_{BE(\text{on})} = V_{G0} - V_T[(\gamma - \alpha) \ln T - \ln(EG)] \quad (4.248)$$

From Fig. 4.44, the output voltage is

$$V_{\text{OUT}} = V_{BE(\text{on})} + MV_T \quad (4.249)$$

Substitution of (4.248) into (4.249) gives

$$V_{\text{OUT}} = V_{G0} - V_T(\gamma - \alpha) \ln T + V_T[M + \ln(EG)] \quad (4.250)$$

This expression gives the output voltage as a function of temperature in terms of the circuit parameters  $G$ ,  $\alpha$ , and  $M$ , and the device parameters  $E$  and  $\gamma$ . Our objective is to make  $V_{\text{OUT}}$  independent of temperature. To this end, we take the derivative of  $V_{\text{OUT}}$  with respect to temperature to find the required values of  $G$ ,  $\gamma$ , and  $M$  to give zero  $TC_F$ . Differentiating (4.250) gives

$$0 = \left. \frac{dV_{\text{OUT}}}{dT} \right|_{T=T_0} = \frac{V_{T0}}{T_0} [M + \ln(EG)] - \frac{V_{T0}}{T_0} (\gamma - \alpha) \ln T_0 - \frac{V_{T0}}{T_0} (\gamma - \alpha) \quad (4.251)$$

where  $T_0$  is the temperature at which the  $TC_F$  of the output is zero and  $V_{T0}$  is the thermal voltage  $V_T$  evaluated at  $T_0$ . Equation 4.251 can be rearranged to give

$$[M + \ln(EG)] = (\gamma - \alpha) \ln T_0 + (\gamma - \alpha) \quad (4.252)$$

This equation gives the required values of circuit parameters  $M$ ,  $\alpha$ , and  $G$  in terms of the device parameters  $E$  and  $\gamma$ . In principle, these values could be calculated directly from (4.252). However, further insight is gained by back-substituting (4.252) into (4.250). The result is

$$V_{\text{OUT}} = V_{G0} + V_T(\gamma - \alpha) \left( 1 + \ln \frac{T_0}{T} \right) \quad (4.253)$$

Thus the temperature dependence of the output voltage is entirely described by the single parameter  $T_0$ , which in turn is determined by the constants  $M$ ,  $E$ , and  $G$ .

Using (4.253), the output voltage at the zero  $TC_F$  temperature ( $T = T_0$ ) is given by

$$V_{\text{OUT}} |_{T=T_0} = V_{G0} + V_{T0}(\gamma - \alpha) \quad (4.254)$$

For example, to achieve zero  $TC_F$  at 27°C, assuming that  $\gamma = 3.2$  and  $\alpha = 1$ ,

$$V_{\text{OUT}} |_{T=T_0=25^\circ\text{C}} = V_{G0} + 2.2V_{T0} \quad (4.255)$$

The band-gap voltage of silicon is  $V_{G0} = 1.205$  V so that

$$V_{\text{OUT}} |_{T=T_0=25^\circ\text{C}} = 1.205 \text{ V} + (2.2)(0.026 \text{ V}) = 1.262 \text{ V} \quad (4.256)$$

Therefore, the output voltage for zero temperature coefficient is close to the band-gap voltage of silicon, which explains the name given to these bias circuits.

Differentiating (4.253) with respect to temperature yields

$$\begin{aligned} \frac{dV_{\text{OUT}}}{dT} &= \frac{1}{T} \left[ V_T(\gamma - \alpha) \left( 1 + \ln \frac{T_0}{T} \right) \right] - \frac{V_T}{T} (\gamma - \alpha) \\ &= (\gamma - \alpha) \frac{V_T}{T} \left( \ln \frac{T_0}{T} \right) \end{aligned} \quad (4.257)$$

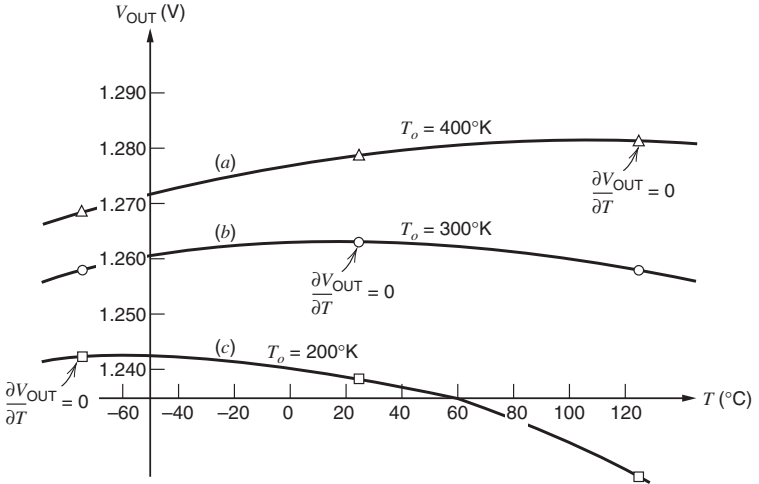


Figure 4.45 Variation of band-gap reference output voltage with temperature.

Equation 4.257 gives the slope of the output as a function of temperature. A typical family of output-voltage-variation characteristics is shown in Fig. 4.45 for different values of  $T_0$  for the special case in which  $\alpha = 0$  and  $I_1$  is temperature independent. The slope of each curve is zero at  $T = T_0$ . When  $T < T_0$ , the slope is positive because the argument of the logarithm in (4.257) is more than unity. Similarly, the slope is negative when  $T > T_0$ . For values of  $T$  near  $T_0$ ,

$$\ln \frac{T_0}{T} = \ln \left( 1 + \frac{T_0 - T}{T} \right) \simeq \frac{T_0 - T}{T} \tag{4.258}$$

and we have

$$\frac{dV_{OUT}}{dT} \simeq (\gamma - \alpha) \frac{V_T}{T} \left( \frac{T_0 - T}{T} \right) \tag{4.259}$$

As shown by (4.257) and (4.259), the temperature coefficient of the output is zero only at one temperature  $T = T_0$ . This result stems from the addition of a weighted thermal voltage to a base-emitter voltage as in Fig. 4.44. Since the temperature coefficient of base-emitter voltage is not exactly constant, the gain  $M$  can be chosen to set the temperature coefficient of the output to zero only at one temperature. In other words, the thermal voltage generator is used to cancel the linear dependence of the base-emitter voltage with temperature. After this cancellation, the changing outputs in Fig. 4.45 stem from the nonlinear dependence of the base-emitter voltage with temperature. Band-gap references that compensate for this nonlinearity are said to be *curvature compensated*.<sup>16,17,18</sup>

■ EXAMPLE

A band-gap reference is designed to give a nominal output voltage of 1.262 V, which gives zero  $TC_F$  at 27°C. Because of component variations, the actual room temperature output voltage is 1.280 V. Find the temperature of actual zero  $TC_F$  of  $V_{OUT}$ . Also, write an equation for  $V_{OUT}$  as a function of temperature, and calculate the  $TC_F$  at room temperature. Assume that  $\gamma = 3.2$  and  $\alpha = 1$ .

From (4.253) at  $T = 27^\circ\text{C} = 300^\circ\text{K}$ ,

$$1.280\text{ V} = 1.205 + (0.026\text{ V})(2.2) \left( 1 + \ln \frac{T_0}{300^\circ\text{K}} \right)$$

and thus

$$T_0 = 300^\circ\text{K} \left( \exp \frac{18\text{ mV}}{57\text{ mV}} \right) = 411^\circ\text{K}$$

Therefore, the  $TC_F$  will be zero at  $T_0 = 411^\circ\text{K} = 138^\circ\text{C}$ , and we can express  $V_{\text{OUT}}$  as

$$V_{\text{OUT}} = 1.205\text{ V} + 57\text{ mV} \left( 1 + \ln \frac{411^\circ\text{K}}{T} \right)$$

From (4.259) with  $T = 300^\circ\text{K}$  and  $T_0 = 411^\circ\text{K}$ ,

$$\frac{dV_{\text{OUT}}}{dT} \simeq (2.2) \frac{26\text{ mV}}{300^\circ\text{K}} \left( \frac{411 - 300}{300} \right) \simeq 70\text{ }\mu\text{V}/^\circ\text{K} = 70\text{ }\mu\text{V}/^\circ\text{C}$$

Therefore, the  $TC_F$  at room temperature is

$$TC_F = \frac{1}{V_{\text{OUT}}} \frac{dV_{\text{OUT}}}{dT} \simeq \frac{70\text{ }\mu\text{V}/^\circ\text{C}}{1.280\text{ V}} \simeq 55\text{ ppm}/^\circ\text{C}$$

To reduce the  $TC_F$ , the constant  $M$  in (4.249)–(4.252) is often trimmed at one temperature so that the band-gap output is set to a desired target voltage.<sup>19</sup> In principle, the target voltage is given by (4.253). In practice, however, significant inaccuracy in (4.253) stems from an approximation in (4.244).<sup>20</sup> As a result, the target voltage is usually determined experimentally by measuring the  $TC_F$  directly for several samples of each band-gap reference in a given process.<sup>21,22</sup> This procedure reduces the  $TC_F$  at the reference temperature to a level of about  $10\text{ ppm}/^\circ\text{C}$ .

A key parameter of interest in reference sources is the variation of the output that is encountered over the entire temperature range. Since the  $TC_F$  expresses the temperature sensitivity only at one temperature, a different parameter must be used to characterize the behavior of the circuit over a broad temperature range. An effective temperature coefficient can be defined for a voltage reference as

$$TC_{F(\text{eff})} = \frac{1}{V_{\text{OUT}}} \left( \frac{V_{\text{MAX}} - V_{\text{MIN}}}{T_{\text{MAX}} - T_{\text{MIN}}} \right) \quad (4.260)$$

where  $V_{\text{MAX}}$  and  $V_{\text{MIN}}$  are the largest and smallest output voltages observed over the temperature range, and  $T_{\text{MAX}} - T_{\text{MIN}}$  is the temperature excursion.  $V_{\text{OUT}}$  is the nominal output voltage. By this standard,  $TC_{F(\text{eff})}$  over the  $-55$  to  $125^\circ\text{C}$  range for case (b) of Fig. 4.45 is  $44\text{ ppm}/^\circ\text{C}$ . If the temperature range is restricted to  $0$  to  $70^\circ\text{C}$ ,  $TC_{F(\text{eff})}$  improves to  $17\text{ ppm}/^\circ\text{C}$ . Thus over a restricted temperature range, this reference is comparable with the standard cell in temperature stability once the zero  $TC_F$  temperature has been set at room temperature. Saturated standard cells (precision batteries) have a  $TC_F$  of about  $\pm 30\text{ ppm}/^\circ\text{C}$ .

Practical realizations of band-gap references in bipolar technologies take on several forms.<sup>15,19,23</sup> One such circuit is illustrated in Fig. 4.46a.<sup>15</sup> This circuit uses a feedback loop to establish an operating point in the circuit such that the output voltage is equal to a  $V_{BE(\text{on})}$  plus a voltage proportional to the difference between two base-emitter voltages. The operation of the feedback loop is best understood by reference to Fig. 4.46b, in which a portion of the circuit is shown. We first consider the variation of the output voltage  $V_2$  as the input voltage  $V_1$  is varied from zero in the positive direction. Initially, with  $V_1 = 0$ , devices  $Q_1$  and  $Q_2$  do not

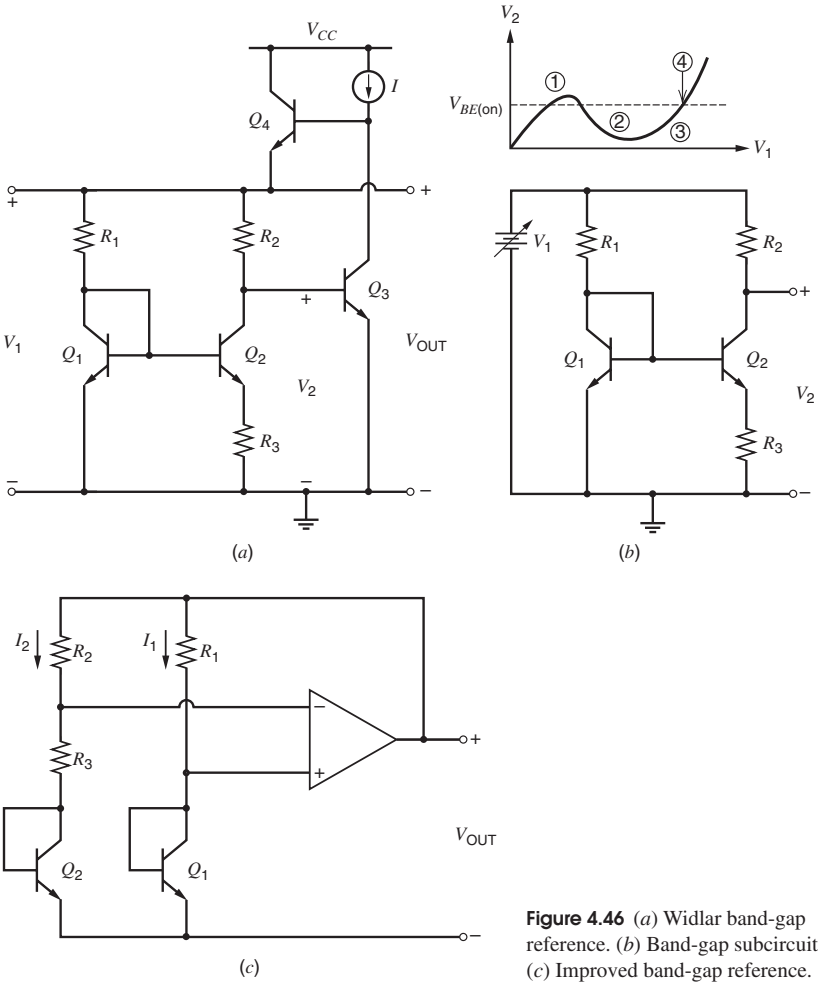


**Figure 4.46** (a) Widlar band-gap reference. (b) Band-gap subcircuit. (c) Improved band-gap reference.

conduct and  $V_2 = 0$ . As  $V_1$  is increased,  $Q_1$  and  $Q_2$  do not conduct significant current until the input voltage reaches about 0.6 V. When  $V_1 < 0.6$  V,  $V_2 = V_1$  since the voltage drop on  $R_2$  is zero. When  $V_1$  exceeds 0.6 V, however,  $Q_1$  begins to conduct current, corresponding to point ① in Fig. 4.46b. The magnitude of the current in  $Q_1$  is roughly equal to  $(V_1 - 0.6 \text{ V})/R_1$ . For small values of this current,  $Q_1$  and  $Q_2$  carry the same current because the drop across  $R_3$  is negligible at low currents. Since  $R_2$  is much larger than  $R_1$ , the voltage drop across  $R_2$  is much larger than  $(V_1 - 0.6 \text{ V})$ , and transistor  $Q_2$  saturates, corresponding to point ② in Fig. 4.46b. Because of the presence of  $R_3$ , the collector current that *would* flow in  $Q_2$  if it were in the forward-active region has an approximately logarithmic dependence on  $V_1$ , exactly as in the Widlar source. Thus as  $V_1$  is further increased, a point is reached at which  $Q_2$  comes out of saturation because  $V_1$  increases faster than the voltage drop across  $R_2$ . This point is labeled point ③ in Fig. 4.46b.

Now consider the complete circuit of Fig. 4.46a. If transistor  $Q_3$  is initially turned off, transistor  $Q_4$  will drive  $V_1$  in the positive direction. This process will continue until enough voltage is developed at the base of  $Q_3$  to produce a collector current in  $Q_3$  approximately equal to  $I$ . Thus the circuit stabilizes with voltage  $V_2$  equal to one diode drop, the base-emitter voltage of  $Q_3$ , which can occur at point ① or point ④ in Fig. 4.46b. Appropriate start-up circuitry must be included to ensure operation at point ④.

Assuming that the circuit has reached a stable operating point at point ④, the output voltage  $V_{OUT}$  is the sum of the base-emitter voltage of  $Q_3$  and the voltage drop across  $R_2$ . The drop across  $R_2$  is equal to the voltage drop across  $R_3$  multiplied by  $R_2/R_3$  because the collector current of  $Q_2$  is approximately equal to its emitter current. The voltage drop across  $R_3$  is equal to the difference in base-emitter voltages of  $Q_1$  and  $Q_2$ . The ratio of currents in  $Q_1$  and  $Q_2$  is set by the ratio of  $R_2$  to  $R_1$ .

A drawback of this reference is that the current  $I$  is set by the power supply and may vary with power-supply variations. A self-biased band-gap reference circuit is shown in Fig. 4.46c. Assume that a stable operating point exists for this circuit and that the op amp is ideal. Then the differential input voltage of the op amp must be zero and the voltage drops across resistors  $R_1$  and  $R_2$  are equal. Thus the ratio of  $R_2$  to  $R_1$  determines the ratio of  $I_1$  to  $I_2$ . These two currents are the collector currents of the two diode-connected transistors  $Q_2$  and  $Q_1$ , assuming base currents are negligible. The voltage across  $R_3$  is

$$V_{R3} = \Delta V_{BE} = V_{BE1} - V_{BE2} = V_T \ln \frac{I_1 I_{S2}}{I_2 I_{S1}} = V_T \ln \frac{R_2 I_{S2}}{R_1 I_{S1}} \quad (4.261)$$

Since the same current that flows in  $R_3$  also flows in  $R_2$ , the voltage across  $R_2$  must be

$$V_{R2} = \frac{R_2}{R_3} V_{R3} = \frac{R_2}{R_3} \Delta V_{BE} = \frac{R_2}{R_3} V_T \ln \frac{R_2 I_{S2}}{R_1 I_{S1}} \quad (4.262)$$

This equation shows that the voltage across  $R_2$  is proportional to absolute temperature (PTAT) because of the temperature dependence of the thermal voltage. Since the op amp forces the voltages across  $R_1$  and  $R_2$  to be equal, the currents  $I_1$  and  $I_2$  are both proportional to temperature if the resistors have zero temperature coefficient. Thus for this reference,  $\alpha = 1$  in (4.247). The output voltage is the sum of the voltage across  $Q_2$ ,  $R_3$ , and  $R_2$ :

$$\begin{aligned} V_{OUT} &= V_{BE2} + V_{R3} + V_{R2} = V_{BE2} + \left(1 + \frac{R_2}{R_3}\right) \Delta V_{BE} \\ &= V_{BE2} + \left(1 + \frac{R_2}{R_3}\right) V_T \ln \frac{R_2 I_{S2}}{R_1 I_{S1}} = V_{BE2} + M V_T \end{aligned} \quad (4.263)$$

The circuit thus behaves as a band-gap reference, with the value of  $M$  set by the ratios of  $R_2/R_3$ ,  $R_2/R_1$ , and  $I_{S2}/I_{S1}$ .

#### 4.4.3.2 Band-Gap-Referenced Bias Circuits in CMOS Technology

Band-gap-referenced biasing also can be implemented using the parasitic bipolar devices inherent in CMOS technology. For example, in a  $n$ -well process, substrate  $pnp$  transistors can be used to replace the  $nnp$  transistors in Fig. 4.46c, as shown in Fig. 4.47. Assume that the CMOS op amp has infinite gain but nonzero input-referred offset voltage  $V_{OS}$ . (The input-referred offset voltage of an op amp is defined as the differential input voltage required to drive the output to zero.) Because of the threshold mismatch and the low transconductance per current of CMOS transistors, the offset of op amps in CMOS technologies is usually larger than in bipolar technologies. With the offset voltage, the voltage across  $R_3$  is

$$V_{R3} = V_{EB1} - V_{EB2} + V_{OS} = \Delta V_{EB} + V_{OS} \quad (4.264)$$

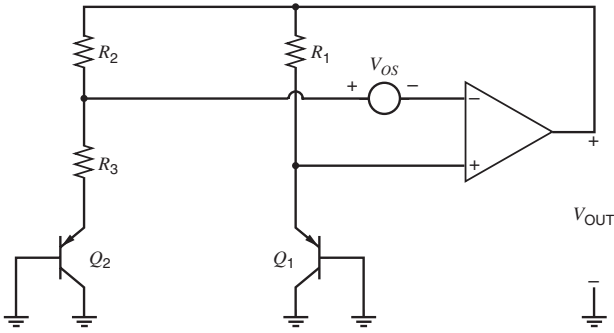


**Figure 4.47** A band-gap reference in *n*-well CMOS.

The emitter-base voltages are used here because the base-emitter voltages of the *pnp* transistors operating in the forward-active region are negative. Then the voltage across  $R_2$  is

$$V_{R2} = \frac{R_2}{R_3} V_{R3} = \frac{R_2}{R_3} (V_{EB1} - V_{EB2} + V_{OS}) = \frac{R_2}{R_3} (\Delta V_{EB} + V_{OS}) \quad (4.265)$$

and the output voltage is <sup>18</sup>

$$\begin{aligned} V_{OUT} &= V_{EB2} + V_{R3} + V_{R2} \\ &= V_{EB2} + \left(1 + \frac{R_2}{R_3}\right) (\Delta V_{EB} + V_{OS}) \end{aligned} \quad (4.266)$$

Since the difference in the base-emitter voltages is proportional to the thermal voltage, comparing (4.266) with  $V_{OS} = 0$  to (4.249) shows that the gain  $M$  here is proportional to  $(1 + R_2/R_3)$ . Rearranging (4.266) gives

$$V_{OUT} = V_{EB2} + \left(1 + \frac{R_2}{R_3}\right) (\Delta V_{EB}) + V_{OS(out)} \quad (4.267)$$

where the output-referred offset is

$$V_{OS(out)} = \left(1 + \frac{R_2}{R_3}\right) V_{OS} \quad (4.268)$$

Equations 4.267 and 4.268 show that the output contains an offset voltage that is a factor of  $(1 + R_2/R_3)$  times bigger than the input-referred offset voltage. Therefore, the same gain that is applied to the difference in the base-emitter voltages is also applied to the input-referred offset voltage.

Assume that the offset voltage is independent of temperature. To set  $TC_F$  of the output equal to zero, the gain must be changed so that temperature coefficients of the  $V_{EB}$  and  $\Delta V_{EB}$  terms cancel. Since the offset is assumed to be temperature independent, this cancellation occurs when the output is equal to the target, where zero offset was assumed, plus the output-referred offset. If the gain is trimmed at  $T = T_0$  to set the output to a target voltage assuming the offset is zero, (4.267) shows that the gain is too small if the offset voltage is positive and that the gain is too big if the offset voltage is negative. Since the gain is applied to the PTAT term, the resulting slope of the output versus temperature is negative when the offset is positive and the gain is too small. On the other hand, this slope is positive when the offset is negative and the gain is too big.

We will now calculate the magnitude of the slope of the output versus temperature at  $T = T_0$ . With zero offset and a target that assumes zero offset, trimming  $R_2$  and/or  $R_3$  to set the output in (4.267) to the target forces the slope of the  $\Delta V_{EB}$  term to cancel the slope of the  $V_{EB}$  term. With nonzero offset but the same target, the factor  $(1 + R_2/R_3)$  differs from its ideal value after trimming by  $-V_{OS(out)}/\Delta V_{EB}$ . Since this error is multiplied by  $\Delta V_{EB}$  in (4.267), the resulting slope of the output versus temperature is

$$\left. \frac{dV_{OUT}}{dT} \right|_{T=T_0} = - \left( \frac{V_{OS(out)}}{\Delta V_{EB}} \right) \frac{d\Delta V_{EB}}{dT} \quad (4.269)$$

Since  $\Delta V_{EB}$  is proportional to the thermal voltage  $V_T$ ,

$$\Delta V_{EB} = HV_T \quad (4.270)$$

where  $H$  is a temperature-independent constant. Substituting (4.270) into (4.269) gives

$$\left. \frac{dV_{OUT}}{dT} \right|_{T=T_0} = - \frac{V_{OS(out)}}{HV_T} \left. \frac{HV_T}{T} \right|_{T=T_0} = - \frac{V_{OS(out)}}{T_0} \quad (4.271)$$

Therefore, when the gain is trimmed at one temperature to set the band-gap output to a desired target voltage, variation in the op-amp offset causes variation in the output temperature coefficient. In practice, the op-amp offset is usually the largest source of nonzero temperature coefficient.<sup>18</sup> Equation 4.271 shows that the temperature coefficient at  $T = T_0$  is proportional to the output-referred offset under these circumstances. Furthermore, (4.268) shows that the output-referred offset is equal to the gain that is applied to the  $\Delta V_{EB}$  term times the input-referred offset. Therefore, minimizing this gain minimizes the variation in the temperature coefficient at the output. Since the reference output at  $T = T_0$  for zero  $TC_F$  is approximately equal to the band-gap voltage, the required gain can be minimized by maximizing the  $\Delta V_{EB}$  term.

To maximize the  $\Delta V_{EB}$  term, designers generally push a large current into a small transistor and a small current into a large transistor, as shown in Fig. 4.48. Ignoring base currents,

$$\Delta V_{EB} = V_{EB1} - V_{EB2} = V_T \ln \left( \frac{I_1 I_{S2}}{I_2 I_{S1}} \right) \quad (4.272)$$

Equation 4.272 shows that maximizing the product of the ratios  $I_1/I_2$  and  $I_{S2}/I_{S1}$  maximizes  $\Delta V_{EB}$ . In Fig. 4.48,  $I_1 > I_2$  is emphasized by drawing the symbol for  $I_1$  larger than the symbol for  $I_2$ . Similarly, the emitter area of  $Q_2$  is larger than that of  $Q_1$  to make  $I_{S2} > I_{S1}$ ,

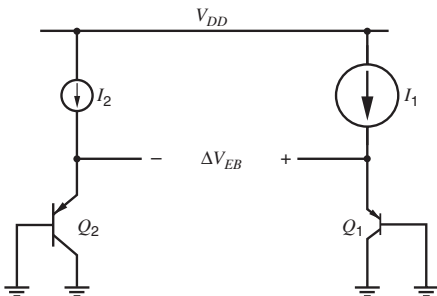


**Figure 4.48** A circuit that increases  $\Delta V_{EB}$  by increasing  $I_1/I_2$  and  $I_{S2}/I_{S1}$ .

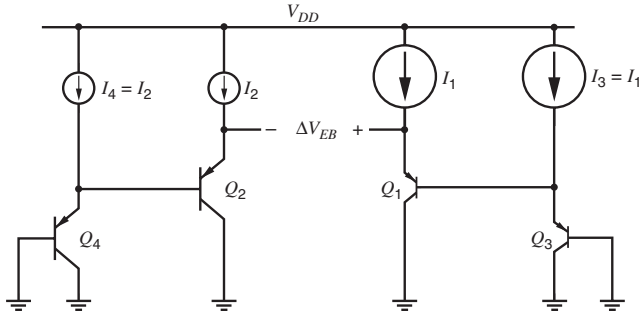


Figure 4.49 A circuit that cascades emitter followers to double  $\Delta V_{EB}$  if  $I_{S3} = I_{S1}$  and  $I_{S4} = I_{S2}$ .

and this relationship is shown by drawing the symbol of  $Q_2$  larger than the symbol of  $Q_1$ .<sup>24</sup> In practice, these ratios are often each set to be about equal to ten, and the resulting  $\Delta V_{EB} \simeq 120$  mV at room temperature. Because the logarithm function compresses its argument, however, a limitation of this approach arises. For example, if the argument is increased by a factor of ten,  $\Delta V_{EB}$  increases by only  $V_T \ln(10) \simeq 60$  mV. Therefore, to double  $\Delta V_{EB}$  to 240 mV,  $(I_1/I_2)(I_{S2}/I_{S1})$  must be increased by a factor of 100 to 10,000. On the other hand, if  $Q_1$  and the transistors that form  $I_2$  are minimum-sized devices when  $(I_1/I_2)(I_{S2}/I_{S1}) = 100$ , the required die area would be dominated by the biggest devices ( $Q_2$  and/or the transistors that form  $I_1$ ). Therefore, increasing  $(I_1/I_2)(I_{S2}/I_{S1})$  from 100 to 10,000 would increase the die area by about a factor of 100 but only double  $\Delta V_{EB}$ .

To overcome this limitation, stages that each contribute to  $\Delta V_{EB}$  can be cascaded.<sup>25</sup> For example, consider Fig. 4.49, where two emitter-follower stages are cascaded. Here

$$\Delta V_{EB} = V_{EB3} - V_{EB4} + V_{EB1} - V_{EB2} \tag{4.273}$$

Assume the new devices in Fig. 4.49 are identical to the corresponding original devices in Fig. 4.48 so that  $I_3 = I_1$ ,  $I_4 = I_2$ ,  $I_{S3} = I_{S1}$ , and  $I_{S4} = I_{S2}$ . Then ignoring base currents

$$\Delta V_{EB} = 2(V_{EB1} - V_{EB2}) = 2V_T \ln \left( \frac{I_1 I_{S2}}{I_2 I_{S1}} \right) \tag{4.274}$$

Thus cascading two identical emitter followers doubles  $\Delta V_{EB}$  while only doubling the required die area.

The effect of the offset in a band-gap reference can also be reduced by using offset cancellation. An example of offset cancellation in a CMOS band-gap reference with curvature correction in addition to an analysis of other high-order effects arising from finite  $\beta_F$ ,  $\beta_F$  mismatch,  $\beta_F$  variation with temperature, nonzero base resistance, and nonzero temperature coefficient in the resistors is presented in Ref. 18.

A high-performance CMOS band-gap reference is shown in Fig. 4.50, where cascoded current mirrors are used to improve supply rejection. A  $V_T$ -dependent current from  $M_{11}$  develops a  $V_T$ -dependent voltage across resistor  $xR$ . A proper choice of the ratio  $x$  can give a band-gap voltage at  $V_{OUT}$ . If desired, a temperature-independent output current can be realized by choosing  $x$  to give an appropriate temperature coefficient to  $V_{OUT}$  to cancel the temperature coefficient of resistor  $R_2$ .



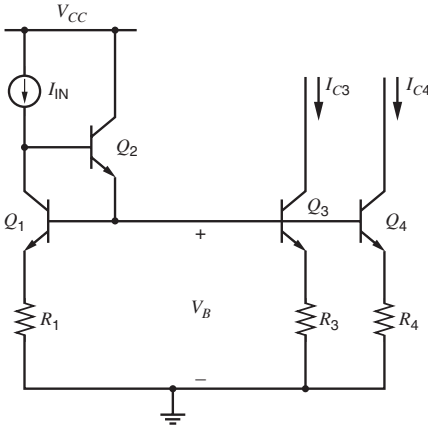


Figure 4.51 Matched bipolar current sources.

We now define *average* and *mismatch* parameters as follows:

$$I_C = \frac{I_{C3} + I_{C4}}{2} \tag{4.278}$$

$$\Delta I_C = I_{C3} - I_{C4} \tag{4.279}$$

$$I_S = \frac{I_{S3} + I_{S4}}{2} \tag{4.280}$$

$$\Delta I_S = I_{S3} - I_{S4} \tag{4.281}$$

$$R = \frac{R_3 + R_4}{2} \tag{4.282}$$

$$\Delta R = R_3 - R_4 \tag{4.283}$$

$$\alpha_F = \frac{\alpha_{F3} + \alpha_{F4}}{2} \tag{4.284}$$

$$\Delta \alpha_F = \alpha_{F3} - \alpha_{F4} \tag{4.285}$$

These relations can be inverted to give the original parameters in terms of the average and mismatch parameters. For example,

$$I_{C3} = I_C + \frac{\Delta I_C}{2} \tag{4.286}$$

$$I_{C4} = I_C - \frac{\Delta I_C}{2} \tag{4.287}$$

This set of equations for the various parameters is now substituted into (4.277). The result is

$$\begin{aligned}
 & V_T \ln \left( \frac{I_C + \frac{\Delta I_C}{2}}{I_C - \frac{\Delta I_C}{2}} \right) - V_T \ln \left( \frac{I_S + \frac{\Delta I_S}{2}}{I_S - \frac{\Delta I_S}{2}} \right) \\
 & + \frac{\left( I_C + \frac{\Delta I_C}{2} \right) \left( R + \frac{\Delta R}{2} \right)}{\alpha_F + \frac{\Delta \alpha_F}{2}} - \frac{\left( I_C - \frac{\Delta I_C}{2} \right) \left( R - \frac{\Delta R}{2} \right)}{\alpha_F - \frac{\Delta \alpha_F}{2}} = 0 \tag{4.288}
 \end{aligned}$$

The first term in this equation can be rewritten as

$$V_T \ln \left( \frac{I_C + \frac{\Delta I_C}{2}}{I_C - \frac{\Delta I_C}{2}} \right) = V_T \ln \left( \frac{1 + \frac{\Delta I_C}{2I_C}}{1 - \frac{\Delta I_C}{2I_C}} \right) \quad (4.289)$$

If  $\Delta I_C/2I_C \ll 1$ , this term can be rewritten as

$$V_T \ln \left( \frac{1 + \frac{\Delta I_C}{2I_C}}{1 - \frac{\Delta I_C}{2I_C}} \right) \simeq V_T \ln \left[ \left( 1 + \frac{\Delta I_C}{2I_C} \right) \left( 1 + \frac{\Delta I_C}{2I_C} \right) \right] \quad (4.290)$$

$$\simeq V_T \ln \left[ 1 + \frac{\Delta I_C}{I_C} + \left( \frac{\Delta I_C}{2I_C} \right)^2 \right] \quad (4.291)$$

$$\simeq V_T \ln \left( 1 + \frac{\Delta I_C}{I_C} \right) \quad (4.292)$$

where the squared term is neglected. The logarithm function has the infinite series

$$\ln(1+x) = x - \frac{x^2}{2} + \dots \quad (4.293)$$

If  $x \ll 1$ ,

$$\ln(1+x) \simeq x \quad (4.294)$$

To simplify (4.292) when  $\Delta I_C/I_C \ll 1$ , let  $x = \Delta I_C/I_C$ . Then

$$V_T \ln \left( \frac{I_C + \frac{\Delta I_C}{2}}{I_C - \frac{\Delta I_C}{2}} \right) \simeq V_T \frac{\Delta I_C}{I_C} \quad (4.295)$$

Applying the same approximations to the other terms in (4.288), we obtain

$$\frac{\Delta I_C}{I_C} \simeq \left( \frac{1}{1 + \frac{g_m R}{\alpha_F}} \right) \frac{\Delta I_S}{I_S} + \frac{\frac{g_m R}{\alpha_F}}{1 + \frac{g_m R}{\alpha_F}} \left( -\frac{\Delta R}{R} + \frac{\Delta \alpha_F}{\alpha_F} \right) \quad (4.296)$$

We will consider two important limiting cases. First, since  $g_m = I_C/V_T$ , when  $g_m R \ll 1$ , the voltage drop on an emitter resistor is much smaller than the thermal voltage. In this case, the second term in (4.296) is small and the mismatch is mainly determined by the transistor  $I_S$  mismatch in the first term. Observed mismatches in  $I_S$  typically range from  $\pm 10$  to  $\pm 1$  percent depending on geometry. Second, when  $g_m R \gg 1$ , the voltage drop on an emitter resistor is much larger than the thermal voltage. In this case, the first term in (4.296) is small and the mismatch is mainly determined by the resistor mismatch and transistor  $\alpha_F$  mismatch in the second term. Resistor mismatch typically ranges from  $\pm 2$  to  $\pm 0.1$  percent depending on geometry, and  $\alpha_F$  matching is in the  $\pm 0.1$  percent range for *npn* transistors. Thus for *npn* current sources, the use of emitter resistors offers significantly improved current matching. On the other hand, for *pnp* current sources, the  $\alpha_F$  mismatch is larger due to the lower  $\beta_F$ , typically around  $\pm 1$  percent. Therefore, the advantage of emitter degeneration is less significant with *pnp* than *npn* current sources.

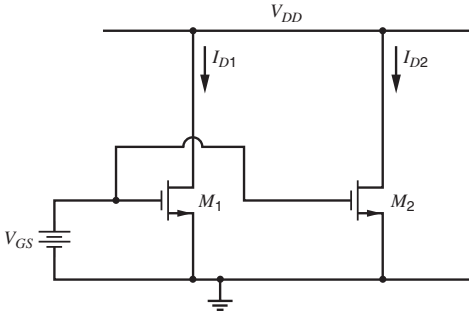


Figure 4.52 Matched MOS current sources.

**A.4.1.2 MOS**

Matched current sources are often required in MOS analog integrated circuits. The factors affecting this mismatch can be calculated using the circuit of Fig. 4.52. The two transistors  $M_1$  and  $M_2$  will have mismatches in their  $W/L$  ratios and threshold voltages. The drain currents are given by

$$I_{D1} = \frac{1}{2} \mu_n C_{ox} \left( \frac{W}{L} \right)_1 (V_{GS} - V_{t1})^2 \tag{4.297}$$

$$I_{D2} = \frac{1}{2} \mu_n C_{ox} \left( \frac{W}{L} \right)_2 (V_{GS} - V_{t2})^2 \tag{4.298}$$

Defining average and mismatch quantities, we have

$$I_D = \frac{I_{D1} + I_{D2}}{2} \tag{4.299}$$

$$\Delta I_D = I_{D1} - I_{D2} \tag{4.300}$$

$$\frac{W}{L} = \frac{1}{2} \left[ \left( \frac{W}{L} \right)_1 + \left( \frac{W}{L} \right)_2 \right] \tag{4.301}$$

$$\Delta \frac{W}{L} = \left( \frac{W}{L} \right)_1 - \left( \frac{W}{L} \right)_2 \tag{4.302}$$

$$V_t = \frac{V_{t1} + V_{t2}}{2} \tag{4.303}$$

$$\Delta V_t = V_{t1} - V_{t2} \tag{4.304}$$

Substituting these expressions into (4.297) and (4.298) and neglecting high-order terms, we obtain

$$\frac{\Delta I_D}{I_D} = \frac{\Delta \frac{W}{L}}{\frac{W}{L}} - \frac{\Delta V_t}{(V_{GS} - V_t)/2} \tag{4.305}$$

The current mismatch consists of two components. The first is geometry dependent and contributes a fractional current mismatch that is independent of bias point. The second is dependent on threshold voltage mismatch and increases as the overdrive ( $V_{GS} - V_t$ ) is reduced. This change occurs because as the overdrive is reduced, the fixed threshold mismatch progressively becomes a larger fraction of the total gate drive that is applied to the transistors and therefore contributes a progressively larger percentage error to the current mismatch. In practice, these

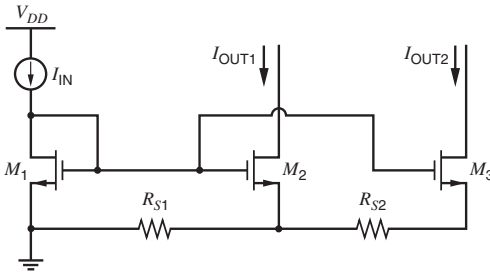


**Figure 4.53** Current mirror with two outputs used to compare voltage- and current-routing techniques.

observations are important because they affect the techniques used to distribute bias signals on integrated circuits.

Consider the current mirror shown in Fig. 4.53, which has one input and two outputs. At first, assume that  $R_{S1} = R_{S2} = 0$ . Also, assume that the input current is generated by a circuit with desirable properties. For example, a self-biased band-gap reference might be used to make  $I_{IN}$  insensitive to changes in the power supply and temperature. Finally, assume that each output current is used to provide the required bias in one analog circuit on the integrated circuit (IC). For example,  $M_2$  and  $M_3$  could each act as the tail current source of a differential pair.

One way to build the circuit in Fig. 4.53 is to place  $M_1$  on the IC near the input current source  $I_{IN}$ , while  $M_2$  and  $M_3$  are placed near the circuits that they bias, respectively. Since the gate-source voltage of  $M_1$  must be routed to  $M_2$  and  $M_3$  here, this case is referred to as an example of the *voltage routing* of bias signals. An advantage of this approach is that by routing only two nodes (the gate and the source of  $M_1$ ) around the IC, any number of output currents can be produced. Furthermore the gains from the input to each output of the current mirror are not affected by the number of outputs in MOS technologies because  $\beta_F \rightarrow \infty$ . (In bipolar technologies,  $\beta_F$  is finite, and the gain error increases as the number of outputs increase, but a beta-helper configuration can be used to reduce such errors as described in Section 4.2.3.)

Unfortunately, voltage routing has two important disadvantages. First, the input and output transistors in the current mirror may be separated by distances that are large compared to the size of the IC, increasing the potential mismatches in (4.305). In particular, the threshold voltage typically displays considerable gradient with distance across a wafer. Therefore, when the devices are physically separated by large distances, large current mismatch can result from biasing current sources sharing the same gate-source bias, especially when the overdrive is small. The second disadvantage of voltage routing is that the output currents are sensitive to variations in the supply resistances  $R_{S1}$  and  $R_{S2}$ . Although these resistances were assumed to be zero above, they are nonzero in practice because of imperfect conduction in the interconnect layers and their contacts. Since  $I_{OUT2}$  flows in  $R_{S2}$  and  $(I_{OUT1} + I_{OUT2})$  flows in  $R_{S1}$ , nonzero resistances cause  $V_{GS2} < V_{GS1}$  and  $V_{GS3} < V_{GS1}$  when  $I_{OUT1} > 0$  and  $I_{OUT2} > 0$ . Therefore, with perfectly matched transistors, the output currents are less than the input current, and the errors in the output currents can be predicted by an analysis similar to that presented in Section 4.4.1 for Widlar current sources. The key point here is that  $R_{S1}$  and  $R_{S2}$  increase as the distances between the input and output transistors increase, increasing the errors in the output currents. As a result of both of these disadvantages, the output currents may have considerable variation from one IC to another with voltage routing, increasing the difficulty of designing the circuits biased by  $M_2$  and  $M_3$  to meet the required specifications even if  $I_{IN}$  is precisely controlled.

To overcome these problems, the circuit in Fig. 4.53 can be built so that  $M_1$ – $M_3$  are close together physically, and the current outputs  $I_{OUT1}$  and  $I_{OUT2}$  are routed as required on the IC. This case is referred to as an example of the *current routing* of bias signals. Current routing reduces the problems with mismatch and supply resistance by reducing the distances

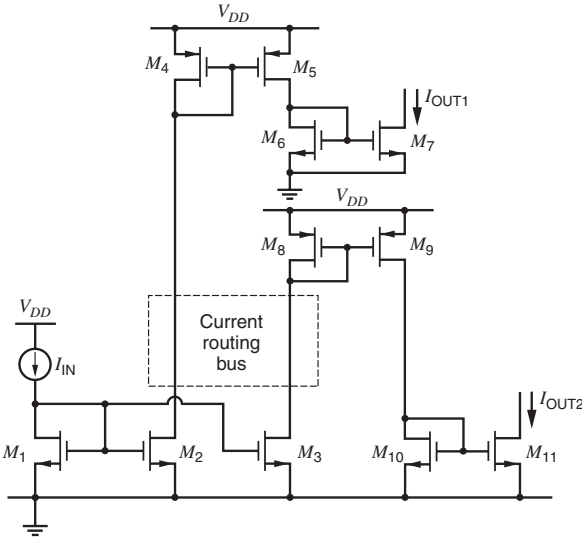


**Figure 4.54** Bias-distribution circuit using both current routing and voltage routing.

between the input and output transistors in the current mirror in Fig. 4.53 compared to voltage routing. One disadvantage of current routing is that it requires one node to be routed for each bias signal. Therefore, when the number of bias outputs is large, the die area required for the interconnect to distribute the bias currents can be much larger than that required with voltage routing. Another disadvantage of current routing is that it can increase the parasitic capacitance on the drains of  $M_2$  and  $M_3$ . If these nodes are connected to circuits that process high-frequency signals, increased parasitic capacitance can reduce performance in some ways. For example, if  $M_2$  and  $M_3$  act as the tail current sources of differential pairs, increased parasitic capacitance will increase the common-mode gain and reduce the common-mode rejection ratio of each differential pair at high frequencies.

In practice, many ICs use a combination of current- and voltage-routing techniques. For example, Fig. 4.54 shows a circuit with five current mirrors, where the input and output currents are still referenced as in Fig. 4.53. If the current routing bus in Fig. 4.54 travels over a large distance, the parasitic capacitances on the drains of  $M_2$  and  $M_3$  may be large. However, the parasitic capacitances on the drains of  $M_7$  and  $M_{11}$  are minimized by using voltage routing within each current mirror. Although simple current mirrors are shown in Fig. 4.54, cascoding is often used in practice to reduce gain errors stemming from a finite Early voltage. In ICs using both current and voltage routing, currents are routed globally and voltages locally, where the difference between global and local routing depends on distance. When the distance is large enough to significantly worsen mismatch or supply-resistance effects, the routing is *global*. Otherwise, it is *local*. An effective combination of these bias distribution techniques is to divide an IC into blocks, where bias currents are routed between blocks and bias voltages within the blocks.

## A.4.2 INPUT OFFSET VOLTAGE OF DIFFERENTIAL PAIR WITH ACTIVE LOAD

### A.4.2.1 BIPOLAR

For the resistively loaded emitter-coupled pair, we showed in Chapter 3 that the input offset voltage arises primarily from mismatches in  $I_S$  in the input transistors and from mismatches in the collector load resistors. In the active-load case, the input offset voltage results from nonzero

base current of the load devices and mismatches in the input transistors and load devices. Refer to Fig. 4.25a. Assume the inputs are grounded. If the matching is perfect and if  $\beta_F \rightarrow \infty$  in  $T_3$  and  $T_4$ ,

$$V_{OUT} = V_{CC} - |V_{BE3}| \quad (4.306)$$

Equation 4.306 holds because only this output voltage forces  $V_{CE3} = V_{CE4}$ , where  $I_{C1} = I_{C2}$  and  $V_{BE1} = V_{BE2}$ , which is required by KVL when  $V_{I1} = V_{I2}$ .

The differential input required to drive the output to the value given by (4.306) is the input-referred offset voltage. With finite  $\beta_F$  in the active-load transistors and/or device mismatch, the offset is usually nonzero. In the active-load, KVL shows that

$$V_{BE3} = V_{BE4} \quad (4.307)$$

Solving (1.58) for  $V_{BE3}$  and  $V_{BE4}$  and substituting in (4.307) gives

$$\frac{I_{C3}}{I_{S3}} \left( \frac{1}{1 + \frac{V_{CE3}}{V_{A3}}} \right) = \frac{I_{C4}}{I_{S4}} \left( \frac{1}{1 + \frac{V_{CE4}}{V_{A4}}} \right) \quad (4.308)$$

Assume that the Early voltages of  $T_3$  and  $T_4$  are identical. Since  $V_{CE3} = V_{CE4}$  when (4.306) is satisfied, (4.308) can be simplified to

$$I_{C4} = I_{C3} \left( \frac{I_{S4}}{I_{S3}} \right) \quad (4.309)$$

Since  $I_{C2} = -I_{C4}$ , (4.309) can be written as

$$I_{C2} = -I_{C3} \left( \frac{I_{S4}}{I_{S3}} \right) \quad (4.310)$$

From KCL at the collector of  $T_3$ ,

$$I_{C1} = -I_{C3} \left[ 1 + \left( \frac{2}{\beta_F} \right) \right] \quad (4.311)$$

where  $\beta_F$  is the ratio of the collector to base current in the active-load devices. From KVL in the input loop,

$$V_{ID} = V_{I1} - V_{I2} = V_{BE1} - V_{BE2} \quad (4.312)$$

Then the input offset voltage,  $V_{OS}$ , is the value of  $V_{ID}$  for which the output voltage is given by (4.306). If the Early voltages of  $T_1$  and  $T_2$  are identical, solving (1.58) for  $V_{BE1}$  and  $V_{BE2}$  and substituting into (4.312) gives

$$V_{OS} = V_{ID} = V_T \ln \left( \frac{I_{C1} I_{S2}}{I_{C2} I_{S1}} \right) \quad (4.313)$$

because  $V_{CE1} = V_{CE2}$  when (4.306) is satisfied. Substituting (4.310) and (4.311) in (4.313) gives

$$V_{OS} = V_T \ln \left[ \frac{I_{S3} I_{S2}}{I_{S4} I_{S1}} \left( 1 + \frac{2}{\beta_F} \right) \right] \quad (4.314)$$

If the mismatches are small, this expression can be approximated as

$$V_{OS} \simeq V_T \left( \frac{\Delta I_{SP}}{I_{SP}} - \frac{\Delta I_{SN}}{I_{SN}} + \frac{2}{\beta_F} \right) \quad (4.315)$$

using the technique described in Section 3.5.6.3, where

$$\Delta I_{SP} = I_{S3} - I_{S4} \quad (4.316)$$

$$I_{SP} = \frac{I_{S3} + I_{S4}}{2} \quad (4.317)$$

$$\Delta I_{SN} = I_{S1} - I_{S2} \quad (4.318)$$

$$I_{SN} = \frac{I_{S1} + I_{S2}}{2} \quad (4.319)$$

In the derivation of (4.315), we assumed that the Early voltages of matched transistors are identical. In practice, mismatch in Early voltages also contributes to the offset, but the effect is usually negligible when the transistors are biased with collector-emitter voltages much less than their Early voltages.

Assuming a worst-case value for  $\Delta I_S/I_S$  of  $\pm 5$  percent and a *pn*p beta of 20, the worst-case offset voltage is

$$V_{OS} \simeq V_T(0.05 + 0.05 + 0.1) = 0.2V_T \simeq 5 \text{ mV} \quad (4.320)$$

To find the worst-case offset, we have added the mismatch terms for the *pn*p and *np*n transistors in (4.320) instead of subtracting them as shown in (4.315) because the mismatch terms are random and independent of each other in practice. Therefore, the polarity of the mismatch terms is unknown in general. Comparing (4.320) to (3.219) shows that the actively loaded differential pair has significantly higher offset than the resistively loaded case under similar conditions. The offset arising here from mismatch in the load devices can be reduced by inserting resistors in series with the emitters of  $T_3$  and  $T_4$  as shown in Section A.4.1. To reduce the offset arising from finite  $\beta_F$  in the load devices, the current mirror in the load can use a beta helper transistor as described in Section 4.2.3.

#### A.4.2.2 MOS

The offset in the CMOS differential pair with active load shown in Fig. 4.25*b* is similar to the bipolar case. If the matching is perfect with the inputs grounded,

$$V_{OUT} = V_{DD} - |V_{GS3}| \quad (4.321)$$

Equation 4.321 holds because only this output voltage forces  $V_{DS3} = V_{DS4}$ , where  $I_1 = I_2$  and  $V_{GS1} = V_{GS2}$ , which is required by KVL when  $V_{I1} = V_{I2}$ .

The differential input required to drive the output to the value given by (4.321) is the input-referred offset voltage. With device mismatch, the offset is usually nonzero.

$$V_{ID} = V_{GS1} - V_{GS2} = V_{I1} + V_{ov1} - V_{I2} - V_{ov2} \quad (4.322)$$

Assume that the Early voltages of  $T_1$  and  $T_2$  are identical. Since  $V_{DS1} = V_{DS2} = V_{DSN}$  when  $V_{ID} = V_{OS}$ , applying (1.165) to  $V_{ov1}$  and  $V_{ov2}$  in (4.322) gives

$$V_{OS} = V_{I1} - V_{I2} + \sqrt{\frac{1}{1 + \lambda_N V_{DSN}}} \left( \sqrt{\frac{2I_1}{k'(W/L)_1}} - \sqrt{\frac{2I_2}{k'(W/L)_2}} \right) \quad (4.323)$$

If the mismatches are small, this expression can be approximated as

$$V_{OS} \simeq V_{I1} - V_{I2} + \frac{V_{ovN}}{2} \left( \frac{\Delta I_N}{I_N} - \frac{\Delta(W/L)_N}{(W/L)_N} \right) \quad (4.324)$$

using the technique described in Section 3.5.6.7, where

$$V_{ovN} = \sqrt{\frac{2I_N}{k'(W/L)_N(1 + \lambda_N V_{DSN})}} \quad (4.325)$$

$$\Delta I_N = I_1 - I_2 \quad (4.326)$$

$$I_N = \frac{I_1 + I_2}{2} \quad (4.327)$$

$$\Delta(W/L)_N = (W/L)_1 - (W/L)_2 \quad (4.328)$$

$$(W/L)_N = \frac{(W/L)_1 + (W/L)_2}{2} \quad (4.329)$$

Since  $I_1 = -I_3$  and  $I_2 = -I_4$

$$\frac{\Delta I_N}{I_N} = \frac{\Delta I_P}{I_P} \quad (4.330)$$

where

$$\Delta I_P = I_3 - I_4 \quad (4.331)$$

$$I_P = \frac{I_3 + I_4}{2} \quad (4.332)$$

To find  $\Delta I_P/I_P$ , we will use KVL in the gate-source loop in the load as follows

$$0 = V_{GS3} - V_{GS4} = V_{i3} + V_{ov3} - V_{i4} - V_{ov4} \quad (4.333)$$

Since  $T_3$  and  $T_4$  are  $p$ -channel transistors, their overdrives are negative. Assume that the Early voltages of  $T_3$  and  $T_4$  are identical. Since  $V_{DS3} = V_{DS4} = V_{DSP}$  when  $V_{ID} = V_{OS}$  (4.333) can be rewritten as

$$0 = V_{i3} - V_{i4} - \sqrt{\frac{1}{1 + |\lambda_P V_{DSP}|}} \left( \sqrt{\frac{2|I_3|}{k'(W/L)_3}} - \sqrt{\frac{2|I_4|}{k'(W/L)_4}} \right) \quad (4.334)$$

In (4.334), absolute value functions have been used so that the arguments of the square-root functions are positive. If the mismatches are small, this expression can be approximated as

$$\frac{\Delta I_P}{I_P} \simeq \frac{V_{i3} - V_{i4}}{\frac{|V_{ovP}|}{2}} + \frac{\Delta(W/L)_P}{(W/L)_P} \quad (4.335)$$

using the technique described in Section 3.5.6.7, where

$$|V_{ovP}| = \sqrt{\frac{2|I_P|}{k'(W/L)_P(1 + |\lambda_P V_{DSP}|)}} \quad (4.336)$$

$$\Delta(W/L)_P = (W/L)_3 - (W/L)_4 \quad (4.337)$$

$$(W/L)_P = \frac{(W/L)_3 + (W/L)_4}{2} \quad (4.338)$$

Substituting (4.335) and (4.330) into (4.324) gives

$$V_{OS} \simeq V_{i1} - V_{i2} + \frac{V_{ovN}}{2} \left( \frac{V_{i3} - V_{i4}}{\frac{|V_{ovP}|}{2}} + \frac{\Delta(W/L)_P}{(W/L)_P} - \frac{\Delta(W/L)_N}{(W/L)_N} \right) \quad (4.339)$$

Comparing (4.339) to (4.315) shows that the MOS differential pair with active load includes terms to account for threshold mismatch but excludes a term to account for finite beta in the active load because  $\beta_F \rightarrow \infty$  in MOS transistors.

### ■ EXAMPLE

Find the input-referred offset voltage of the circuit in Fig. 4.25*b* using the transistor parameters in the table below.

Transistor	$V_i$ (V)	$W$ ( $\mu\text{m}$ )	$L$ ( $\mu\text{m}$ )	$k'$ ( $\mu\text{A}/\text{V}^2$ )
$T_1$	0.705	49	1	100
$T_2$	0.695	51	1	100
$T_3$	-0.698	103	1	50
$T_4$	-0.702	97	1	50

Assume that  $I_{\text{TAIL}} = 200 \mu\text{A}$  and that  $\lambda_N V_{\text{DSN}} \ll 1$  and  $|\lambda_P V_{\text{DSP}}| \ll 1$ . From (4.327) and KCL,

$$I_N = \frac{I_1 + I_2}{2} = \frac{I_{\text{TAIL}}}{2} = 100 \mu\text{A} \quad (4.340)$$

Substituting (4.340) and (4.329) into (4.325) gives

$$V_{\text{ovN}} \simeq \sqrt{\frac{200}{100(49 + 51)/2}} \text{ V} = 0.2 \text{ V} \quad (4.341)$$

Similarly, from (4.332) and KCL

$$I_P = \frac{I_3 + I_4}{2} = -\frac{I_{\text{TAIL}}}{2} = -100 \mu\text{A} \quad (4.342)$$

Substituting (4.342) and (4.338) into (4.336) gives

$$|V_{\text{ovP}}| \simeq \sqrt{\frac{200}{50(103 + 97)/2}} \text{ V} = 0.2 \text{ V} \quad (4.343)$$

Substituting (4.337) and (4.328) into (4.339) gives

$$\begin{aligned} V_{\text{OS}} &\simeq 0.705 \text{ V} - 0.695 \text{ V} \\ &+ 0.1 \left( \frac{-0.698 + 0.702}{0.1} + \frac{103 - 97}{(103 + 97)/2} - \frac{49 - 51}{(49 + 51)/2} \right) \text{ V} \\ &\simeq 0.01 \text{ V} + 0.1(0.04 + 0.06 + 0.04) \text{ V} = 0.024 \text{ V} \end{aligned} \quad (4.344)$$

In this example, the mismatches have been chosen so that the individual contributions to the offset add constructively to give the worst-case offset.

## PROBLEMS

For the bipolar transistors in these problems, use the high-voltage device parameters given in Fig. 2.30 and Fig. 2.35, unless otherwise specified. Assume that  $r_b = 0$  and  $r_\mu \rightarrow \infty$  in all problems. Assume all bipolar transistors operate in the forward-active region, and neglect base currents in bias calculations unless otherwise specified.

**4.1** Determine the output current and output resistance of the bipolar current mirror shown in Fig. 4.55. Find the output current if  $V_{\text{OUT}} = 1 \text{ V}$ ,  $5 \text{ V}$ , and  $30 \text{ V}$ . Ignore the effects of nonzero base currents. Compare your answer with a SPICE simulation.

**4.2** Repeat Problem 4.1 including the effects of nonzero base currents.

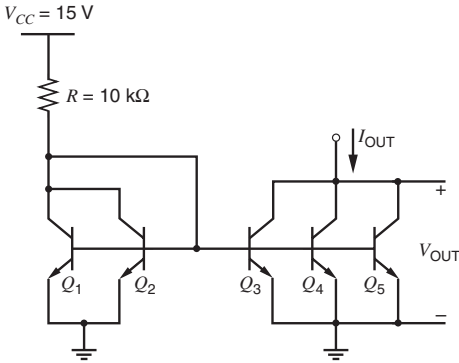


Figure 4.55 Circuit for Problem 4.1.

4.3 Design a simple MOS current mirror of the type shown in Fig. 4.4 to meet the following constraints:

- (a) Transistor  $M_2$  must operate in the active region for values of  $V_{OUT}$  to within 0.2 V of ground.
- (b) The output current must be 50  $\mu\text{A}$ .
- (c) The output current must change less than 1 percent for a change in output voltage of 1 V.

Make  $M_1$  and  $M_2$  identical. You are to minimize the total device area within the given constraints. Here the device area will be taken to be the total gate area ( $W \times L$  product). Assume  $X_d = 0$  and take other device data from Table 2.4.

4.4 Calculate an analytical expression for the small-signal output resistance  $R_o$  of the bipolar cascode current mirror of Fig. 4.8. Assume that the input current source is not ideal and that the nonidealness is modeled by placing a resistor  $R_1$  in parallel with  $I_{IN}$ . Show that for large  $R_1$ , the output resistance approaches  $\beta_0 r_o / 2$ . Calculate the value of  $R_o$  if  $V_{CC} = 5\text{ V}$ ,  $I_{IN} = 0$ , and  $R_1 = 10\text{ k}\Omega$ , and estimate the value of  $V_{OUT}$  below which  $R_o$  will begin to decrease substantially. Use SPICE to check your calculations and also to investigate the  $\beta_F$  sensitivity by varying  $\beta_F$  by  $-50$  percent and examining  $I_{OUT}$ . Use SPICE to plot the large-signal  $I_{OUT}$ - $V_{OUT}$  characteristic.

4.5 Calculate the output resistance of the circuit of Fig. 4.9, assuming that  $I_{IN} = 100\ \mu\text{A}$  and the devices have drawn dimensions of  $100\ \mu\text{m}/1\ \mu\text{m}$ . Use the process parameters given in Table 2.4, and assume for all devices that  $X_d = 0$ . Also, ignore the body effect for simplicity. Compare your answer with a SPICE simulation and also use SPICE to plot the  $I_{OUT}$ - $V_{OUT}$  characteristic for  $V_{OUT}$  from 0 to 3 V.

4.6 Using the data given in the example of Section 1.9, include the effects of substrate leakage in the

calculation of the output resistance for the circuit of Problem 4.5. Let  $V_{OUT} = 2\text{ V}$  and  $3\text{ V}$ .

4.7 Design the circuit of Fig. 4.11b to satisfy the constraints in Problem 4.3 except the output resistance objective is that the output current change less than 0.02 percent for a 1 V change in the output voltage. Ignore the body effect for simplicity. Make all devices identical except for  $M_4$ . Use SPICE to check your design and also to plot the  $I_{OUT}$ - $V_{OUT}$  characteristic for  $V_{OUT}$  from 0 to 3 V.

4.8 For the circuit of Fig. 4.56, assume that  $(W/L)_8 = (W/L)$ . Ignoring the body effect, find  $(W/L)_6$  and  $(W/L)_7$  so that  $V_{DS6} = V_{DS7} = V_{ov8}$ . Draw the schematic of a double-cascode current mirror that uses the circuit of Fig. 4.56 to bias both cascode devices in the output branch. For this current mirror, calculate the output resistance, the minimum output voltage for which all three transistors in the output branch operate in the active region, the total voltage across all the devices in the input branch, and the systematic gain error.

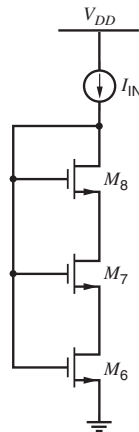
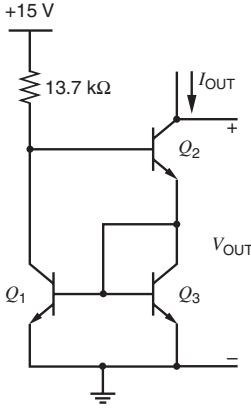


Figure 4.56 Circuit for Problem 4.8.

4.9 Calculate the output resistance of the Wilson current mirror shown in Fig. 4.57. What is the percentage change in  $I_{OUT}$  for a 5-V change in  $V_{OUT}$ ? Compare your answer with a SPICE simulation using a full device model. Use SPICE to check the  $\beta_F$  sensitivity by varying  $\beta_F$  by  $-50$  percent and examining  $I_{OUT}$ . Also, use SPICE to plot the large-signal  $I_{OUT}$ - $V_{OUT}$  characteristic for  $V_{OUT}$  from 0 to 15 V.

4.10 Calculate the small-signal voltage gain of the common-source amplifier with active load in Fig. 4.16b. Assume that  $V_{DD} = 3\text{ V}$  and that all the transistors operate in the active region. Do the calculations for values of  $I_{REF}$  of 1 mA, 100  $\mu\text{A}$ , 10  $\mu\text{A}$ , and 1  $\mu\text{A}$ .



**Figure 4.57**  
Circuit for Problem 4.9.

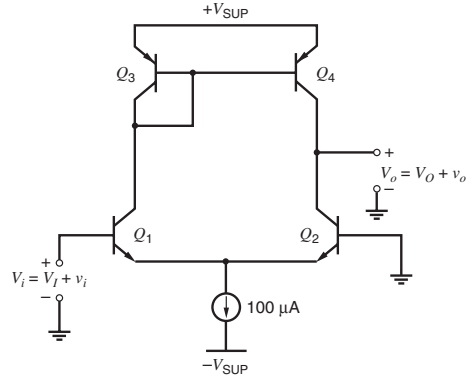


**Figure 4.58** Circuit for Problem 4.12.

Assume that the drawn dimensions of each transistor are  $W = 100 \mu\text{m}$  and  $L = 1 \mu\text{m}$ . Assume  $X_d = 0$  and use Table 2.4 for other parameters.

- (a) At first, assume the transistors operate in strong inversion in all cases.
- (b) Repeat part (a) including the effects of weak inversion by using (1.253) with  $n = 1.5$  to calculate the transconductance of  $M_1$ . Assume that a transistor operates in weak inversion when its overdrive is less than  $2nV_T$ , as given in (1.255).
- (c) Use SPICE to check your calculations for both parts (a) and (b).

**4.11** Calculate the small-signal voltage gain of a common-source amplifier with depletion load in Fig. 4.20, including both the body effect and channel-length modulation. Assume that  $V_{DD} = 3 \text{ V}$  and that the dc input voltage is adjusted so that the dc output voltage is  $1 \text{ V}$ . Assume that  $M_1$  has drawn dimensions of  $W = 100 \mu\text{m}$  and  $L = 1 \mu\text{m}$ . Also, assume that  $M_2$  has drawn dimensions of  $W = 10 \mu\text{m}$  and  $L = 1 \mu\text{m}$ . For  $M_2$ , assume  $V_{t0} = -1 \text{ V}$ . For both transistors, assume that  $X_d = 0$ . Use Table 2.4 for other parameters of both transistors.

**4.12** Determine the unloaded voltage gain  $v_o/v_i$  and output resistance for the circuit of Fig. 4.58. Check with SPICE and also use SPICE to plot out the large-signal  $V_O-V_I$  transfer characteristic for  $V_{SUP} = 2.5 \text{ V}$ . Use SPICE to determine the CMRR if the current-source output resistance is  $1 \text{ M}\Omega$ .

**4.13** Repeat Problem 4.12, but now assuming that  $2\text{-k}\Omega$  resistors are inserted in series with the emitters of  $Q_3$  and  $Q_4$ .

**4.14** Repeat Problem 4.12 except replace  $Q_1$  and  $Q_2$  with  $n$ -channel MOS transistors  $M_1$  and  $M_2$ . Also, replace  $Q_3$  and  $Q_4$  with  $p$ -channel MOS transistors  $M_3$  and  $M_4$ . Assume  $W_n = 50 \mu\text{m}$  and  $W_p = 100 \mu\text{m}$ .

For all transistors, assume  $L_{drwn} = 1 \mu\text{m}$  and  $X_d = 0$ . Use Table 2.3 for other parameters.

**4.15** Repeat Problem 4.14, but now assuming that  $2 \text{ k}\Omega$  resistors are inserted in series with the sources of  $M_3$  and  $M_4$ . Ignore the body effect.

**4.16** Determine the unloaded voltage gain  $v_o/v_i$  and output resistance for the circuit of Fig. 4.59. Neglect  $r_{\mu}$ . Verify with SPICE and also use SPICE to plot the large-signal  $V_O-V_I$  transfer characteristic for  $V_{SUP} = 2.5 \text{ V}$ .

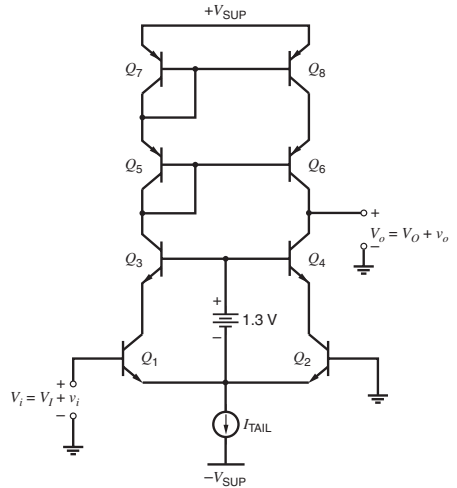


**Figure 4.59** Cascode active-load circuit for Problem 4.16.

**4.17** Repeat Problem 4.16 except replace the  $nnp$  and  $pnp$  transistors with  $n$ -channel and  $p$ -channel MOS transistors, respectively. Assume  $W_n = 50 \mu\text{m}$  and  $W_p = 100 \mu\text{m}$ . For all transistors, assume  $L_{drwn} = 1 \mu\text{m}$  and  $X_d = 0$ . Let  $I_{TAIL} = 100 \mu\text{A}$ . Ignore

the body effect. Use Table 2.3 for other parameters.

**4.18** Find  $G_m[dm]$  of a source-coupled pair with a current-mirror load with nonzero mismatch (Fig. 4.29b) and show that it is approximately given by (4.184). Calculate the value of  $G_m[dm]$  using the following data:

	$T_1$	$T_2$	$T_3$	$T_4$	$T_5$
$g_m$ (mA/V)	1.05	0.95	1.1	0.9	2.0
$r_o$ (M $\Omega$ )	0.95	1.05	1.0	1.0	0.5

Compare your answer with a SPICE simulation. Also, compare your answer to the result that would apply without mismatch.

**4.19** Although  $G_m[cm]$  of a differential pair with a current-mirror load can be calculated exactly from a small-signal diagram where mismatch is allowed, the calculation is complicated because the mismatch terms interact, and the results are difficult to interpret. In practice, the mismatch terms are often a small fraction of the corresponding average values, and the interactions between mismatch terms are often negligible. Using the following steps as a guide, calculate an approximation to  $G_m[cm]$  including the effects of mismatch.

(a) Derive the ratio  $i_2/v_{ic}$  included in (4.165) and show that this ratio is approximately  $1/2r_{tail}$  as shown in (4.185) if  $\epsilon_d \ll 2$ ,  $g_{m2}r_{o2} \gg 1$ , and  $2g_{m2}r_{tail} \gg 1$ .

(b) Use (4.173) to calculate  $\epsilon_d$  with perfect matching, where  $\epsilon_d$  represents the gain error of the differential pair with a pure common-mode input and is defined in (4.161).

(c) Calculate  $\epsilon_d$  if  $1/g_{m3} = 0$  and if the only mismatch is  $g_{m1} \neq g_{m2}$ .

(d) Calculate  $\epsilon_d$  if  $1/g_{m3} = 0$  and if the only mismatch is  $r_{o1} \neq r_{o2}$ .

(e) Now estimate the total  $\epsilon_d$  including mismatch by adding the values calculated in parts (b), (c), and (d). Show that the result agrees with (4.186) if  $g_{m3}r_{o(dp)} \gg 1$ .

(f) Calculate  $\epsilon_m$ , which represents the gain error of the current mirror and is defined in (4.133). Show that the result agrees with (4.187).

(g) Calculate the value of  $G_m[cm]$  using (4.185) and the CMRR for the data given in Problem 4.18. Compare your answer with a SPICE simulation. Also, compare your answer to the result that would apply without mismatch.

**4.20** Design a Widlar current source using *npn* transistors that produces a 5- $\mu$ A output current. Use

Fig. 4.31a with identical transistors,  $V_{CC} = 30$  V, and  $R_1 = 30$  k $\Omega$ . Find the output resistance.

**4.21** In the design of a Widlar current source of Fig. 4.31a to produce a specified output current, two resistors must be selected. Resistor  $R_1$  sets  $I_{IN}$ , and the emitter resistor  $R_2$  sets  $I_{OUT}$ . Assuming a supply voltage of  $V_{CC}$  and a desired output current  $I_{OUT}$ , determine the values of the two resistors so that the total resistance in the circuit is minimized. Your answer should be given as expressions for  $R_1$  and  $R_2$  in terms of  $V_{CC}$  and  $I_{OUT}$ . What values would these expressions give for Problem 4.20? Are these values practical?

**4.22** Determine the output current in the circuit of Fig. 4.60.

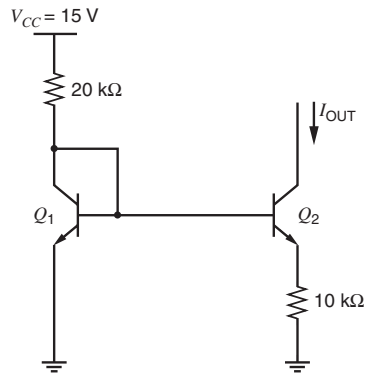


Figure 4.60 Circuit for Problem 4.22.

**4.23** Design a MOS Widlar current source using the circuit shown in Fig. 4.31b to meet the following constraints with  $V_{DD} = 3$  V:

(a) The input current should be 100  $\mu$ A, and the output current should be 10  $\mu$ A.

(b)  $V_{ov1} = 0.2$  V.

(c) Transistor  $M_2$  must operate in the active region if the voltage from the drain of  $M_2$  to ground is at least 0.2 V.

(d) The output resistance should be 50 M $\Omega$ .

Ignore the body effect. Assume  $L_{drwn} = 1$   $\mu$ m and  $X_d = L_d = 0$ . Use Table 2.4 for other parameters.

**4.24** Design the MOS peaking current source in Fig. 4.34 so that  $I_{OUT} = 0.1$   $\mu$ A.

(a) First, let  $I_{IN} = 1$   $\mu$ A and find the required value of  $R$ .

(b) Second, let  $R = 10$  k $\Omega$  and find the required  $I_{IN}$ .

In both cases, assume that both transistors are identical and operate in weak inversion with  $I_t = 0.1$   $\mu$ A and  $n = 1.5$ . Also, find the minimum  $W/L$

in both cases, assuming that  $V_{GS} - V_t < 0$  is required to operate a transistor in weak inversion as shown in Fig. 1.45.

**4.25** Determine the output current and output resistance of the circuit shown in Fig. 4.61.

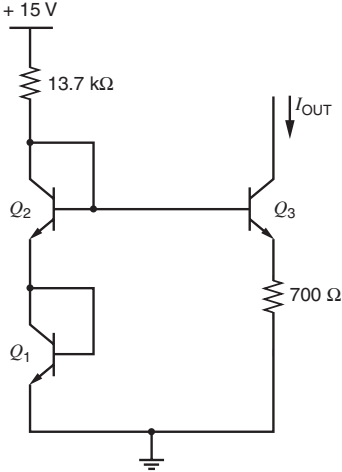


Figure 4.61 Circuit for Problem 4.25.

**4.26** Determine the value of sensitivity  $S$  of output current to supply voltage for the circuit of Fig. 4.62, where  $S = (V_{CC}/I_{OUT})(\partial I_{OUT}/\partial V_{CC})$ .

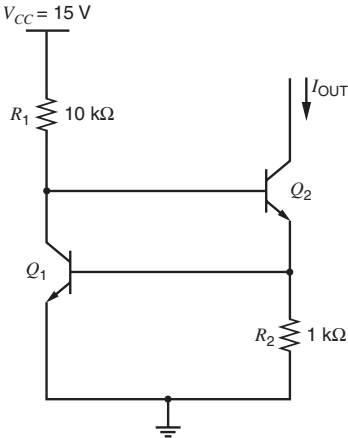


Figure 4.62 Circuit for Problem 4.26.

**4.27** In the analysis of the hypothetical reference of Fig. 4.44, the current  $I_1$  was assumed proportional to temperature. Assume instead that this current is derived from a diffused resistor, and thus has a  $TC_F$  of  $-1500 \text{ ppm}/^\circ\text{C}$ . Determine the new value of  $V_{OUT}$  required to achieve zero  $TC_F$  at  $25^\circ\text{C}$ . Neglect base current.

**4.28** The circuit of Fig. 4.46c is to be used as a band-gap reference. If the op amp is ideal, its differential input voltage and current are both zero and

$$V_{OUT} = (V_{BE1} + I_1 R_1) = (V_{BE1} + I_2 R_2)$$

$$V_{OUT} = V_{BE1} + R_2 \left( \frac{V_{BE1} - V_{BE2}}{R_3} \right)$$

Assume that  $I_1$  is to be made equal to  $200 \mu\text{A}$ , and that  $(V_{BE1} - V_{BE2})$  is to be made equal to  $100 \text{ mV}$ . Determine  $R_1$ ,  $R_2$ , and  $R_3$  to realize zero  $TC_F$  of  $V_{OUT}$  at  $25^\circ\text{C}$ . Neglect base currents.

**4.29** A band-gap reference like that of Fig. 4.47 is designed to have nominally zero  $TC_F$  at  $25^\circ\text{C}$ . Due to process variations, the saturation current  $I_S$  of the transistors is actually twice the nominal value. Assume  $V_{OS} = 0$ . What is  $dV_{OUT}/dT$  at  $25^\circ\text{C}$ ? Neglect base currents.

**4.30** Simulate the band-gap reference from Problem 4.29 on SPICE. Assume that the amplifier is just a voltage-controlled voltage source with an open-loop gain of 10,000 and that the resistor values are independent of temperature. Also assume that  $I_{S1} = 1.25 \times 10^{-17} \text{ A}$  and  $I_{S2} = 1 \times 10^{-16} \text{ A}$ . In SPICE, adjust the closed-loop gain of the amplifier (by choosing suitable resistor values) so that the output  $TC_F$  is zero at  $25^\circ\text{C}$ . What is the resulting target value of  $V_{OUT}$ ? Now double  $I_{S1}$  and  $I_{S2}$ . Use SPICE to adjust the gain so that  $V_{OUT}$  is equal to the target at  $25^\circ\text{C}$ . Find the new  $dV_{OUT}/dT$  at  $25^\circ\text{C}$  with SPICE. Compare this result with the calculations from Problem 4.29.

**4.31** Repeat Problem 4.29 assuming that the values of  $I_S$ ,  $R_2$ , and  $R_1$  are nominal but that  $R_3$  is 1 percent low. Assume  $V_{BE(\text{on})} = 0.6 \text{ V}$ .

**4.32** A band-gap reference circuit is shown in Fig. 4.63. Assume that  $\beta_F \rightarrow \infty$ ,  $V_A \rightarrow \infty$ ,  $I_{S1} = 1 \times 10^{-15} \text{ A}$ , and  $I_{S2} = 8 \times 10^{-15} \text{ A}$ . Assume the op amp is ideal except for a possibly nonzero offset voltage  $V_{OS}$ , which is modeled by a voltage source in Fig. 4.63.

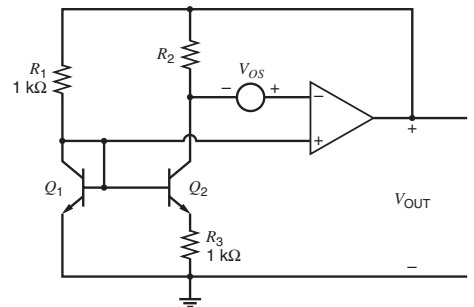


Figure 4.63 Band-gap reference circuit for Problem 4.32.

(a) Suppose that  $R_2$  is trimmed to set  $V_{OUT}$  equal to the target voltage for which  $dV_{OUT}/dT = 0$  at  $T = 25^\circ\text{C}$  when  $V_{OS} = 0$ . Find  $dV_{OUT}/dT$  at  $T = 25^\circ\text{C}$  when  $V_{OS} = 30\text{ mV}$ .

(b) Under the conditions in part (a), is  $dV_{OUT}/dT$  positive or negative? Explain.

**4.33** For the circuit of Fig. 4.64, find the value of  $W/L$  for which  $dV_{GS}/dT = 0$  at  $25^\circ\text{C}$ . Assume that the threshold voltage falls 2 mV for each  $1^\circ\text{C}$  increase in temperature. Also, assume that the mobility temperature dependence is given by (4.243) with  $n = 1.5$ . Finally, use Table 2.4 for other parameters at  $25^\circ\text{C}$ , and let  $I = 200\ \mu\text{A}$ .

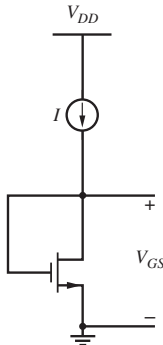


Figure 4.64 Circuit for Problem 4.33.

**4.34** Calculate the bias current of the circuit shown in Fig. 4.65 as a function of  $R$ ,  $\mu_n C_{ox}$ ,  $(W/L)_1$ , and  $(W/L)_2$ . Comment on the temperature behavior of the bias current. For simplicity, assume that  $X_d = L_d = 0$  and ignore the body effect. Assume  $M_4$  is identical to  $M_3$ .

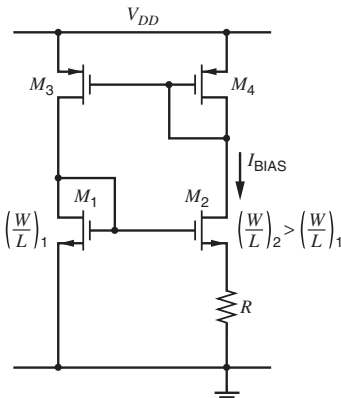


Figure 4.65 Circuit for Problem 4.34.

**4.35** The circuit of Fig. 4.65 produces a supply-insensitive current. Calculate the ratio of small-signal

variations in  $I_{BIAS}$  to small-signal variations in  $V_{DD}$  at low frequencies. Ignore the body effect but include finite transistor  $r_o$  in this calculation.

**4.36** For the bias circuit shown in Fig. 4.66, determine the bias current. Assume that  $X_d = L_d = 0$ . Neglect base currents and the body effect. Comment on the temperature dependence of the bias current. Assume a channel mobility and oxide thickness from Table 2.4. Compare your calculations to a SPICE simulation using a full circuit model from Table 2.4, and also use SPICE to determine the supply-voltage sensitivity of  $I_{BIAS}$ .

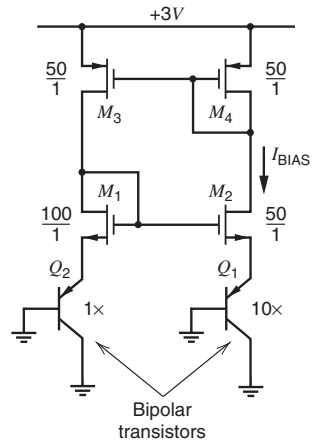


Figure 4.66 Circuit for Problem 4.36.

**4.37** A pair of bipolar current sources is to be designed to produce output currents that match with  $\pm 1$  percent. If resistors display a worst-case mismatch of  $\pm 0.5$  percent, and transistors a worst-case  $V_{BE}$  mismatch of 2 mV, how much voltage must be dropped across the emitter resistors?

**4.38** Determine the worst-case input offset voltage for the circuit of Fig. 4.58. Assume the worst-case  $I_S$  mismatches in the transistors are  $\pm 5$  percent and  $\beta_F = 15$  for the *pnp* transistors. Assume the dc output voltage is  $V_{SUP} - |V_{BE(on)}|$ .

**4.39** Repeat Problem 4.38, but assume that 2-k $\Omega$  resistors are placed in series with the emitters of  $Q_3$  and  $Q_4$ . Assume the worst-case resistor mismatch is  $\pm 0.5$  percent and the worst-case *pnp*  $\beta_F$  mismatch is  $\pm 10$  percent.

**4.40** Repeat Problem 4.38 but replace the bipolar transistors with MOS transistors as in Problem 4.14. Assume the worst-case  $W/L$  mismatches in

the transistors are  $\pm 5$  percent and the worst-case  $V_t$  mismatches are  $\pm 10$  mV. Assume the dc output voltage to ground is  $V_{SUP} - |V_{GS3}|$ . Also, assume

that  $(W/L)_1 + (W/L)_2 = 20$  and  $(W/L)_3 + (W/L)_4 = 60$ . Use Table 2.4 to calculate the transconductance parameters.

## REFERENCES

1. Y. P. Tsividis. *Operation and Modeling of the MOS Transistor*; McGraw Hill, New York, 1987, p. 139.
2. J.-B. Shyu, G. C. Temes, and F. Krummenacher. "Random Error Effects in Matched MOS Capacitors and Current Sources," *IEEE Journal of Solid-State Circuits*, Vol. SC-19, pp. 948–955, December 1984.
3. K. R. Lakshmikummar, R. A. Hadaway, and M. A. Copeland. "Characterisation and Modeling of Mismatch in MOS Transistors for Precision Analog Design," *IEEE Journal of Solid-State Circuits*, Vol. SC-21, pp. 1057–1066, December 1986.
4. M. J. M. Pelgrom, A. C. J. Duinmaijer, and A. P. G. Welbers. "Matching Properties of MOS Transistors," *IEEE Journal of Solid-State Circuits*, Vol. 24, pp. 1433–1440, October 1989.
5. W.-J. Hsu, B. J. Sheu, and S. M. Gowda. "Design of Reliable VLSI Circuits Using Simulation Techniques," *IEEE Journal of Solid-State Circuits*, Vol. 26, pp. 452–457, March 1991.
6. T. C. Choi, R. T. Kaneshiro, R. W. Brodersen, P. R. Gray, W. B. Jett, and M. Wilcox. "High-Frequency CMOS Switched-Capacitor Filters for Communications Application," *IEEE Journal of Solid-State Circuits*, Vol. SC-18, pp. 652–664, December 1983.
7. N. S. Sooch. "MOS Cascode Current Mirror," U.S. Patent 4,550,284, October 1985.
8. G. R. Wilson. "A Monolithic Junction FET— $n$ - $p$ - $n$  Operational Amplifier," *IEEE Journal of Solid-State Circuits*, Vol. SC-3, pp. 341–348, December 1968.
9. D. Fullagar. "A New-Performance Monolithic Operational Amplifier," *Fairchild Semiconductor Applications Brief*, May 1968.
10. R. J. Widlar. "Some Circuit Design Techniques for Linear Integrated Circuits," *IEEE Transactions on Circuit Theory*, Vol. CT-12, pp. 586–590, December 1965.
11. R. J. Widlar. "Design Techniques for Monolithic Operational Amplifiers," *IEEE Journal of Solid-State Circuits*, Vol. SC-4, pp. 184–191, August 1969.
12. M. Nagata. "Constant Current Circuits," Japanese Patent 628,228, May 6, 1971.
13. T. M. Frederiksen. "Constant Current Source," U.S. Patent 3,659,121, April 25, 1972.
14. C. Y. Kwok. "Low-Voltage Peaking Complementary Current Generator," *IEEE Journal of Solid-State Circuits*, Vol. SC-20, pp. 816–818, June 1985.
15. R. J. Widlar. "New Developments in IC Voltage Regulators," *IEEE Journal of Solid-State Circuits*, Vol. SC-6, pp. 2–7, February 1971.
16. C. R. Palmer and R. C. Dobkin. "A Curvature Corrected Micropower Voltage Reference," *International Solid-State Circuits Conference*, pp. 58–59, February 1981.
17. G. C. M. Meijer, P. C. Schmale, and K. van Zalinge. "A New Curvature-Corrected Bandgap Reference," *IEEE Journal of Solid-State Circuits*, Vol. SC-17, pp. 1139–1143, December 1982.
18. B.-S. Song and P. R. Gray. "A Precision Curvature-Compensated CMOS Bandgap Reference," *IEEE Journal of Solid-State Circuits*, Vol. SC-18, pp. 634–643, December 1983.
19. A. P. Brokaw. "A Simple Three-Terminal IC Bandgap Reference," *IEEE Journal of Solid-State Circuits*, Vol. SC-9, pp. 388–393, December 1974.
20. Y. P. Tsividis. "Accurate Analysis of Temperature Effects in  $I_C - V_{BE}$  Characteristics with Application to Bandgap Reference Sources," *IEEE Journal of Solid-State Circuits*, Vol. SC-15, pp. 1076–1084, December 1980.
21. A. P. Brokaw. Private Communication.
22. R. A. Pease. Private Communication.
23. K. E. Kuijk. "A Precision Reference Voltage Source," *IEEE Journal of Solid-State Circuits*, Vol. SC-8, pp. 222–226, June 1973.
24. T. R. Viswanathan. Private Communication.
25. E. A. Vittoz and O. Neyroud. "A Low-Voltage CMOS Bandgap Reference," *IEEE Journal of Solid-State Circuits*, Vol. SC-14, pp. 573–577, June 1979.